

Chapter One

Introduction

1-1 Biomedical Inorganic Chemistry:

Metal ions are essential to life (plant and animal); this has long been recognized although their role is uncertain in many cases. The list of essential "trace elements" has grown steadily over the years, as has the list of biological functions in which metals are known to be involved. Only recently we have begun to understand the structural chemistry operating at the biological sites where metal ions are found⁽¹⁾. These metals include most the first row transition metals but only molybdenum and perhaps tungsten from the heavier transition metals are important in mammalian biochemistry⁽²⁾.

Inorganic Compounds play crucial roles in biological and biomedical processes, and it is evident that many organic compounds used in medicine do not have a purely organic mode of action, some are activated or biotransformed by metal ions including metalloenzymes, other have direct or indirect effect on metal ion metabolism⁽³⁾.

Bioinorganic chemistry is a rapidly developing field and there is enormous potential for applications in medicine, not only for the 24 essential elements (H, C, N, O, F, Na, Mg, Si, P, S, Cl, K, Ca, V, Mn, Fe, Co, Ni, Cu, Zn, Se, Mo, Sn, and I) and also for nonessential and even radioactive elements⁽³⁾.

Biomedical inorganic chemistry (elemental medicine) is an important new area of biochemistry. The elements of medical importance (Pd, Pt, Cu, and Au) offer the potential for the design of novel therapeutic and diagnosis agents and hence for the treatment and understanding of diseases which are currently intractable⁽³⁾.

The use of metals in drug design provides new opportunities in the development of new generation antitumor drugs. The large number of metals available, combined with access to a range of coordination geometries and types of complexes, and the almost infinite number of organic ligands that may be coordinated to the metal centre, provides access to a huge number of metal complexes that could be screened for activity⁽³⁾.

The important of metal ions to the vital functions of living organism, hence their health and well being has become increasingly apparent. As a result, the long – neglected field of “bioinorganic chemistry” is now developing at a rapid pace⁽⁴⁾.

1-2 Chemotherapy:

Chemotherapy may be defined as the use of chemical agents in the treatment of diseases. Chemicals, that employed are referred to be chemotherapeutic agents, the most essential feature of good chemotherapeutic agents must show a high degree of selective toxicity towards a microorganism, so that, it can be given in sufficient doses to inhibit or kill the microorganism throughout the body without harming the body cells⁽⁵⁾.

Chemotherapy is an important method of anti-tumor therapy, including platinum compounds, in particular, cisplatin, is the drug of choice in the treatment of the majority of solid tumor⁽⁶⁾.

1-3 New Metal Complexes as Potential Therapeutics:

The key areas in the design of active compounds are the control of toxicity (side-effect) and targeting of the metal to specific tissues, organs, or cells where activity is needed. The toxicity of an element will depend on the element itself, its oxidation state, and the nature and number of coordinated ligands, as well as on the dose, mode of administration, and

biochemical status of the host. Moreover the effect of one element may depend on the presence or availability of another⁽⁷⁾.

Designing ligands that will interact with free or protein-bound metal ions is also a recent focus of medicinal inorganic research. For example, chelating ligands for copper and zinc are being investigated as a potential treatment for Al-Zheimer's disease⁽⁸⁾.

Developing metal complexes as drugs, however, is not an easy task. Accumulation of metal ions in the body can lead to deleterious effects. Thus biodistribution and clearance of the metal complex as well as its pharmacological specificity are to be considered. Favorable physiological responses of the candidate drugs need to be demonstrated by *in vitro* study with targeted biomolecules and tissues as well as *in vivo* investigation with xenografts and animal models before they enter clinical trials⁽⁸⁾.

A mechanistic understanding of how metal complexes achieve their activities is crucial to their clinical success, as well as to the rational design of new compounds with improved potency⁽⁸⁾.

1-3-1 Platinum Complexes:

The many activities of metal ions in biology have stimulated the development of metal-based therapeutics. Cisplatin [cisdiamminedichloroplatinum (II)] Figure (1-1), as one of the leading metal-based drugs, is widely used in treatment of cancer, being especially effective against genitourinary tumors such as testicular with 90% cure rate⁽⁸⁾.

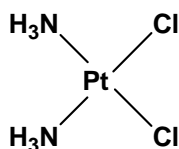


Figure (1-1): Cisplatin [cis-diamminedichloroplatinum (II)]⁽⁸⁾

Cisplatin enters cells by passive diffusion and also, as recently discovered, by active transport mediated by the copper transporter in yeast and mammals. The cytotoxicity of Cisplatin originates from its binding to DNA and the formation of covalent cross-links. Binding of cisplatin to DNA causes significant distortion of helical structure and results in inhibition of DNA replication and transcription⁽⁸⁾.

The clinical success of cisplatin is limited by significant side effects and acquired or intrinsic resistance.

Drug Resistance:

The development of cellular resistance after prolonged treatment with cisplatin can be a problem in the clinic. The major resistance mechanisms are⁽⁷⁾:

- (i) reduced transport across the cell membrane (pt pumped out via transmembrane p-glycoprotein),
- (ii) formation of unreactive adducts with thiol ligands of the tripeptide glutathione and the protein metallothionein, and
- (iii) repair of DNA damage by excision-repair enzymes.

Cisplatin is administered to cancer patients intravenously as a sterile saline solution (that is, containing salt—specifically, sodium chloride). Once cisplatin is in the bloodstream, it remains intact due the relatively high concentration of chloride ions (~100 mM). The neutral compound then enters the cell by either passive diffusion or active uptake by the cell. Inside the cell, the neutral cisplatin molecule undergoes hydrolysis, in which a chloride ligand is replaced by a molecule of water, generating a positively charged species, as shown below and in Figure (1-2) Hydrolysis occurs inside the cell due to a much lower concentration of chloride ion (~3-20 mM)—and therefore a higher concentration of water⁽⁹⁾.

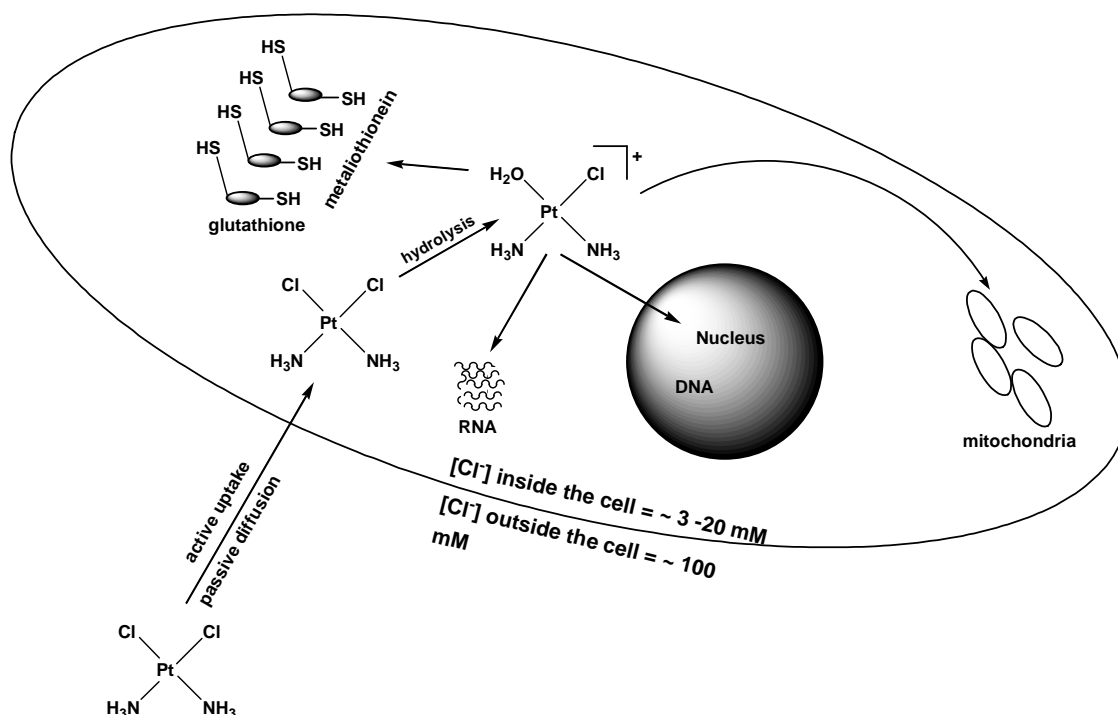
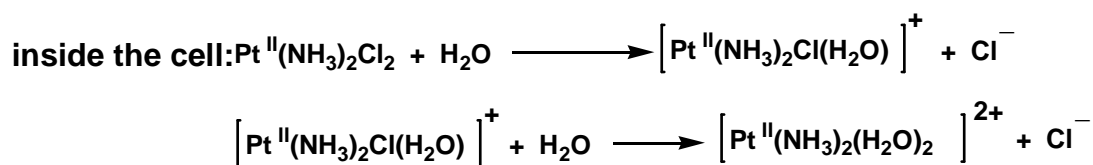


Figure (1-2): The cellular uptake of cisplatin and its targets⁽⁹⁾.

As seen in Figure (1-2), once inside the cell, cisplatin has a number of possible targets: DNA; RNA; sulfur-containing enzymes such as metallothionein and glutathione; and mitochondria. The effects of DNA on mitochondria are not well understood, but it is possible that damage to mitochondrial DNA resulting from cisplatin treatment contributes to cell death. The interaction of cisplatin with sulfur-containing enzymes is better understood and is believed to be involved in resistance of cells to cisplatin⁽⁹⁾.

Therefore, much attention has focused on designing new platinum compounds with improved pharmacological properties and a broader range of antitumor activity. Several platinum complexes Figure (1-3)⁽¹⁰⁾ are currently in clinical trials, but these new complexes have not yet demonstrated significant advantages over cisplatin⁽⁸⁾.

Oxaliplatin has been approved for clinical use in Europe, China and, for colorectal cancer, the United States. Strategies for developing new platinum anticancer agents include the incorporation of carrier groups that can target tumor cells with high specificity. Also of interest is to develop platinum complexes that bind to DNA in a fundamentally different manner than cisplatin in an attempt to overcome the resistance pathways that have evolved to eliminate the drug. These complexes may provide a broader spectrum of antitumor activity⁽⁸⁾.

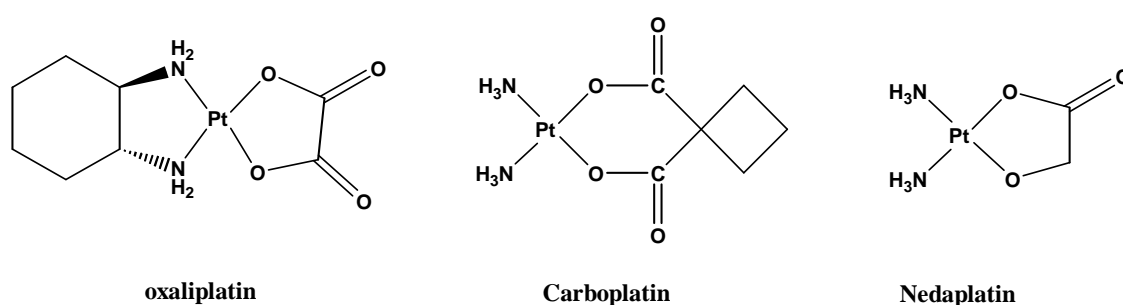


Figure (1-3): Platinum (II) complexes in worldwide clinical use, oxaliplatin (left), carboplatin (middle) and Nedaplatin (right)⁽¹⁰⁾.

1-3-2 Palladium Complexes:

Pd (II) complexes are usually isostructural with those of Pt (II). However, substitution reactions are much more rapid than those of Pt (II) (ca $\times 10^4 - 10^5$ times) and so, with some exceptions, they tend to undergo side reactions before reaching the DNA target⁽⁷⁾.

Following the discovery of Cisplatin, metal complexes, derived from a range of metals, have been shown to have anticancer activity. Metal complexes of gold, iron, ruthenium, rhodium, iridium, palladium, and tin have shown some promising antitumor activity but have not yet been introduced into clinical trials. These metal complexes, along with many others, have been screened in either *in vitro* studies or *in vivo* studies Figure (1-4)⁽¹¹⁾.

Periodic Table of Elements

1											18						
1 H	2											13	14	15	16	17	2 He
3 Li	4 Be											5 B	6 C	7 N	8 O	9 F	10 Ne
11 Na	12 Mg	3	4	5	6	7	8	9	10	11	12	13 Al	14 Si	15 P	16 S	17 Cl	18 Ar
19 K	20 Ca	21 Sc	22 Ti	23 V	24 Cr	25 Mn	26 Fe	27 Co	28 Ni	29 Cu	30 Zn	31 Ga	32 Ge	33 As	34 Se	35 Br	36 Kr
37 Rb	38 Sr	39 Y	40 Zr	41 Nb	42 Mo	43 Tc	44 Ru	45 Rh	46 Pd	47 Ag	48 Cd	49 In	50 Sn	51 Sb	52 Te	53 I	54 Xe
55 Cs	56 Ba	57 La	72 Hf	73 Ta	74 W	75 Re	76 Os	77 Ir	78 Pt	79 Au	80 Hg	81 Tl	82 Pb	83 Bi	84 Po	85 At	86 Rn

Magenta: Complexes of these metals have entered clinical trials for their antitumor activity

Red: Complexes of these metals show antitumor activity *in vitro* or/and *in vivo*

Green: Metallocene complexes of these metals show sporadic antitumor activity *in vivo*

Blue: Metallocene complexes of these metals show no antitumor activity *in vivo*

* Cisplatin is widely used in chemotherapy treatments

Figure (1-4): Periodic table of elements showing metals derived from active antitumour complexes⁽¹¹⁾.

1-3-3 Gold Complexes:

Metallic gold is quite inert, not reacting with oxygen or sulfur at any temperature; for this reason, it is considered to be the most noble of all the metals. It has the lowest oxidation potential of any metal; therefore, the preparation of positive oxidation state gold complexes requires a relatively strong oxidizing agent (*e.g.* Fe (III)) and a good ligand for gold (*e.g.* Cl⁻).

Despite the low reactivity of metallic gold, a large number of gold complexes have been successfully prepared⁽¹²⁾.

1-3-3-1 History of Gold as a Therapeutic Agent:

The earliest recorded medicinal use of gold was by the Chinese around 2500 BC.

In 1890, Robert Koch reported that potassium aurocyanide, $\text{KAu}(\text{CN})_2$, inhibited the growth of *Tubercle bacilli*, the organism responsible for tuberculosis, which at that time was also known as the 'white plague'. This gave a biological basis for gold treatment and stimulated many studies⁽¹²⁾.

Potassium aurocyanide was too toxic for clinical use, which is not surprising for a compound of cyanide, but over the next thirty years, several gold(I) thiolates were introduced for the treatment of tuberculosis; the period from 1925-1935 has been called the "gold decade" in tuberculosis treatment. In the late 1920s, Dr.K.Landé and Dr.J.Forestier, because of a belief that rheumatoid arthritis is a chronic infectious disease like tuberculosis, independently introduced gold(I) complexes for the treatment of arthritis⁽¹²⁾.

Recently new gold containing drugs have been prepared and tested as antineoplastic agents.

A series of square planer gold (III) complexes have been synthesized by Calamai *et. al.*, all containing at least two gold chloride bonds in cis position and tested their activity *in vitro* cytotoxicity on a panel of established human tumor cell line⁽¹³⁾.

1-3-3-2 Gold (III):

This is a very common and relatively stable oxidation state for gold. Gold (III) complexes are diamagnetic and most have 4- coordinate square – planar stereo chemistry with a low spin $5d^8$ electron configurations. The most common example of a gold (III) complex, $[\text{AuCl}_4]^-$, is easily prepared by dissolving gold metal in aqua regia, and is the precursor of most other gold complexes.

Five coordinate gold (III) complexes are rare but when they are found, they have a square pyramidal or a distorted square pyramidal geometry. The neutral AuF_3 is rare examples of gold (III) compound in which the gold atoms are 6- coordinate in its crystal structure⁽¹²⁾. There are two criteria which can be followed to stabilized Au (III) complexes these are (i) the ligand should have more than one donor atom (multidentate) and (ii) contain two nitrogen atoms. These two criteria were previously reported to enhance the stability of Au (III) complexes under physiological conditions⁽⁸⁾.

1-3-3-3 Overview of Gold Drugs:

The chemical formulae of a number of gold thiol complexes, which are presently being used or have been used for medicinal purposes, are shown in Figure (1-5). Each of these are gold (I) thiol complexes, with the exception of aurothioglucose, for which the commonly represented stoichiometry indicates a +III oxidation state for gold, though, it is not well characterized⁽¹²⁾.

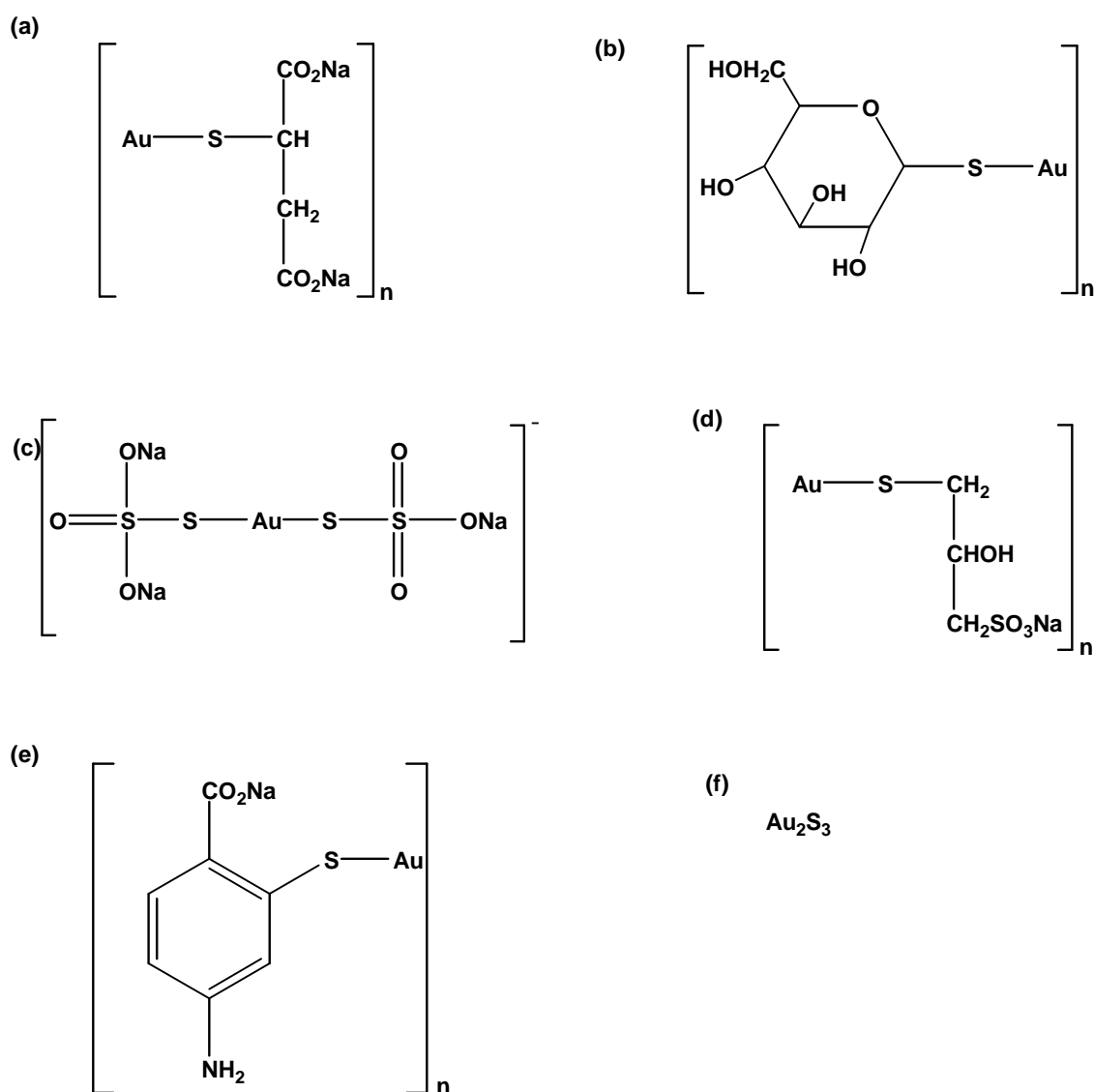


Figure (1-5):Some representative gold (I) thiol complexes of medicinal interest: (a) gold sodium thiomalate (GST;Myochryesine; Marketed in Britain, the united states (USA) and Canada) ; (b) gold B-D thioglucose (Solganal;marketed in the USA) ; (C) gold sodium thiosulfate (Sanochryesine; marketed in Europe) ; (d) gold Sodium 3- thio –2- propanol –1-Sulfonate (Allochryesine; Marketed in Europe) ; (e) gold Sodium 4- amino –2- Mercapto benzoate (Krysolgan; not currently used in medicine) ; (F) gold sulfide (AuroI Sulfide; not currently used in medicine)⁽¹²⁾.

Messori *et.al.*⁽¹⁴⁾ and Buckley *et.al.*⁽¹⁵⁾ used en,dien and damp as multidentate nitrogen-containing ligands to prepare gold (III) complex, which were found to be active against human cancer cell lines. Also a recent *in vitro* cytotoxicity study demonstrated promising activity of two gold(III) complexes with bipyridyl ligands, (dihydroxy(2,2'-

bipyridyl)gold(III)ion)[Au(bipy)-(OH)₂]PF₆ and [Au(bipy-H)(OH)]PF₆ Figure (1-6) and (1-7)⁽¹⁶⁾.

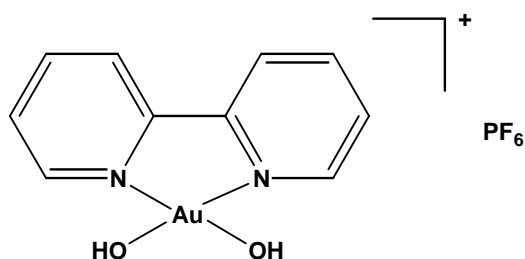


Figure (1-6): The structure of (dihydroxy(2,2'-bipyridyl) gold (III) ion) [Au(bipy)(OH)₂]PF₆⁽¹⁶⁾.

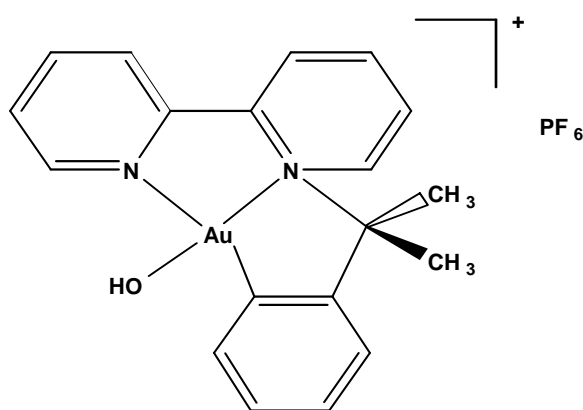


Figure (1-7): The structure of [Au(bipy-H)(OH)]PF₆⁽¹⁶⁾.

1-3-3-4 In Vivo Chemistry of Gold Drugs

Metabolism of Gold Complexes

Most pharmacological gold studies have been conducted with Myochrysine (Fig 1.5-a); however, because all of the gold drugs have many common effects, common metabolites may mediate their *in vivo* chemistry⁽¹³⁾.

Myochrysine is absorbed quickly after its intramuscular injection and maximal plasma gold levels are attained after 2 hours. Peak plasma concentrations of gold during long-term treatment with Myochrysine vary greatly between patients but are approximately 5 mg/L at 50 mg/week of the drug. Most of the circulating gold is bound to plasma proteins, with the highest concentrations in the albumin fraction. The major plasma species is

thought to have the general formula albumin –S-Au-thiol, where the thiol is an endogenous compound such as glutathione or cysteine. Gold accumulates in the liver, spleen and kidneys and the inflamed joints of arthritic patient contain more than twice as much gold as healthy joints. It was assumed that *in vivo* gold remains in the Au (I) state; however, recent work provides evidence that oxidation to Au (III) is also possible. Elimination of gold from the body occurs mainly by urinary and faecal excretion and elimination rates vary greatly between patients⁽¹²⁾.

1-3-3-5 Mechanism of Action⁽¹²⁾:

Since rheumatoid arthritis is an inflammatory disease, some of the cells involved in the disease pathogenesis are lymphocytes, macrophages, plasma cells, leucocytes and platelets. Many studies have shown that gold complexes interact with these cells both *in vitro* and *in vivo*.

A proposed theory known as the “aurocyanide hypothesis”. According to the aurocyanide hypothesis, the cellular effects of the gold drugs is that cyanide, produced by activated polymorphonuclear leucocytes, reacts with the complexes to produce aurocyanide, $[\text{Au}(\text{CN})_2]^-$, which has been shown to inhibit the oxidative burst of polymorphonuclear leucocytes and thus may slow the progression of rheumatoid arthritis .

Aurocyanide has also been shown to be the probable agent responsible for the uptake of gold by red blood cells and this is consistent with the significant increase of the level of gold in the red blood cells of smokers. That aurocyanide is a common metabolite of different gold drugs was confirmed and evidence for a “sulfhydryl shuttle” mechanism for uptake of aurocyanide by red blood cells was recently presented. A crystal structure of an aurocyanide complex with human carbonic anhydrase I enzyme reported and it lends support to the possibility of aurocyanide acting as an enzyme inhibitor.

1-3-4 Copper Complexes:

1-3-4-1 Biochemistry of Copper:

The most common complexes in the human body are that of copper, its ratio is about 2.1-4mg/Kg of body weight. It is important because all the tissues need it in the ordinary metabolic process. Copper is stored inside the liver and released in the form of complex of proteins called (ceruloplasmin)⁽¹⁷⁾.

Copper is the important key for the making of the metalloenzymes that contribute to melanin formation and very important in the process of hemopiosis and maintains the structure of the vessels, arteries and muscles. Copper plays an important role in the action of nervous system⁽¹⁷⁾.

Tranexamic acid (Trans-4-aminomethylcyclohexane carboxylic acid-C₈H₁₅NO₂) is the drevitive of amino acid lysine. This drug inhibits the proteolytic activity of plasmin and the conversion of plasminogen to plasmin by plasminogen activators. It is used for its antiplasminic, hemostatic, antiallergic and anti-inflammatory activities⁽¹⁸⁾.

1-3-4-2 Copper Anticancer Agents:

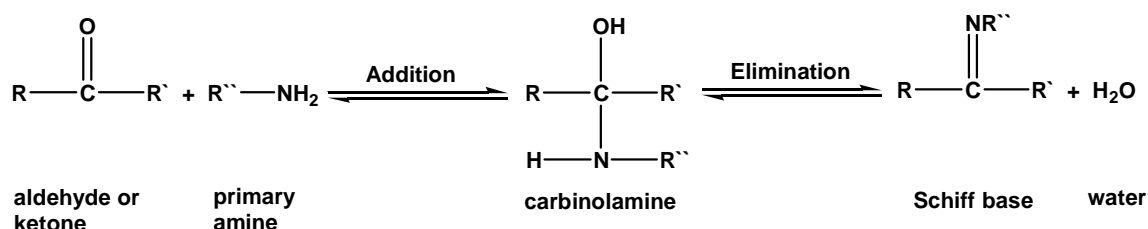
The literature which deal with the copper-containing chemotherapeutic agents are very rare, later a number of studies have been reported which show the potency of various copper complexes as antineoplastic agents. Arena *et.al.* investigated the cytotoxicity of some copper (II) compounds against the mouse cancer cell line, Murine, human KB cells, and fibroblasts. All the studied copper (II) systems tested were shown to have pronounced toxicity against transformed cells and a cytostatic effects against untransformed cells, i.e, human fibroblasts, they found also, that *in vitro* condition copper (II) is essentially present as mixed complexes formed with the amino acids of the culture medium, [cu (glutamine)(histidine)] being the main species. It was found that the cytotoxic activity is related to the amount of copper (II) contained in the tested compounds⁽¹⁹⁾.

1-4 Schiff Bases:

During the past two decades, considerable attention has been paid to the chemistry of the metal complexes of SB containing nitrogen and other donors. This may be attributed to their stability, biological activity and potential application in many fields such as oxidation catalysis, electrochemistry, etc⁽²⁰⁾.

The term "Schiff bases" (SB) was firstly used to define those organic compounds which contain the functional group -C=N- , these Schiff bases have several names: Anils, Imines, Azomethines, Benzanils, and benzylideneaniline. Schiff bases were firstly prepared by Schiff in 1864, from simple condensation reaction of aldehyde or ketones with primary amines and for this reason; these imines were called "Schiff bases".

In the first stage of the reaction the amine added to the carbonyl group to give a species known as carbinolamine. Once formed the carbinolamine undergoes dehydration to yield the product of the reaction, an N-alkyl-or-N-aryl substituted Schiff base (imine) as illustrated by the following scheme^(19,21).



Scheme (1-1): General preparation steps for the preparation of Schiff bases ⁽²¹⁾.

Later years have witnessed a great deal of interest in the synthesis and characterization of transition metal complexes containing SB as a ligand, due to their important as catalysts for many reactions. Staab prepared SB by removing water which is formed by condensation of aldehyde with the amine by refluxing it in benzene and then residual solution is distilled under vacuum⁽¹⁹⁾.

Kuhn also prepared SB, which are derived from ketones and primary amines, through preparation of silver iodide complexes from these bases with a few changes. Also these bases can be prepared by reflux of equimolar quantities of aldehyde or ketones with amine or by slow melting for 10 min and then isolation and purifying the product by recrystallization, or sublimation under reduced pressure⁽¹⁹⁾.

Pokhariyal and Sharma⁽²²⁾ prepared complexes of Rh (III) and Pt (IV) with the SB, N-4-methylphenacylidene anthranilic acid (MPAA) and N-4-methylphenacylidene-o-amino-phenol (MPAP) have been isolated and assigned octahedral structures on the basis of analytical, magnetic susceptibility, electronic and ir spectral data. Electronic spectral studies indicated that the ligand field bands observed for Rh (III) complexes were analogous to those observed in Pt (IV) complexes.

The imino nitrogen atom in monodentate SB is coordinated to metal ion. Also bidentate SB have been among those that are extensively used in preparing metal complexes; these ligands are described according to their donor set, e.g. N, N-donor Schiff bases and N, O-donor Schiff bases.

Tridentate SB may be generally considered as derived from the bidentate analogues by adding another donor group. These have been utilized as anionic ligands having (N, N, O)⁽²³⁻²⁵⁾, (N, O, O)⁽²⁶⁻²⁸⁾, (N, N, S)⁽²³⁾ and (N, S, O)⁽²⁹⁾ donor sets.

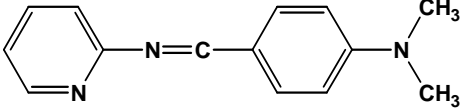
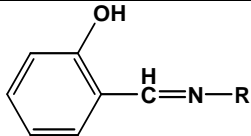

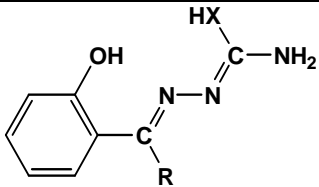
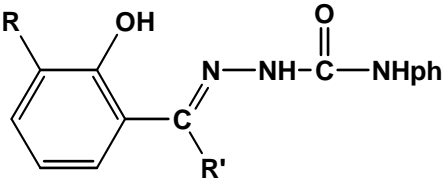
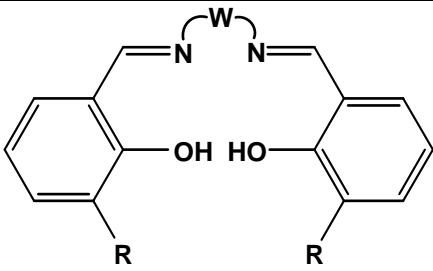
Tetradentate SB with a N₂O₂ donor atom set is well known to coordinate with various metal ions, and this has attracted many authors. Complexes of SB ligands have been studied for their dioxygen uptake and oxidative catalysis. Also complexes of transition metals (II), which involve derivatives of salicylaldehyde and diamine, have gotten considerable attention⁽³⁰⁻³³⁾.

1-4-1 Schiff bases as Ligands in Biologically Important Complexes:

SB and metal complexes have received a great deal of attention during the last years to prepare new sets of these bases and their transition metal complexes. These complexes have proven to be antitumor and have carcinostatic activity⁽³⁴⁾. Many metal complexes have been prepared that contain SB, in their structure because of their efficiency against cancer, like leukemia⁽³⁵⁾.

The biological activity of SB is attributed to the formation of stable chelates with transition metals presents in cell; they are known to exhibit a wide variety of pharmacological properties⁽³⁶⁻³⁸⁾. Such as anti-inflammatory, antimalarial, antithelamentic, antiviral, antifungal, Table (1-1)⁽²¹⁾.

Table (1-1): Some types of schiff bases and their biological activities⁽²¹⁾

No.	Structure of Schiff base	Donor atoms	Donor type	Biological Activity
1		N	Monodentate	Antifungal
2	 <p>R = ph, 2-MeC₆H₄, 3-C₆H₄ 4-MeC₆H₄</p>		Bidentate	Antifungal
3	 <p>R = H, H, Me, Me X = S, O, S, O</p>	ONS/ONN	Tridentate	Antibacterial
4	 <p>R = H, H, OCH₃ R' = H, CH₃, H</p>	ONO	Tridentate	Antibacterial
5	 <p>R = H, OMe W = (CH₂)₂, (CHMeCH₂), (CH₂)₄</p>	ONNO	Quadridentate	Antifungal

1-5 Glutathione:

Living cells defend themselves from toxicants/xenobiotics present in the environment through biotransformation of these compounds to relatively non-toxic metabolites and their subsequent elimination through transport mechanisms⁽³⁹⁾.

Glutathione and its S-transferase enzyme (GSTs) play a central role in the detoxification of exogenous as well as the endogenous electrophiles which can alkylate cellular DNA and proteins leading to cellular dysfunction and toxicity⁽³⁹⁾.

1-5-1 Structure and Function of Glutathione:

Glutathione (GSH, γ -glutamylcysteinylglycine) is the major intracellular low-molecular weight sulfhydryl compound in animals, plants and in most microorganisms⁽⁴⁰⁾.

Glutathione exists in the thiol-reduced (GSH) and disulfideoxidized (GSSG) forms Figure (1-8)⁽⁴¹⁾. Eukaryotic cells have three major reservoirs of GSH. Almost 90% of cellular GSH are in the cytosol, 10% in the mitochondria, and a small percentage in the endoplasmic reticulum. In the endoplasmic reticulum, where GSH is implicated in protein disulfide bond formation, the GSH to GSSG ratio is 3:1. In the cytoplasm and mitochondria, ratios exceed 10:1. Cytosolic GSH in the rat liver turns over rapidly with a half-life of 2–3 h⁽⁴⁰⁾.

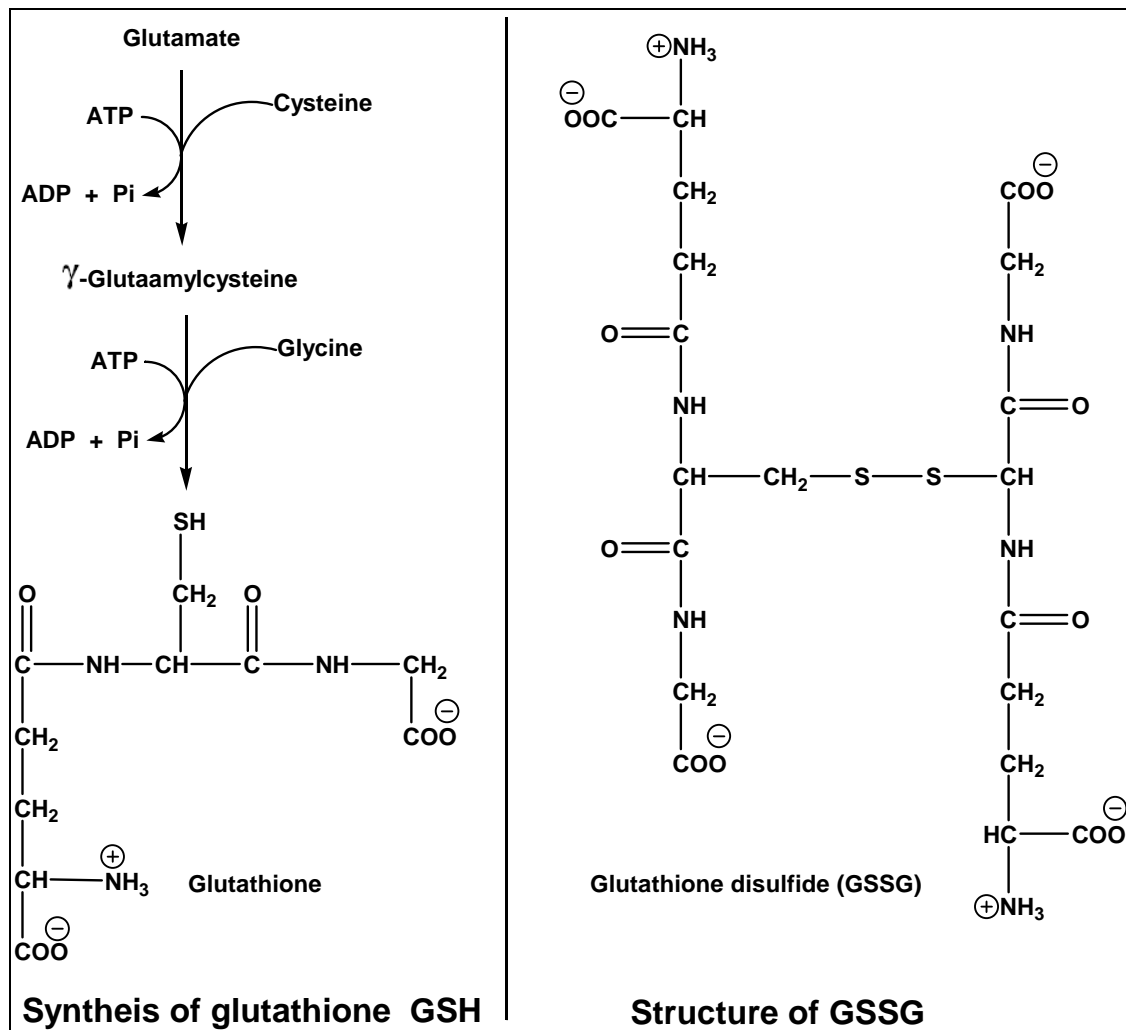


Figure (1-8): Glutathione synthesis and forms ⁽⁴¹⁾.

The γ -glutamyl linkage promotes intracellular stability and the sulfhydryl group is required for GSH's functions Figure (1-9). The peptide bond linking the amino-terminal glutamate and the cysteine residue of GSH is through the γ -carboxyl group of glutamate rather than the conventional α -carboxyl group. This unusual arrangement resists degradation by intracellular peptidases and is subject to hydrolysis by only one known enzyme, γ -glutamyltranspeptidase (GGT), which is on the external surfaces of certain cell types. Furthermore, the carboxyl-terminal glycine moiety of GSH protects the molecule against cleavage by intracellular γ -glutamylcyclotransferase. As a consequence, GSH resists intracellular degradation and is only metabolized extracellularly⁽⁴⁰⁾.

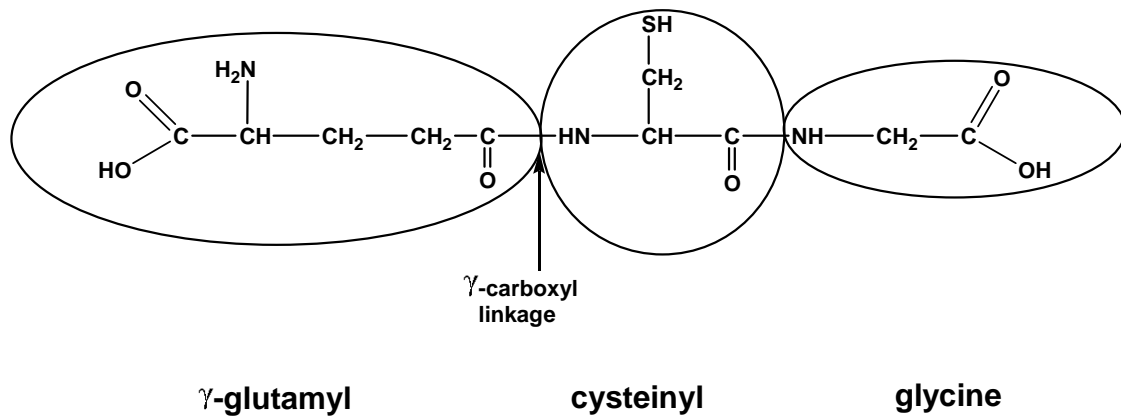


Figure (1-9): The structure of glutathione, γ -glutamylcysteinylglycine. The amino-terminal glutamate and cysteine are linked by the γ -carboxyl group of glutamate⁽⁴⁰⁾.

The key functional element of the GSH molecule is the cysteinyl moiety, which provides the reactive thiol group and is responsible for the many functions of GSH⁽⁴²⁾, including

- 1) Detoxifying electrophiles.
- 2) Maintaining the essential thiol status of proteins by preventing oxidation of -SH groups or by reducing disulfide bonds induced by oxidant stress.
- 3) Scavenging free radicals;
- 4) Providing a reservoir for cysteine.
- 5) Modulating critical cellular processes such as DNA synthesis.

GSH binds endogenous metals, such as copper, selenium, chromium, and zinc, via nonenzymatic reactions. It also forms metal complexes via nonenzymatic reactions. GSH is one of the most versatile and pervasive metal binding ligands and plays an important role in metal transport, storage, and metabolism. as⁽⁴²⁾.

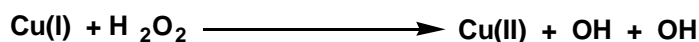
- (a) In the mobilization and delivery of metals between ligands,
- (b) In the transport of metal across cell membranes,
- (c) As a source of cysteine for metal binding,
- (d) as a reductant or cofactor in redox reactions involving metals.

1-5-2 Examples of Detoxifying Functions of GSH:

GSH plays a major role in detoxifying many reactive metabolites by either spontaneous conjugation or by a reaction catalyzed by the GSH S-transferases⁽⁴³⁾. GSH S-transferases have broad and overlapping substrate specificities, which allow them to participate in the detoxification of a chemically diverse group of compounds. The most common reactions involve nucleophilic attack by GSH on an electrophilic carbon: saturated carbon atoms (e.g., alkyl halides, lactones and epoxides), unsaturated carbon atoms (e.g., α,β -unsaturated compounds, quinones and quinonimines, and esters), or aromatic carbon atoms (e.g., aryl halides and aryl nitro compounds). The substrates have in common a degree of hydrophobicity and possess electrophilic centers that undergo nucleophilic substitution, nucleophilic addition to α,β -unsaturated ketones or epoxides or, in the case of hydroperoxides, nucleophilic attack on electrophilic oxygen, resulting in reduction⁽⁴⁰⁾.

Detoxification of xenobiotics or their metabolites is one of the major functions of GSH. These compounds are electrophiles and form conjugates with GSH either spontaneously or enzymatically in reactions catalyzed by GSH S-transferase. The conjugates formed are usually excreted from the cell and, in the case of hepatocytes, into bile. The metabolism of GSH conjugates begins with cleavage of the γ -glutamyl moiety by GGT, leaving a cysteinyl-glycine conjugate. The cysteinyl-glycine bond is cleaved by dipeptidase, resulting in a cysteinyl conjugate. This is followed by N-acetylation of the cysteine conjugate, forming a mercapturic acid Figure (1-10). The metabolism of GSH conjugates to mercapturic acid begins either in the biliary tree, intestine, or kidney, but the formation of the N-acetylcysteine conjugate usually occurs in the kidney. In addition to exogenous compounds, many endogenously formed compounds also follow similar metabolic pathways. Some examples include estradiol-17-b, leukotrienes, and prostaglandins. Although the majority of the conjugation

The interaction between H_2O_2 and Cu can potentially result in generation of the highly toxic $\text{OH}^{(50)}$.



1-5-3 Glutathione Depletion:

Glutathione depletion has been associated with an increased risk of chemical toxicity. Because GSH can be depleted by different agents, combinations of compounds in chemical mixtures are likely to enhance risk over that seen with individual chemicals⁽⁵¹⁾. Erythrocyte glutathione (GSH) can be rapidly depleted by incubating the cells with 1-chloro-2, 4-dinitrobenzene (CDNB), which forms 2, 4-dinitrophenyl-S-glutathione with GSH through the reaction catalyzed by glutathione S-transferase. GSH-CDNB conjugate thus formed stays undegraded within the erythrocytes. This indicates that in the erythrocytes, mercapturic pathway is inoperative. Depletion of GSH in the intact erythrocytes by CDNB results in rapid oxidation of large amounts of hemoglobin to methemoglobin. When glutathione S-transferase-free hemolysate of erythrocytes is incubated with CDNB, the depletion of GSH as well as methemoglobin formation a minimal. Glutathione peroxidase and glutathione reductase activities of the erythrocytes are not affected by CDNB. These studies provide a specific enzymatic method for rapid removal of erythrocyte GSH and also indicate that GSH is vital in maintaining a reduced environment within the erythrocytes⁽⁴⁷⁾.

1-6 Glutathione S-Transferases:

The environmental pollutants are highly mutagenic and carcinogenic⁽⁵²⁾. These xenobiotic pollutants induce, phase II detoxification enzymes, which protect animals and their cells against the toxic and neoplastic effects of the carcinogens, electrophiles and products of oxidative stress. The most important phase II detoxification pathway is Glutathione S-transferases⁽⁵²⁾.

The Glutathione S-transferases (EC 2.5.1.18) (GSTs), are a family of enzymes that play an important role in detoxification by catalyzing the conjugation of many hydrophobic and electrophilic compounds with reduced glutathione⁽⁵³⁻⁵⁵⁾.

The glutathione transferases are normally present in large quantities, representing about 10% of the extractable protein of rat liver but can be induced to greater than 20%. Most of the research has been carried out with enzymes from rat and human liver. But human erythrocytes and placenta, as well as sheep and mouse liver have also been sources for homogenous preparations. The enzymes have been found in all mammalian tissue tested as well as in insects, protozoa, algae, fungi, and bacteria⁽⁵⁶⁾.

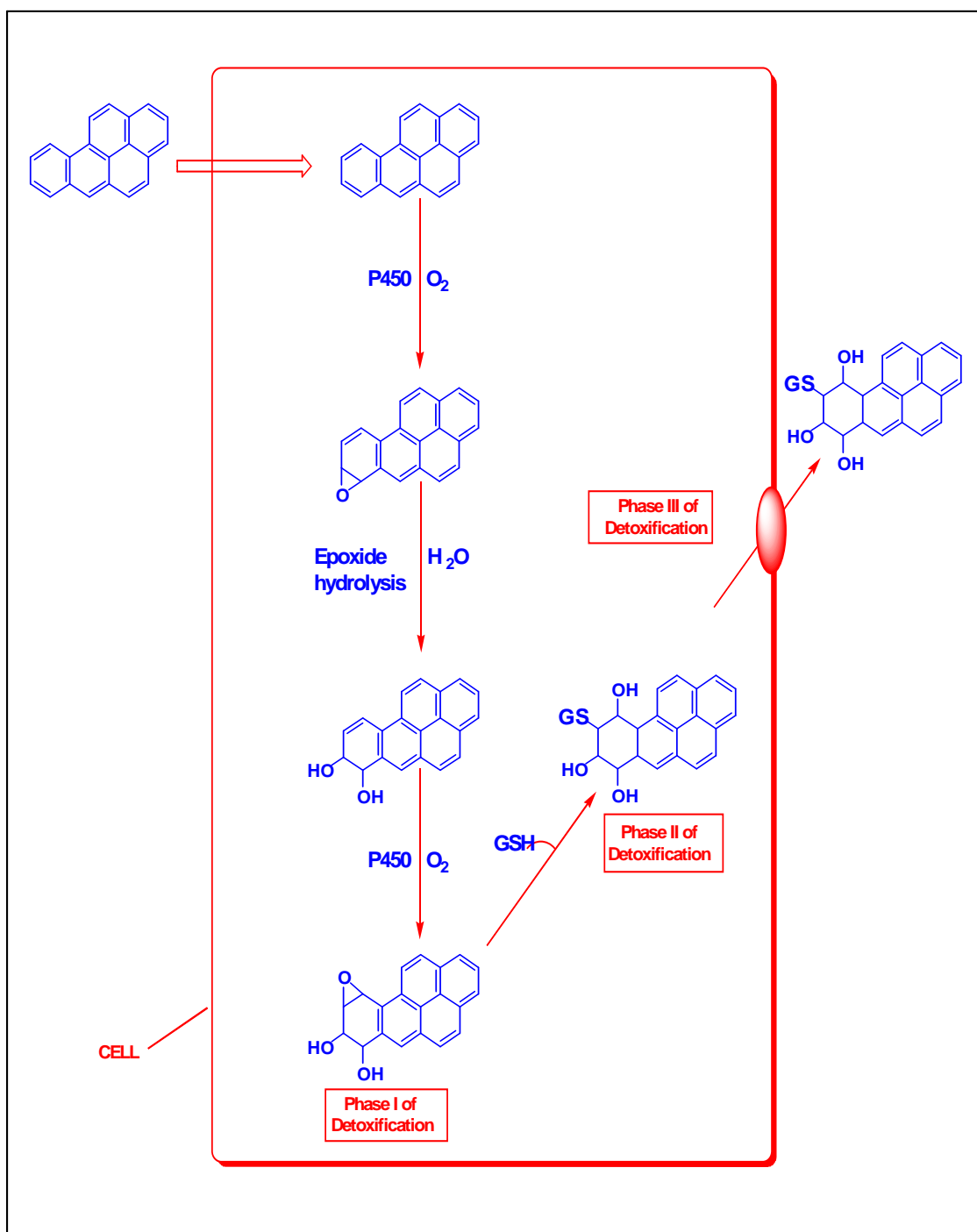
1-6-1 Role of GSTs in Enzymic Detoxification:

Biotransformation is an important biochemical protection mechanism against toxic chemical species. Cells possess an impressive array of enzymes capable of biotransforming a wide range of different chemical structures and functionalities. The enzymic detoxification of xenobiotics has been classified into three distinct phases which act in a tightly integrated manner⁽⁵⁷⁾.

Phases I and II involve the conversion of a lipophilic, non-polar xenobiotic into a more water-soluble and therefore less toxic metabolite, which can then be eliminated more easily from the cell (phase III; Scheme 1-2). Phase I is catalysed mainly by the cytochrome P450 system⁽⁵⁷⁾.

This family of microsomal proteins is responsible for a range of reactions, of which oxidation appears to be the most important. Phase II enzymes catalyse the conjugation of activated xenobiotics to an endogenous water-soluble substrate, such as reduced glutathione (GSH), UDP-glucuronic acid or glycine⁽⁵⁷⁾.

Quantitatively, conjugation to GSH, which is catalysed by the GSTs, is the major phase II reaction in many species. GSTs can catalyse nucleophilic aromatic substitutions, Michael additions to a unsaturated ketones and epoxide ring-opening reactions, all of which result in the formation of GSH conjugates and the reduction of hydroperoxides, resulting in the formation of oxidized glutathione (GSSG)^(57,58).



Scheme (1-2): Overview of enzymatic detoxification ⁽⁵⁷⁾.

GSTs are dimeric, mainly cytosolic, enzymes that have extensive ligand binding properties in addition to their catalytic role in detoxification⁽⁵⁹⁾. They have also been implicated in a variety of resistance phenomena involving cancer chemotherapy agents⁽⁶⁰⁾, insecticides⁽⁵⁷⁾, herbicides⁽⁵⁷⁾ and microbial Antibiotics⁽⁵⁷⁾. A separate microsomal class of GSTs exists which is quite distinct from the cytosolic enzymes, and is designated as membrane-associated proteins in eicosanoid and glutathione' metabolism (MAPEG)⁽⁵⁷⁾.

1-6-2 Classification of GSTs:

The GSTs comprise a complex and widespread enzyme superfamily that has been subdivided further into an ever-increasing number of classes based on a variety of criteria, including amino acid, nucleotide sequence, and immunological, kinetic and tertiary quaternary structural properties⁽⁵⁷⁾.

Most of the well characterized liver GSTs can be grouped into five classes of soluble proteins termed Alpha, Mu, Pi, Theta and Sigma. Two additional classes of soluble GSTs with unusual enzymic activities, Omega and Zeta, were described recently in a variety of organisms, including mammals^(61,62). Table 1-2 summarized some useful classification of GSTs⁽⁵⁷⁾.

Table (1-2): Some useful classification criteria for GSTs⁽⁵⁷⁾.

Criteria	Example
Primary structure comparisons	Alpha/Mu/Pi classes Theta class Kappa class Zeta class Omega class
Immunoblotting	Alpha/Mu MIF Insect classes I and II <i>Fasciola hepatica</i>
Kinetic properties Substrate specificity/affinity	Alpha/Mu/Pi Mu Theta
Inhibitor sensitivity Tertiary structure: active site	Alpha/Mu/Pi Alpha/Mu/Pi Theta Omega Beta Sigma
Quaternary structure Ability to hybridize into dimers Inter-subunit interface	Mu/Alpha Hydrophobic lock and key in Alpha/Mu/Pi/Theta classes Polar interface in Beta class

All four glutathione transferases have a molecular weight of 45,000 Dalton and are dissociable into subunits of approximately 25,000 Daltons⁽⁶³⁾.

1-6-3 Crystal Structure of GSTs:

The cytosolic GSTs, in general contain two binding sites-a GSH binding site (G site) and a second substrate-binding site (H site) (Figure 1-11). Each subunit comprises the following two domains⁽⁵²⁾:

1. The smaller N-terminal α/β helices, domain I, which includes residues 1-78 of α and θ class, 1-82 of class μ , 1-74 of class π and σ . Most of the amino acids form the G site;

2. The large α helix, domain II, includes residues 86-222 of class α , 90-217 of class μ , 81-207 of class π , 81-202 of class σ and 85-208 of class θ . Most of these amino acids form the H site. The H-site is specific for each subunit, whereas the G-site may be common to all GST subunits. The substrate specificity of GST isozymes was determined by a number of residues in the H-site. The association between two subunits will generate an intrasubunit binding site for ligands, which enables a GSH-conjugate formed by one subunit to be sequestered by the adjacent subunit and thereby limiting the product inhibition^(52, 64).

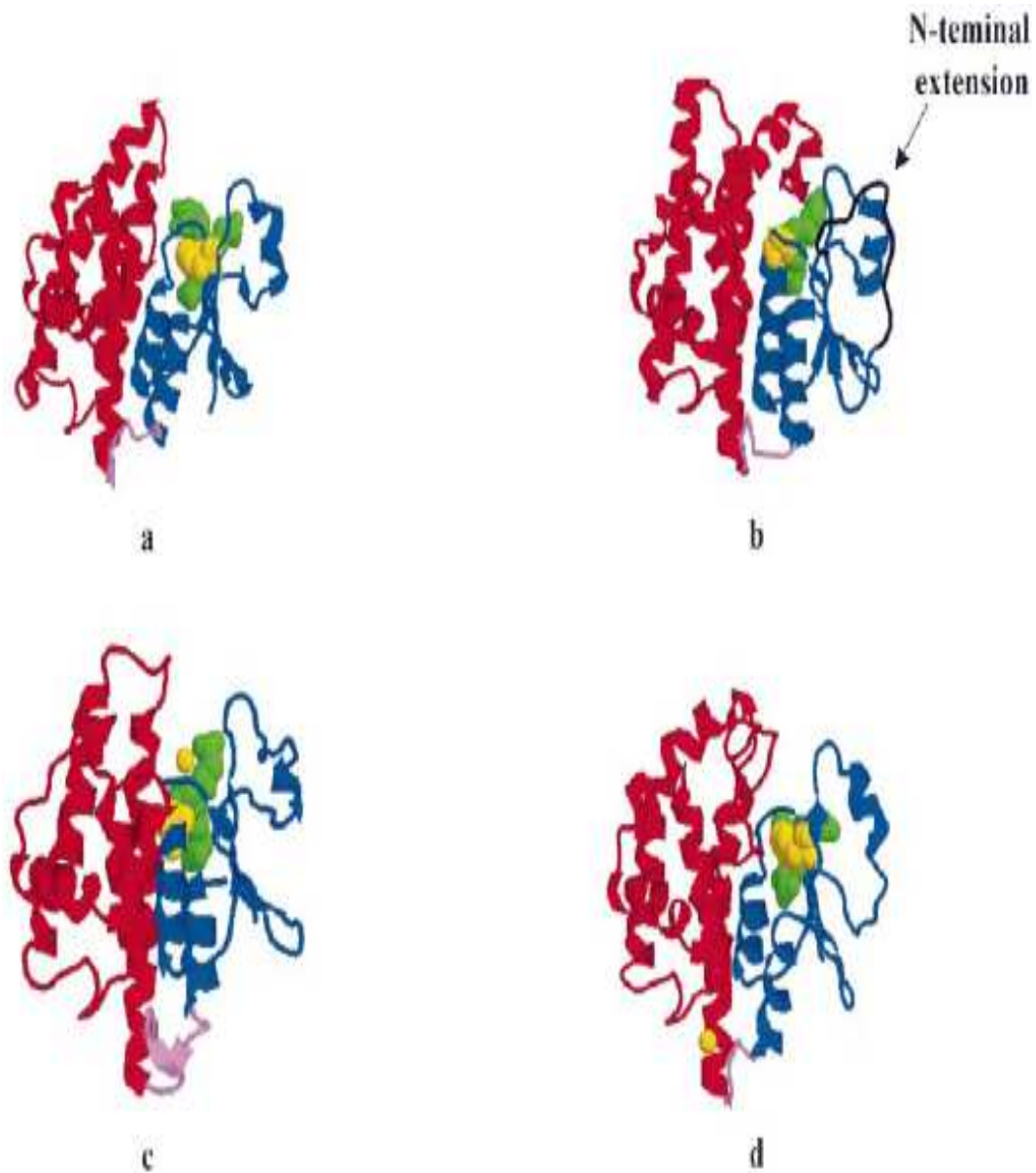


Figure (1-11): Domain structures of GST subunits

Three-dimensional structures of individual GST subunits are shown. The N-terminal domain 1 is coloured blue, while the C-terminal domain 2 is red. Catalytically essential residues (tyrosine in *a* and *d*; cysteine in *b* and *c*) are coloured yellow and presented in space-filling mode, while ligands with which the protein was co-crystallized are shown in green. Linker strands connecting the two domains are shown in violet.

Aim of the Work

Because of the importance of Schiff bases and their derivatives in life, and to study the synergetic effect of metal ions on the biological activity Schiff bases, the research goals are:

1. Preparing new metal complexes using three different Schiff bases with biologically important transition elements Pt(IV), Au(III), Pd(II) and Cu(II).
2. Characterization of these new ligands and their new complexes using standard techniques which include elemental analysis, Infrared and Ultraviolet-Visible Spectrophotometry, Conductivity and magnetic measurements, also measuring their melting points.
3. Isolation and purification of Glutathione S-transferase (GSTs) from rat liver.
4. Studying the reactivity of the prepared complexes toward GSH to estimate their efficiency as substrates to GSTs enzyme by studying the interaction of GSH with the prepared complexes in presence and absence of the enzyme.

Chapter three
Results and Discussion

3-1 Physical Properties of the Prepared Complexes:

The importance of preparing a new set of Schiff bases arises from their virility as starting materials for the synthesis of many complexes especially with transition metal ions due to the expected biological activity of these ligands and their complexes. Table (3-1) shows the physical data for ligands and their new complexes. The metal complexes showed higher melting points than their respective ligands.

Table (3-1):The physical data for the prepared ligands and complexes.

Comp	Colour	M.P. /°C	Yield %	Elemental analysis %			
					C	H	N
L_1	Yellow	-	89.65	-	-	-	-
L_1Pt	Orange	220	41	Cal	28.44	3.82	2.55
				Found	28.51	4.56	3.00
L_1Au	Deep Red	150-152	42	Cal	33.26	3.41	2.98
				Found	33.53	3.39	2.78
L_1Pd	Yellowish-Green	244-246	60	Cal	59.10	6.30	5.20
				Found	59.60	5.69	5.04
L_1Cu	Reddish-Brown	160	54.5	Cal	66.66	7.15	7.47
				Found	66.50	6.33	6.20
L_2	Yellow	125-127	83.54	Cal	75.48	7.08	11.00
				Found	75.44	6.66	10.78
L_2Pt	Orange	205-207	70	Cal	41.03	5.98	4.91
				Found	40.64	4.29	5.63
L_2Au	Brown	163-165	31	Cal	63.10	5.91	9.18
				Found	64.19	6.24	9.13
L_2Pd	Orange	215-217	31.44	Cal	53.30	5.54	7.75
				Found	53.83	5.00	7.58
L_2Cu	Deep Brown	>300	60	Cal	54.41	5.85	7.93
				Found	54.85	4.59	9.28
L_3	Yellow	93-95	95.31	Cal	77.88	5.40	5.04
				Found	78.15	5.21	4.92
L_3Pt	Yellow-Orange	180-182	77.56	Cal	46.56	3.66	3.02
				Found	46.37	3.66	3.49
L_3Au	Red	200-202	30	Cal	48.39	3.73	3.07
				Found	48.00	3.28	2.97
L_3Pd	Yellow	193-195	89.13	Cal	66.02	4.58	4.23
				Found	65.75	4.45	2.32
L_3Cu	Brown	230-232	52	Cal	69.93	4.53	4.53
				Found	69.38	4.47	4.60

Table (3-2): Descriptions of Symbols, Molecular formula and Names of the prepared ligands and complexes.

Symbol	Molecular formula	Name
L ₁	C ₁₃ H ₁₇ NO	2-[(cyclohexylimino)methyl] phenol.
L ₁ Pt	[PtL ₁ Cl ₄]	[Tetra chloro(2-[(cyclohexylimino)methyl] phenolate) Platinum(IV)].
L ₁ Au	[AuL ₁ Cl ₂]	[Dichloro(2-[(cyclohexylimino)methyl] phenolate) Gold(III)].
L ₁ Pd	[Pd(L ₁) ₂].H ₂ O	[Bis(2-[(cyclohexylimino)methyl] phenolate) Palladium(II)]. Water(1).
L ₁ Cu	[Cu ₂ (L ₁) ₈ (ONO ₂) ₂]	[Bis-μ-(2-[(cyclohexylimino)methyl]phenolate).Bis[nitratotri(2-[(cyclohexylimino)methyl] phenol)] copper(II)].
L ₂	C ₁₆ H ₁₈ N ₂ O	N-[4-(diethylamino)benzylidene]-N-(4-methoxyphenyl)amine.
L ₂ Pt	[Pt ₂ (L ₂) ₄ Cl ₆].Cl ₂ .10H ₂ O	[Bis-μ-Chloro.Bis[dichlorodi(N-[4-(diethylamino)benzylidene]-N-(4-methoxyphenyl)amine)] platinum(IV)].chloride.water(10)
L ₂ Au	[Au(L ₂) ₆]Cl ₃	[Hexakis(N-[4-(diethylamino)benzylidene]-N-(4-methoxyphenyl)amine)Gold(III)].Chloride.
L ₂ Pd	[Pd ₂ (L ₂) ₄ (H ₂ O) ₂ Cl ₄].2H ₂ O	[Bis-μ-Chloro.Bis[chloro hydro di(N-[4-(diethylamino)benzylidene]-N-(4-methoxyphenyl)amine)] Palladium(II)]. Water(2).
L ₂ Cu	[Cu (L ₂) ₃ (H ₂ O) ₂ (ONO ₂)]NO ₃	[Nitratodihydrotri(N-[4-(diethylamino)benzylidene]-N-(4-methoxyphenyl)amine) Copper(II)]. Nitrate
L ₃	C ₁₈ H ₁₅ NO ₂	1-[(4-methoxyphenyl)imino)methyl]-2-naphthol.
L ₃ Pt	[Pt(L ₃) ₂ Cl ₂]Cl ₂ .2H ₂ O	[Dichlorobis(1-[(4-methoxyphenyl)imino)methyl]-2-naphthol) Platinum(IV)]. Chloride. Water(2).
L ₃ Au	[Au(L ₃) ₂]Cl ₃ .2H ₂ O	[Bis(1-[(4-methoxyphenyl)imino)methyl]-2-naphthol) Gold(III)]. Chloride. Water(2).
L ₃ Pd	[Pd ₂ (L ₃) ₆]Cl ₂ .H ₂ O	[Bis-μ-(1-[(4-methoxyphenyl)imino)methyl]-2-naphthol).Bis(di(1-[(4-methoxyphenyl)imino)methyl]-2-naphthol)Palladium(II)]. Chloride. Water(1).
L ₃ Cu	[Cu(L ₃) ₂]	[Bis(1-[(4-methoxyphenyl)imino)methyl]-2-naphthol)Copper(II)].

3-2 Infrared Spectra of the Prepared New Ligands:

All the spectra were recorded in the solid state using CsI disk in the range (4000-200) cm^{-1} .

The ligands L_1 , L_2 and L_3 have an important group; this is azomethine group ($-\overset{|}{\text{C}}=\text{N}-$). In general azomethine stretching absorption frequency occurs in the region (1690-1570) cm^{-1} depending on nature of groups linked to it^(81,82). The compounds containing azomethine group show basic behavior toward metal ions coordinating via the nitrogen atoms, this coordination shifts the stretching frequency of ($-\overset{|}{\text{C}}=\text{N}-$) group either toward higher value in some complexes⁽⁸³⁻⁸⁷⁾ or toward lower values in others⁽⁸⁸⁻⁹¹⁾. The increase in frequency may be due to the simultaneous stretching of the ($-\overset{|}{\text{C}}=\text{N}-$) bond due to an increase in both sigma overlap and electrostatic attraction which is possible on account of the coordination of the azomethine nitrogen to metal ion⁽⁸³⁾. The decrease in frequency indicates a decrease in the stretching force constant of ($-\overset{|}{\text{C}}=\text{N}-$) group as a consequence of the coordination through azomethine nitrogen. The double bond character between carbon and nitrogen is reduced⁽⁹²⁾.

3-2-1 Spectra of Ligand (L_1) and their Metal Complexes:

The FT.IR spectrum of (L_1), figure (3-1), showed the azomethine ($\overset{|}{\text{C=N}}$) stretching band at $1627 \text{ cm}^{-1(93-94)}$. The ring ν (C=C) appeared at 1496 cm^{-1} , $1454 \text{ cm}^{-1(30, 95)}$. Another set of bands were also observed at 1078 cm^{-1} for ring C-H in plane bending and at 758 cm^{-1} for out of plane C-H bending of disubstituted phenyl moiety. The phenolic (C-O) stretching vibration that appeared at 1309 cm^{-1} in the Schiff bases⁽⁹⁶⁻⁹⁷⁾ undergoes a shift towards higher frequencies by $(10-43) \text{ cm}^{-1}$ in the complexes. This shift confirms the participation of oxygen in the (C-O-M) bond⁽⁹⁸⁻⁹⁹⁾. Generally a broad band may appear in the region $2700-3100 \text{ cm}^{-1}$ due to hydrogen bonded OH group^(82, 90), in the spectrum of L_1 , Figure (3-1), the position of this band could not be assigned due to the appearance of several strong bands in this region. A medium sharp band was observed at 663 cm^{-1} assigned to the hydrogen bonded out-of the plane O-H bending vibration^(100,101). The last band has no corresponding bands in the metal chelates, except in the spectrum of Pt (IV) complex, Figure (3-2). The ν C-H of the aromatic moiety appeared around 3058 cm^{-1} in the free ligand and its metal complexes⁽¹⁰²⁾. Table (3-3) shows the most characteristic bands of (L_1).

A- Spectrum of the Platinum (IV) Complex ($L_1\text{Pt}$):

The most significant difference in the FT.IR spectra of the ligand and its Platinum complex, Figure (3-2), was the shift of ($\overset{|}{\text{C=N}}$) stretching frequency of (L_1) to a higher value due to metal-ligand coordination by $24 \text{ cm}^{-1(83-87)}$. The phenolic (C-O) frequency shifts from 1309 cm^{-1} to 1352 cm^{-1} indicates the participation of the oxygen atom in the coordination with Pt atom⁽³⁰⁾. We noticed that the band correspond to out of plane O-H bending (663 cm^{-1}) in the free ligand have a correspond band of similar intensity in the spectrum of the Pt(IV) complex, this lend as to conclude that the hydrogen of the phenol group did not ionized,

which was more indicated by the appearance of sharp band at 3190 cm^{-1} due to $\nu_{\text{O-H}}$. The proton of the O-H group is not expected to ionize during the formation of the platinum (IV) complex, since the reaction mixture was highly acidic due to the use of chloroplatinic acid (H_2PtCl_6). Furthermore, new bands have been observed around 560, 455 and 340 cm^{-1} which may be due to $\nu(\text{Pt-N})$, $\nu(\text{Pt-O})$ and $\nu(\text{Pt-Cl})^{(103)}$ respectively. Table (3-3) shows the most characteristic bands of L_1Pt .

B- Spectrum of the Gold (III) Complex (L_1Au):

The most significant difference between the F.T.IR spectrum of the ligand and the complex, Figure (3-3), was the shift of ($-\text{C}=\text{N}$) stretching frequency to lower frequency by 15 cm^{-1} due to metal-ligand coordination⁽⁹⁰⁻⁹¹⁾. The $\nu(\text{C-O})$ frequency shifts from 1309 cm^{-1} to 1328 cm^{-1} which indicates the coordination of the oxygen with the Au (III) ion. No bands were observed at 663 and 3190 cm^{-1} , which are due to out of plane O-H bending and O-H stretching vibration. This indicates the displaced the metal hydrogen. The new bands which have been observed around 565, 461 and 370 cm^{-1} were attributed to $\nu(\text{Au-N})$, $\nu(\text{Au-O})$ and $\nu(\text{Au-Cl})^{(103)}$ respectively, as shown in Table (3-3).

C- Spectrum of the Palladium (II) Complex (L_1Pd):

In the spectrum of L_1Pd , Figure (3-4), azomethine absorption frequency was shifted to 1612 cm^{-1} , indicating the coordination through azomethine nitrogen⁽⁸³⁻⁸⁸⁾. Phenolic $\nu(\text{C-O})$ frequency was shifted to 1319 cm^{-1} , this blue shift indicate the coordination through oxygen⁽⁹⁶⁻⁹⁷⁾. The two bands corresponding to O-H bending and O-H stretching frequencies disappeared in the Pd (II) spectrum. The bands at 551 and 462 cm^{-1} can be attributed to $\nu(\text{Pd-N})$, $\nu(\text{Pd-O})^{(103)}$, respectively. Table (3-3) contains the most characteristic bands of L_1Pd .

D- Spectrum of the Copper (II) Complex (L₁Cu):

In copper complex spectrum, Figure (3-5), the azomethine absorption frequency shifts to lower frequency by 15 cm⁻¹, indicates the complexation via azomethine nitrogen^(81,88). The phenolic ν (C-O) frequency was shifted from 1309 to 1323 cm⁻¹, indicating the coordination through oxygen⁽⁹⁶⁻⁹⁷⁾. New bands have been observed around 570 cm⁻¹ which is attributed to ν (Cu-N)⁽³⁰⁾, another one at 466 cm⁻¹ due to ν (Cu-O)⁽³⁰⁾. The expected NO stretching bands of the nitrate group for the monodentate symmetry (c_{2v}) could not easily assigned, since another bands absorb at the expected wave number⁽¹⁰³⁾. Table (3-3) contains the most characteristic bands of L₁Cu.

3-2-2 Spectrum of Ligand (L₂) and their Metal Complexes:

The ligand (L₂), Figure (3-6), Table (3-3), showed the azomethine stretching band at 1606 cm⁻¹⁽⁹³⁾, the ν_{as} (C-O-C) at 1238 cm⁻¹, ν_s (C-O-C) at 1031 cm⁻¹⁽⁸²⁾, another band appeared at 1359 cm⁻¹ due to ν (Ar-N) band characteristic of the tertiary aromatic amines⁽⁸²⁾.

A- Spectrum of the Platinum (IV) Complex (L₂Pt):

In the spectrum of L₂Pt complex, Figure (3-7), two bands were observed in the $\nu_{C=N}$ region, due to the splitting in this band, indicating the coordination through azomethine nitrogen⁽⁸³⁻⁸⁸⁾. Furthermore, new bands have been observed around 526 and 378 cm⁻¹ which can be attributed to ν (Pt-N) and ν (Pt-Cl) respectively. Table (3-3) contains the most characteristic bands of L₂Pt.

B- Spectrum of the Gold (III) Complex (L_2Au):

In the spectrum of L_2Au complex, Figure (3-8), two bands were observed in the $\nu_{C=N}$ region, due to the splitting in this band, indicating the coordination through azomethine nitrogen⁽⁸³⁻⁸⁸⁾. Furthermore, new band have been observed around 524 cm^{-1} due to $\nu(\text{Au-N})$ ⁽¹⁰³⁾, as shown in Table (3-3).

C- Spectrum of the Palladium (II) Complex (L_2Pd):

In palladium complex spectrum, Figure (3-9), the azomethine stretching frequency shifts from 1606 to 1585 cm^{-1} , this red shift indicates complexation via azomethine nitrogen⁽⁸⁸⁻⁸⁹⁾, which was more indicated by the splitting in this band with reduced intensity. Another group of bands appeared at $524, 343\text{ cm}^{-1}$ may be attributed to $\nu(\text{Pd-N}), \nu(\text{Pd-Cl})$ ⁽¹⁰⁴⁾ respectively, as shown in Table (3-3).

D- Spectrum of the Copper (II) Complex (L_2Cu):

In the spectrum of L_2Cu complex, Figure (3-10), The azomethine stretching band was splitted and shifted with reduced intensity, this means that coordination may took place through nitrogen of azomethine group.

New three bands were observed at $1508, 1298, 829\text{ cm}^{-1}$ due to the expected NO stretching bands of the nitrate group for the monodentate symmetry (C_2V)⁽¹⁰³⁾, Furthermore, new bands have been observed around $518, 428\text{ cm}^{-1}$ which are due to $\nu(\text{Cu-N}), \nu(\text{Cu-O})$ ⁽¹⁰³⁾, respectively, as shown in Table (3-3), another broad band at 3452 cm^{-1} due to H_2O .

3-2-3 Spectrum of Ligand (L_3) and their Metal Complexes:

The FT.IR of (L_3), Figure (3-11), showed a weak band at 632 cm^{-1} assigned to hydrogen-bonded out-of-plane O-H bending vibration⁽³⁰⁾. This assignment is supported by disappearance of the band when the hydroxy hydrogen is replaced by a metal. The phenolic (C-O) stretching vibrations, that appeared at 1294 cm^{-1} in the Schiff bases^(96,97), underwent a shift towards higher frequencies in the complexes. This shift confirms the participation of oxygen in the C-O-M bond^(98, 99), the $\nu_{\text{as}}(\text{C-O-C})$ at 1244 cm^{-1} , $\nu_{\text{s}}(\text{C-O-C})$ at 1024 cm^{-1} ⁽¹⁸²⁾. Also a strong band appeared at about 1614 cm^{-1} in the free ligand, underwent a shift towards higher or lower frequencies in the complexes. This band was attributed to the $(\overset{|}{\text{C}}=\text{N})$ stretching vibration^(98,100). Table (3-3) contains the most characteristic bands in the FTIR spectrum of (L_3).

A- Spectrum of the Platinum (IV) Complex ($L_3\text{Pt}$):

The FT.IR spectrum of $L_3\text{Pt}$, Figure (3-12), Table (3-3) shows some changes in which azomethine band, which appeared at 1614 cm^{-1} in (L_3) underwent shift to 1625 cm^{-1} upon complexation, this means that coordination may took place through nitrogen of azomethine. The phenolic (C-O) frequency was shifted to 1298 cm^{-1} , this blue shift indicate the participation of oxygen atom in the coordination with Pt atom⁽³⁰⁾. We noticed that the band correspond to out of plane O-H bending (632 cm^{-1}) in the free ligand have a correspond band of similar intensity in the spectrum of the Pt(IV) complex, this lend as to conclude that the hydrogen of the phenol group did not get ionized, which was more indicated by the appearance of strong sharp band at 3193 cm^{-1} for $\nu_{\text{O-H}}$. The proton of the O-H group is not expected to ionize during the formation of the platinum (IV) complex, since the reaction mixture was highly acidic due to the use of chloroplatinic acid (H_2PtCl_6).

No appreciable change took place in the ν_s (C-O-C) and ν_{as} (C-O-C) modes, which excludes the possibility of the participation of the oxygen atom of the methoxy group in coordination with Pt atom. Furthermore, new weak bands have been observed around 520 assigned to ν (Pt-N) , ν (Pt-O) at 443 cm^{-1} , and ν (Pt-Cl) at 325 cm^{-1} (103) as strong band.

B- Spectrum of the Gold (III) Complex (L_3Au):

The FT.IR spectrum of L_3Au , Figure (3-13), Table (3-3) shows the blue shift of ν (C=N) by 13 cm^{-1} , this indicates coordination through nitrogen. The phenolic (C-O) frequency was shifted with lower intensity to 1296 cm^{-1} , this indicates the participation of oxygen atom in the coordination with Au atom. We noticed that the band correspond to out of plane O-H bending in the free ligand have a correspond band of similar intensity in the spectrum of the Au (III) complex, this lend as to conclude that the hydrogen of the phenol group did not get ionized, The proton of the O-H group is not expected to ionize during the formation of the Au (III) complex, since the reaction mixture was highly acidic due to the use of $HAuCl_4$. Furthermore, new bands have been observed at 543, 449 cm^{-1} , due to ν (Au-N) , ν (Au-O), respectively .Table (3-3) contains the most characteristic bands of L_3Au .

C- Spectrum of the Palladium (II) Complex (L_3Pd):

The most significant difference in the FT.IR spectrum of the ligand and its palladium complex, Figure (3-14), was the shift of (C=N) stretching frequencies of (L_3) to lower value by 6 cm^{-1} due to metal-ligand coordination⁽⁸³⁾. The phenolic (C-O) frequency was shifted to 1303 cm^{-1} , this blue shift indicate the participation of the oxygen atom in the coordination with Pd atom⁽³⁰⁾.

Since no band characteristic to free C=N group was appeared in the L₃Pd spectrum, a bridged dig and structure can be suggested. No appreciable change took place in the ν_s (C-O-C) and ν_{as} (C-O-C) modes, which exclude the possibility O atom of methoxy group participation in coordination with Pd atom. Furthermore, new bands have been observed at 525 and 435 cm⁻¹ due to ν (Pd-N) and ν (Pd-O) respectively as shown in Table (3-3).

D- Spectrum of the Copper (II) complex (L₃Cu):

In the copper complex spectrum, Figure (3-15), the azomethine stretching frequency shifts from 1614 to 1608 cm⁻¹, this shift indicates complexation via azomethine nitrogen⁽⁸⁸⁻⁸⁹⁾. The out of plane O-H bending was disappeared upon complexation, this indicates coordination through oxygen, also this was more confirmed by the appearance a new bands at 530 and 450 cm⁻¹ due to ν (Cu-N) and ν (Cu-O)⁽¹⁰⁵⁾. The phenolic C-O shifted from 1294 to 1304 cm⁻¹, which is more indicates the coordination through phenolic oxygen. Table (3-3) shows the most diagnostic bands of L₃Cu.

Table (3-3): Number of the most bands of F.T.IR to prepared ligands and their complexes in (cm⁻¹).

Comp.	ν C=N	ν C-H Arm.	Phenolic ν C-O	γ O-H Out-of- plane bending	ν Ar-N	ν M-N	ν M-O	ν M-Cl
L ₁	1627	3058	1309	663	-	-	-	-
L ₁ Pt	1651	3006	1352	659	-	560	455	340
L ₁ Au	1612	3050	1328	-	-	565	461	370
L ₁ Pd	1612	3043	1319	-	-	551	462	-
L ₁ Cu	1612	3050	1323	-	-	570	466	-
L ₂	1606	3000	-	-	1359	-	-	-
L ₂ Pt	1649 1606	3000	-	-	1367	526	-	378
L ₂ Au	1645 1606	3100	-	-	1390	524	-	-
L ₂ Pd	1585	3124	-	-	1373	524	-	343
L ₂ Cu	1598	3080	-	-	1382	518	428	
L ₃	1614	3057	1294	632	-	-	-	-
L ₃ Pt	1625	3072	1298	632	-	520	443	325
L ₃ Au	1627	3050	1296	640	-	543	449	-
L ₃ Pd	1608	3060	1303	-	-	525	435	-
L ₃ Cu	1608	3018	1304	-	-	530	450	-

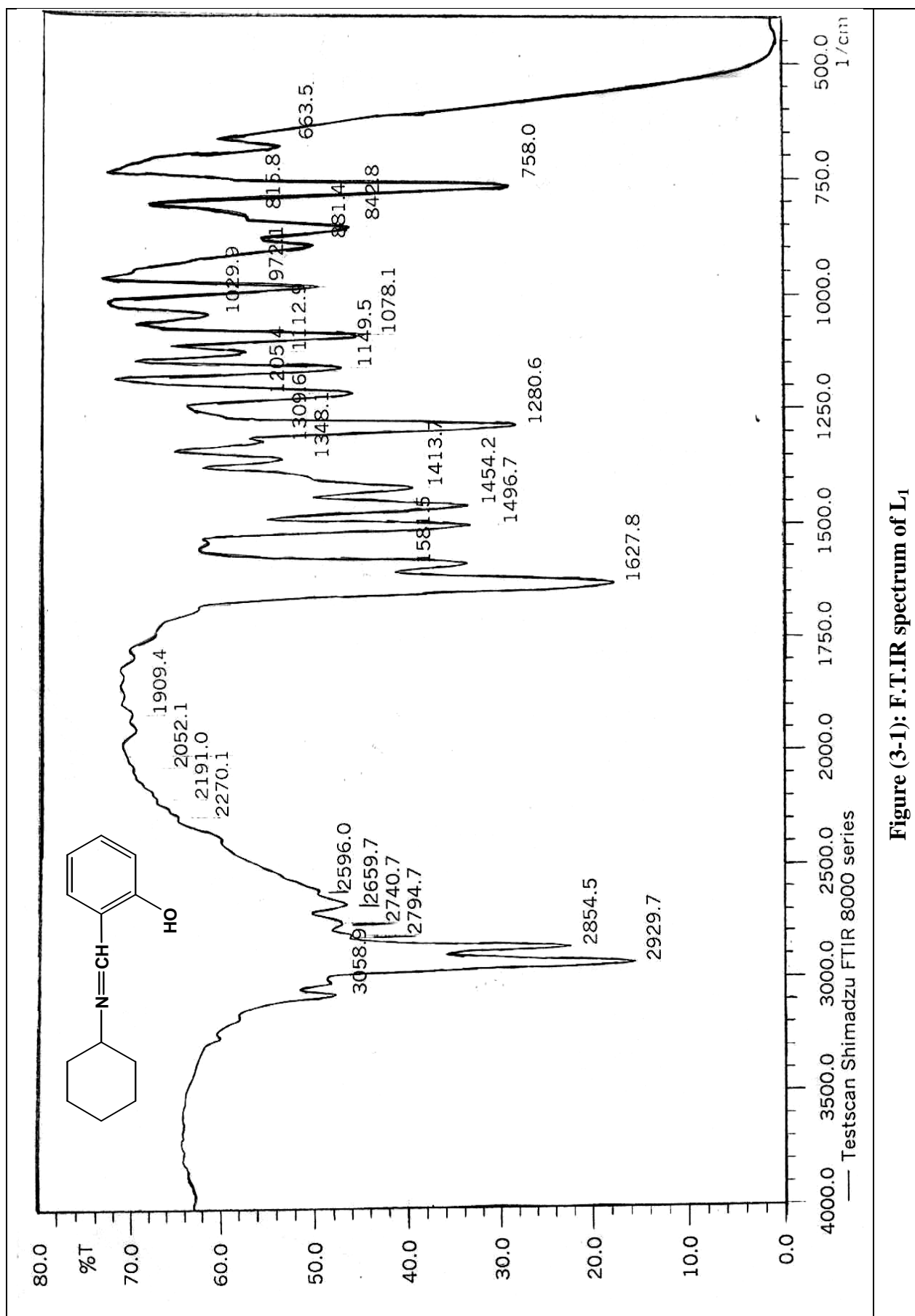


Figure (3-1): F.T.IR spectrum of L₁

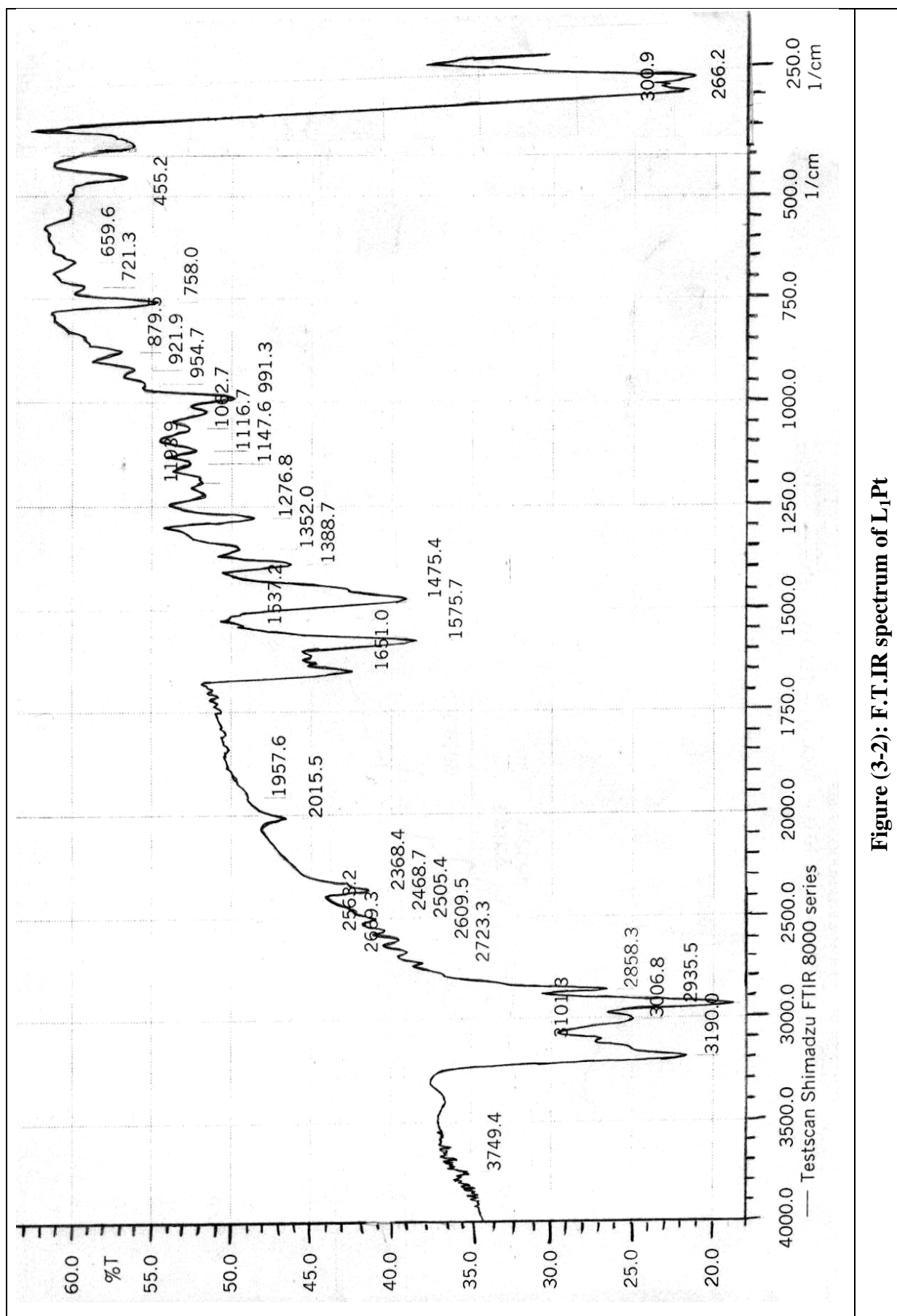
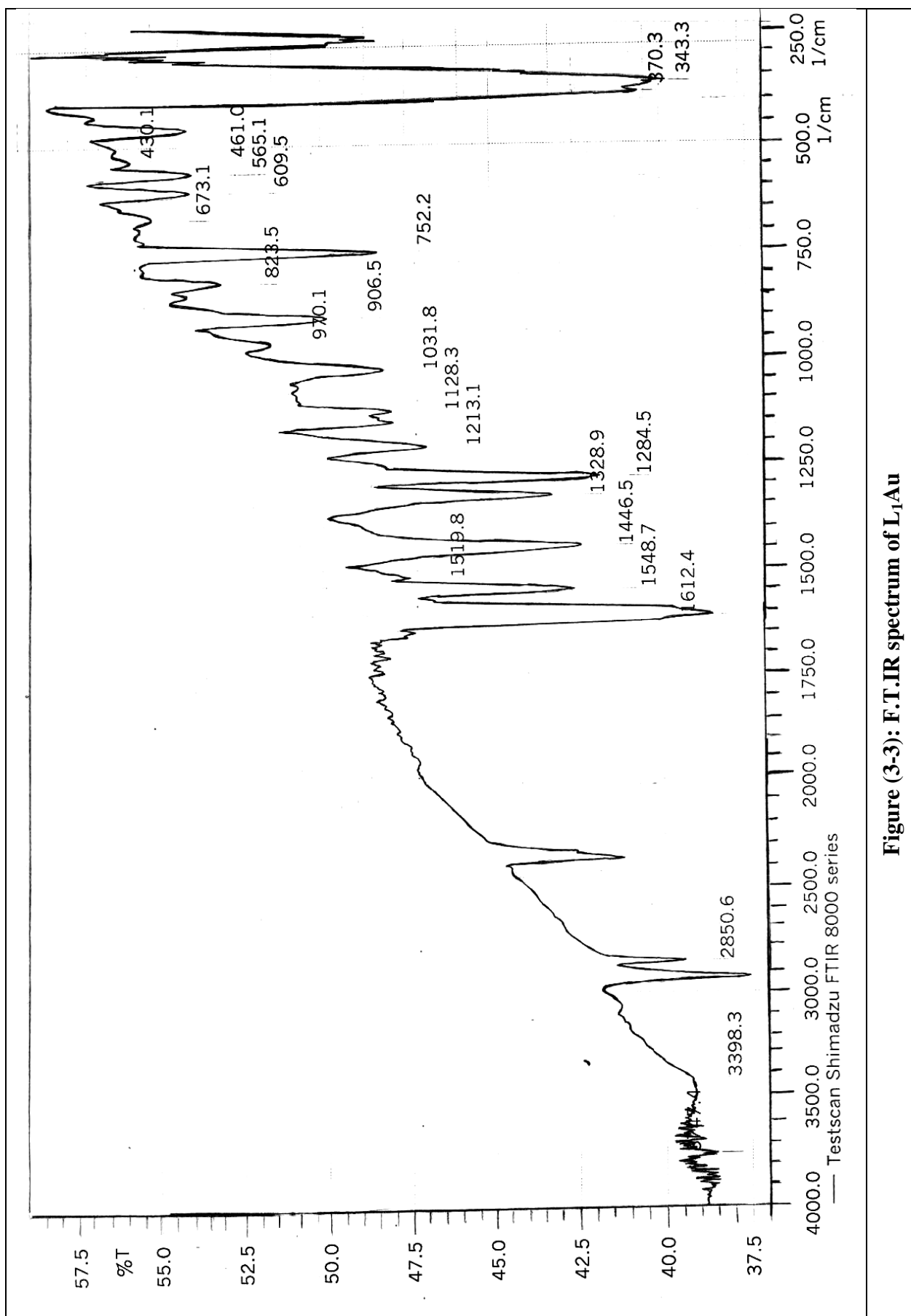
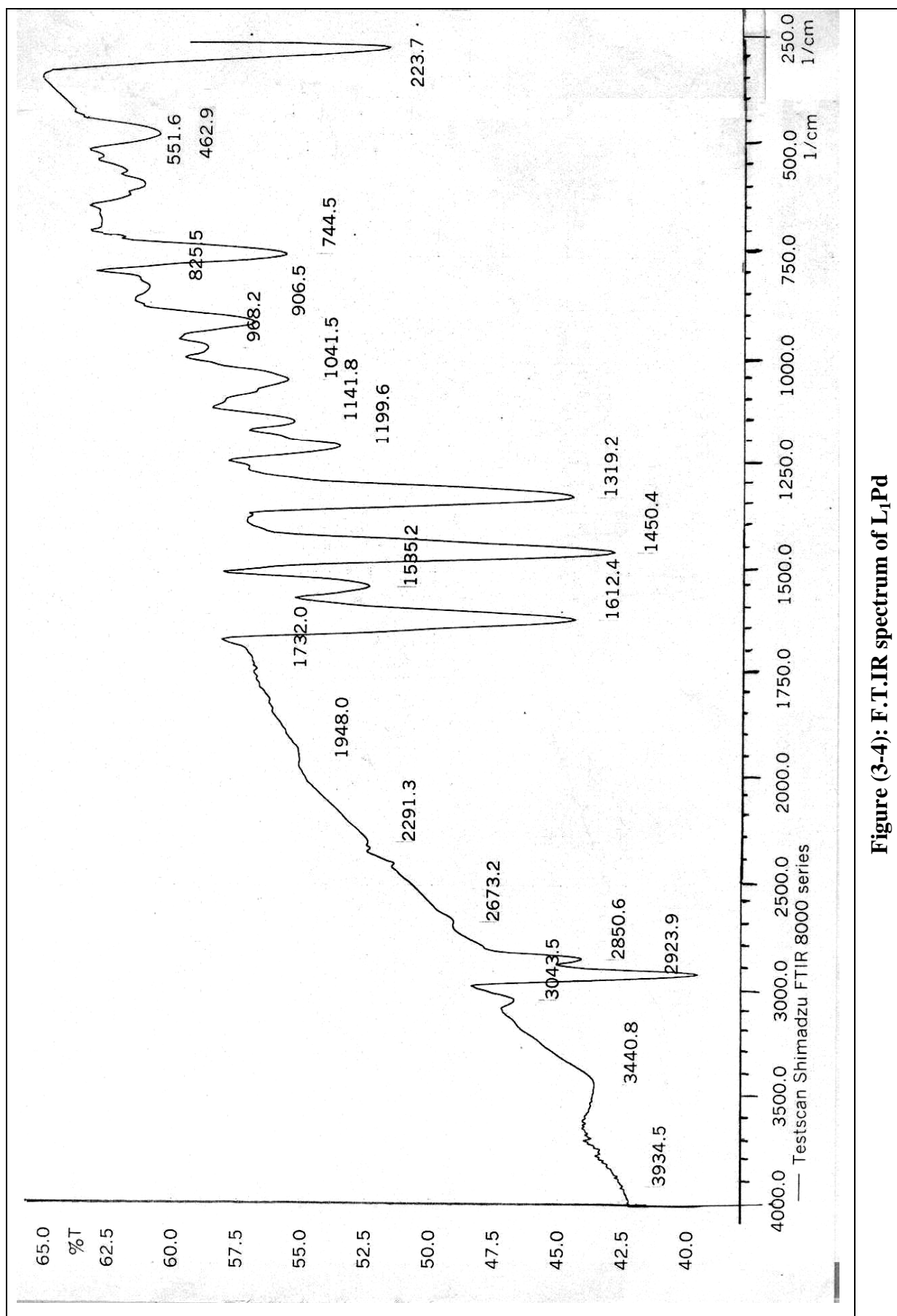
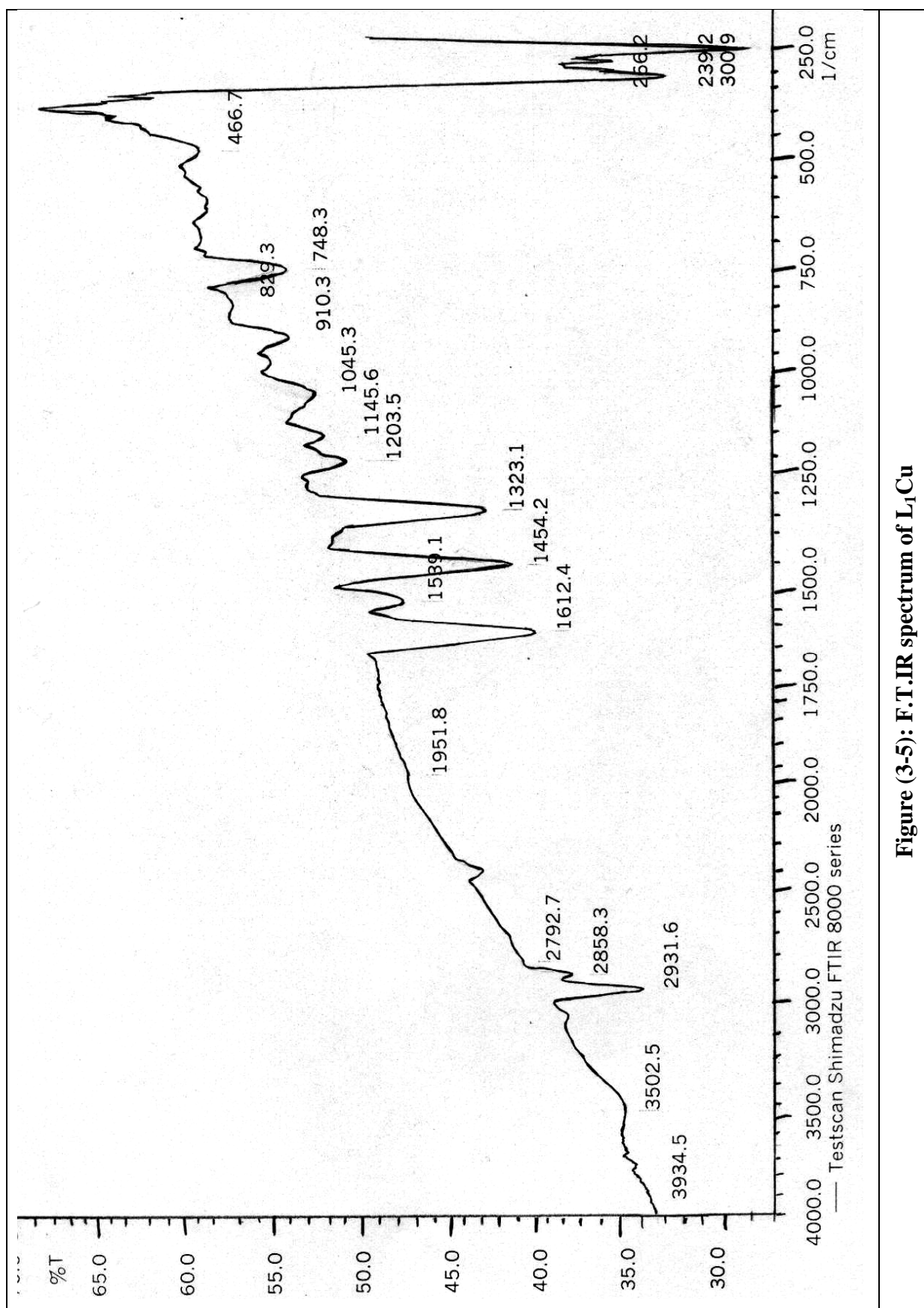


Figure (3-2): F.T.IR spectrum of L₁Pt

Figure (3-3): F.T.IR spectrum of L₁Au

Figure (3-4): F.T.IR spectrum of L₁Pd

Figure (3-5): F.T.IR spectrum of L₁Cu

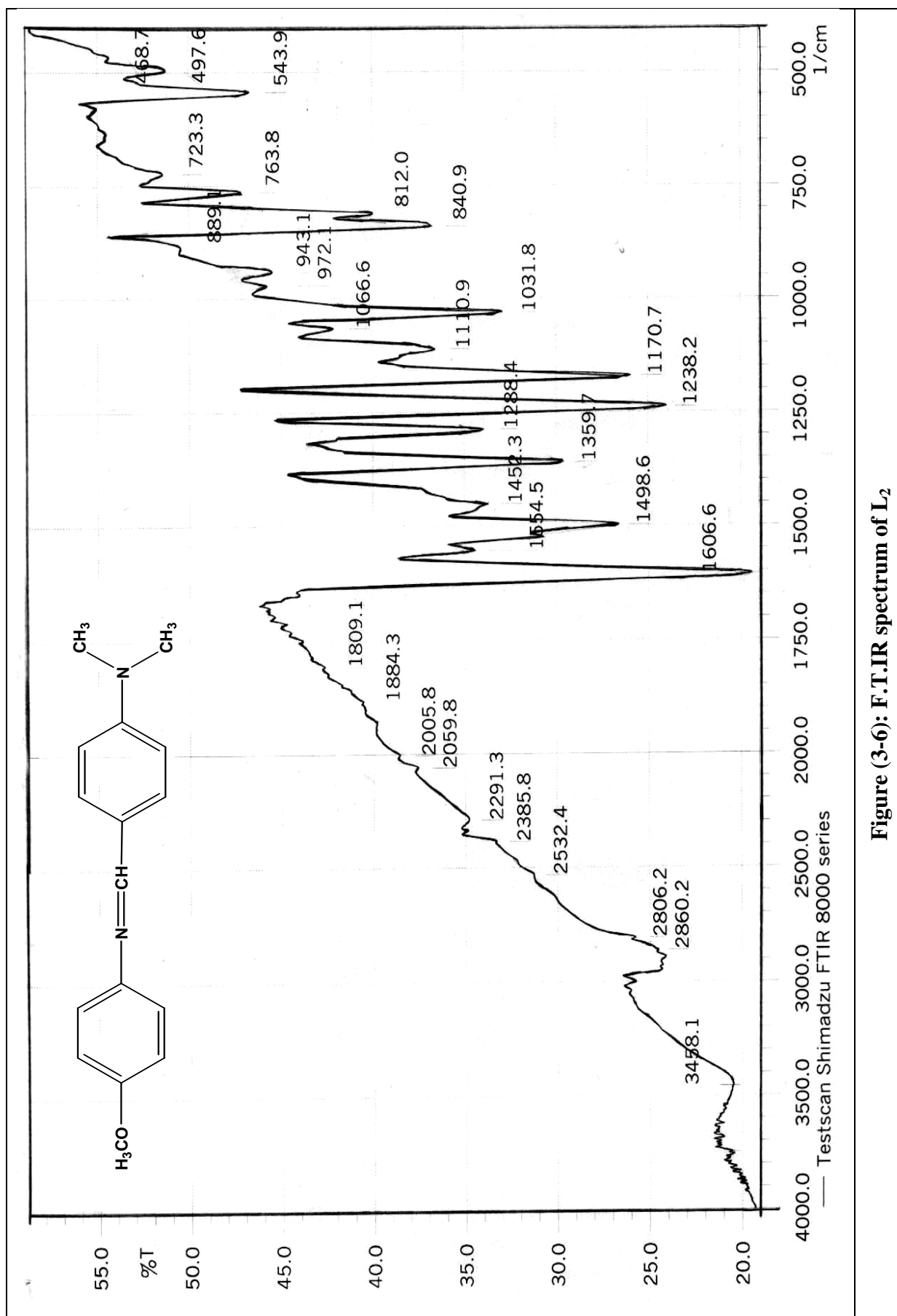
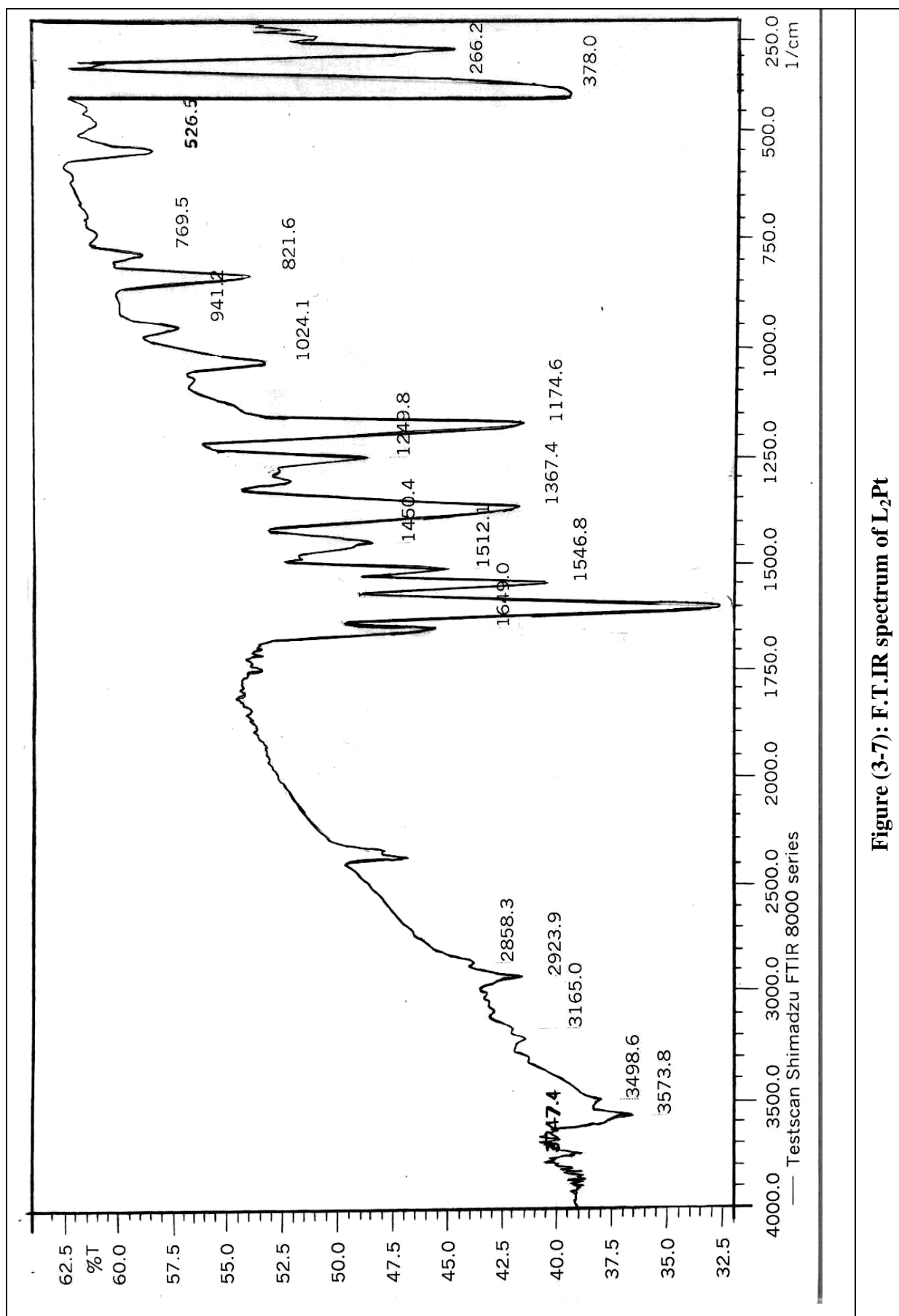
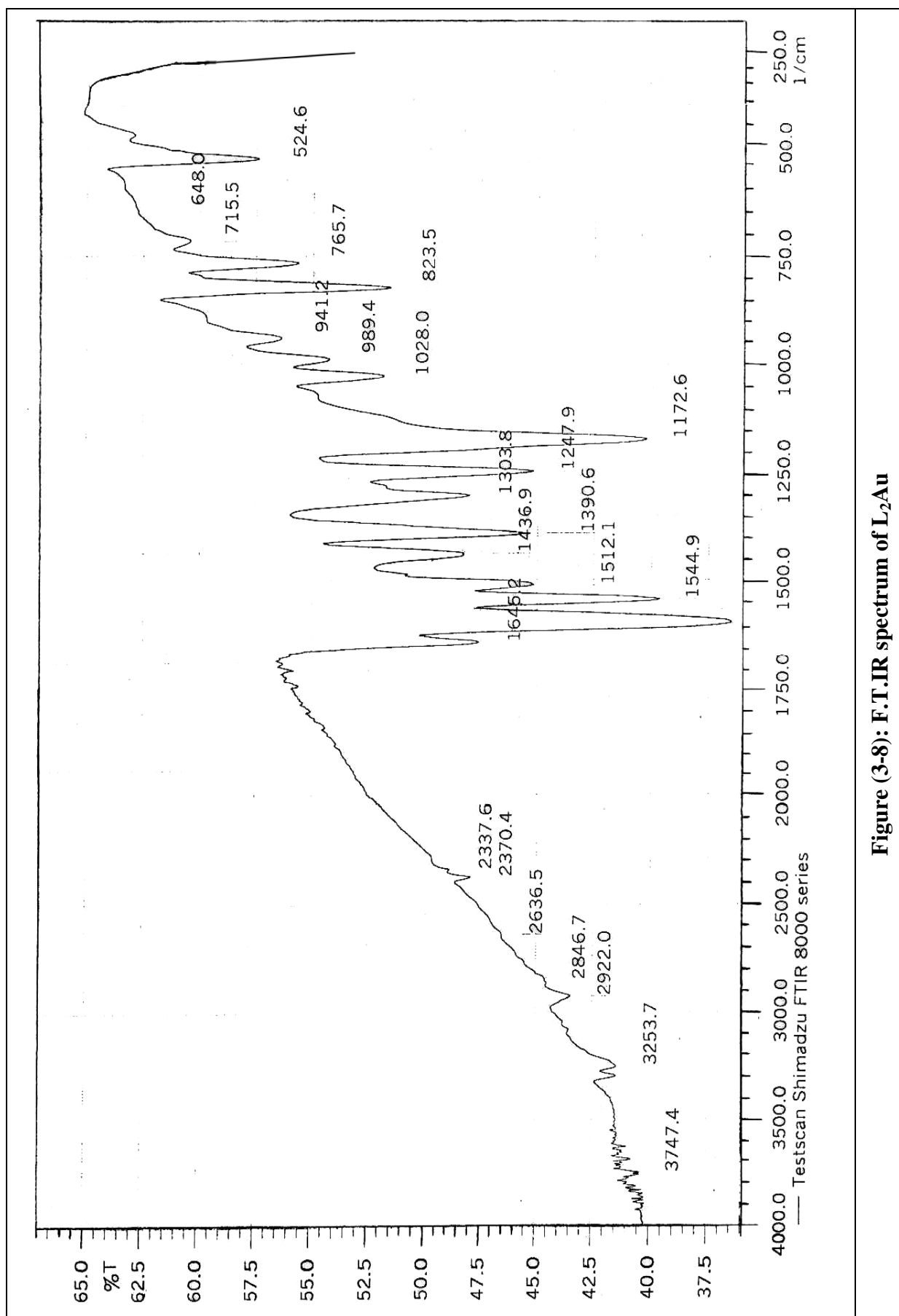
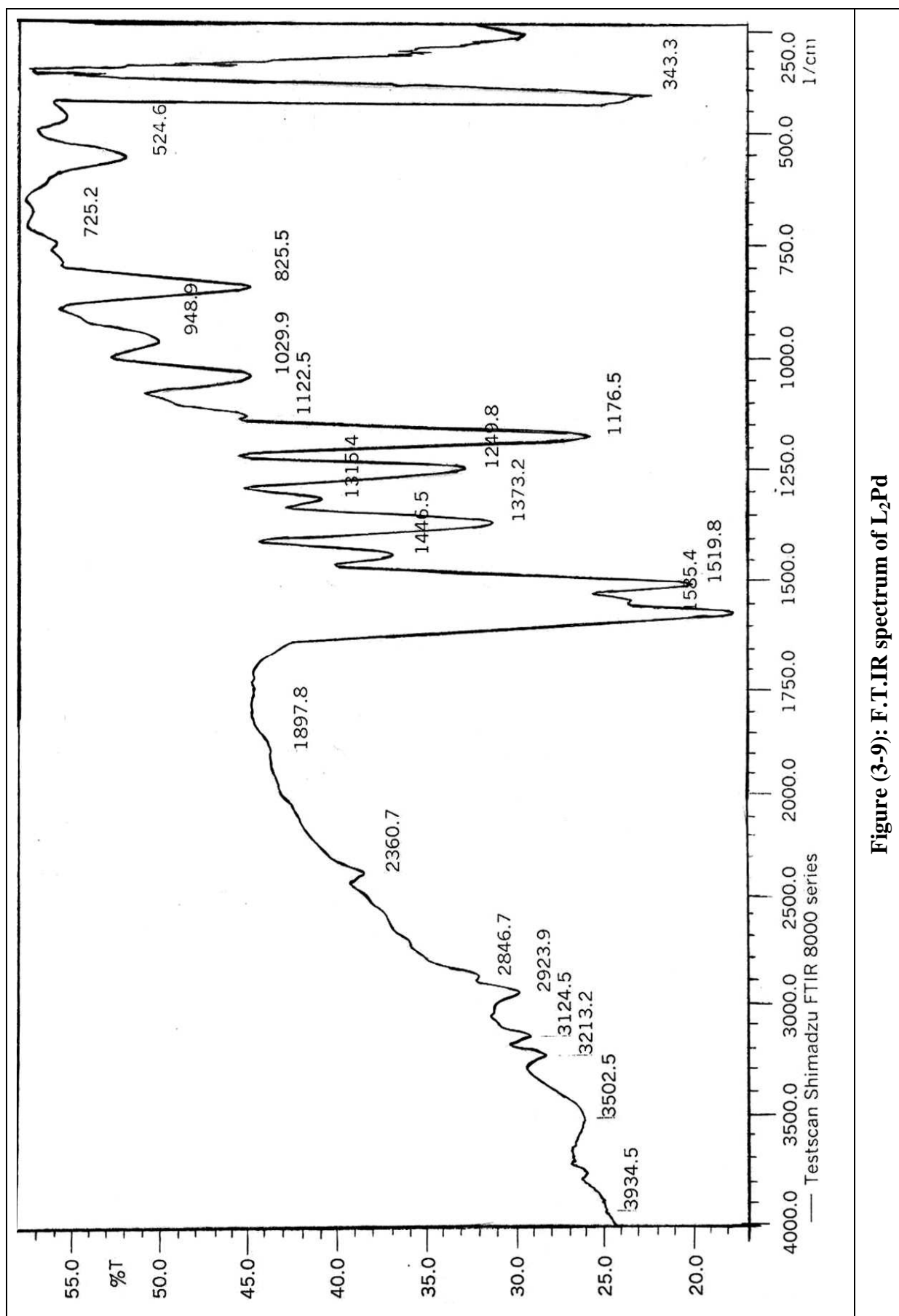


Figure (3-6): F.T.IR spectrum of L₂

Figure (3-7): F.T. IR spectrum of L₂Pt

Figure (3-8): F.T.IR spectrum of L₂Au

Figure (3-9): F.T.IR spectrum of L₂Pd

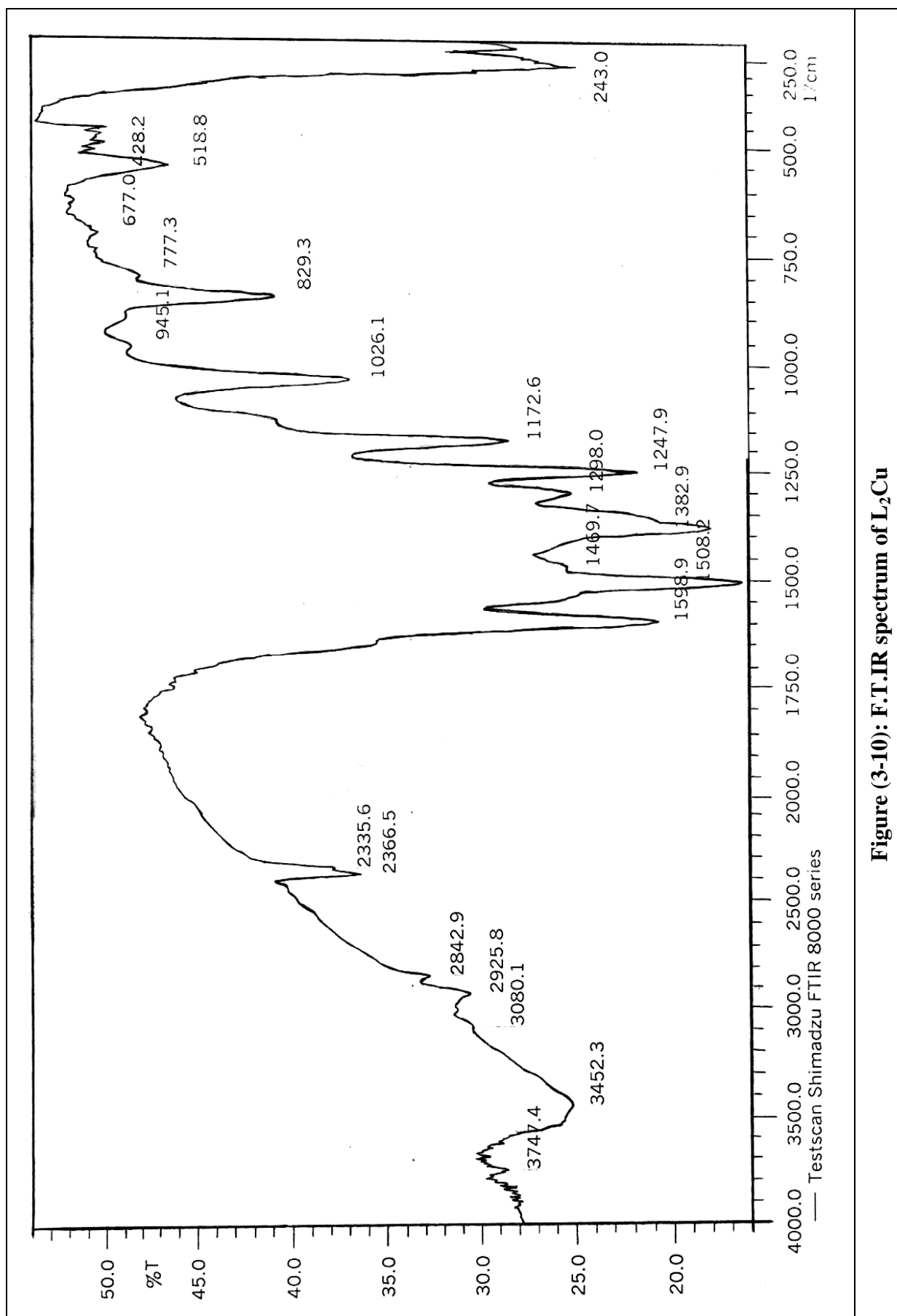
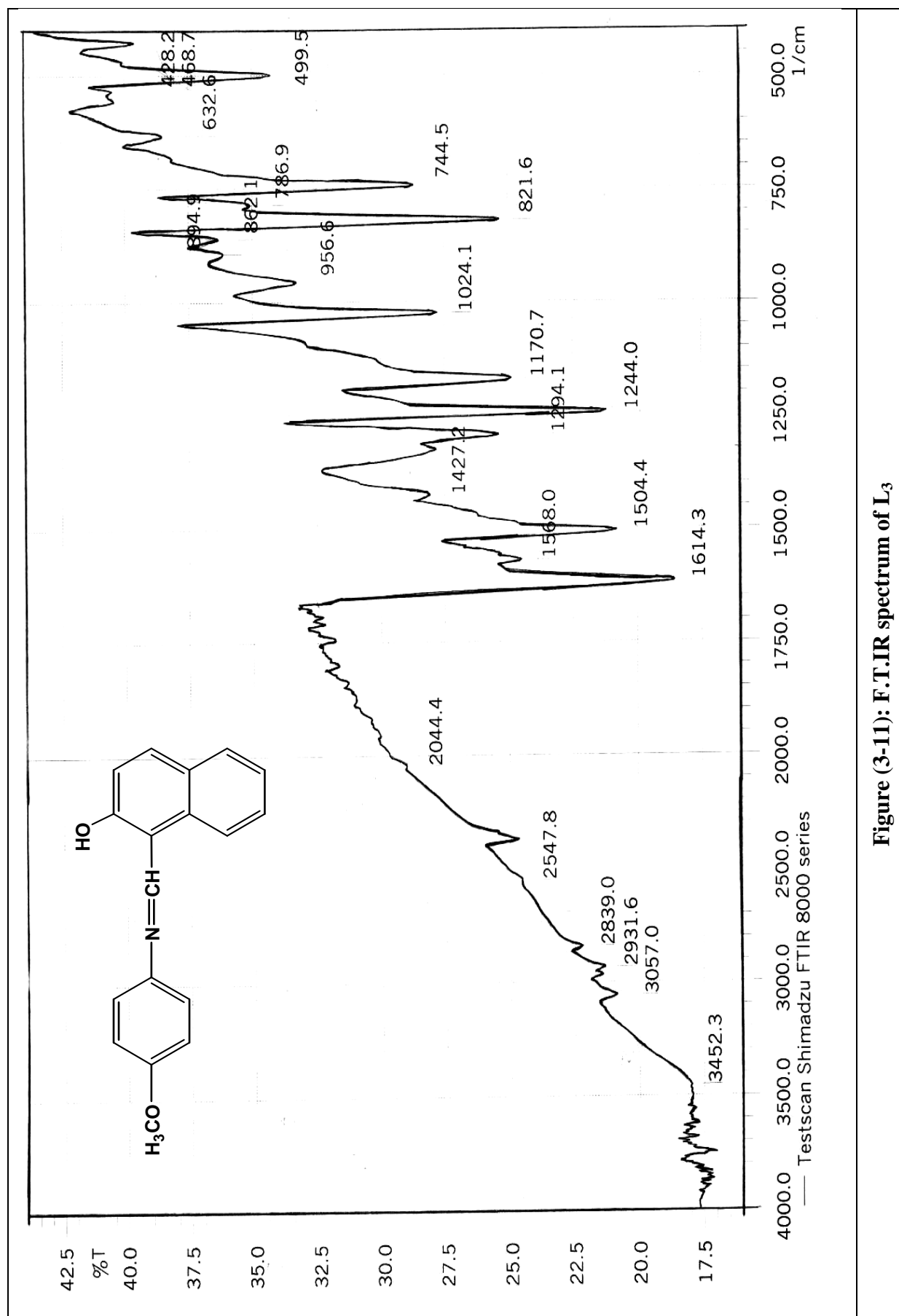


Figure (3-10): F.T.IR spectrum of L₂Cu

Figure (3-11): F.T.IR spectrum of L_3

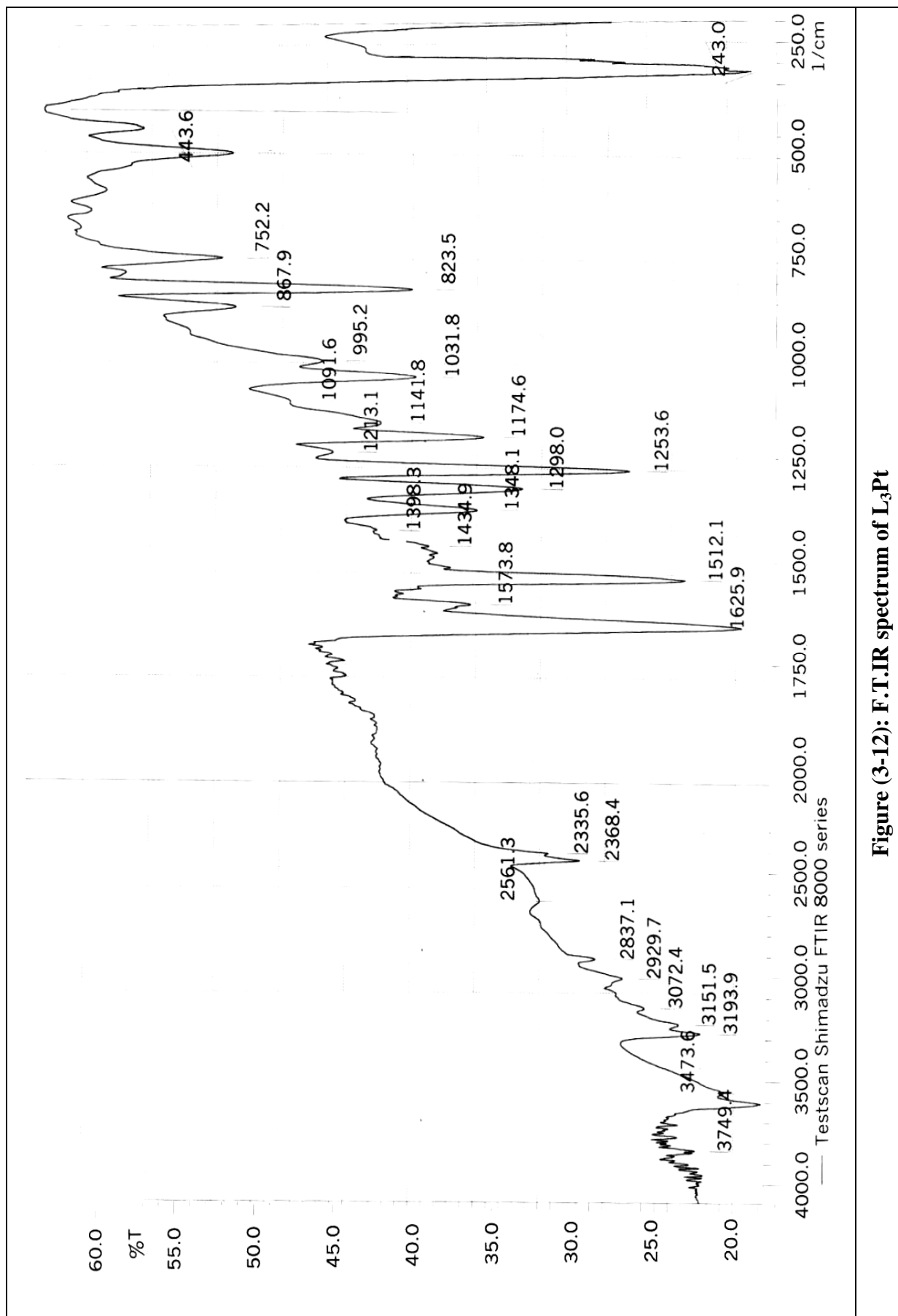
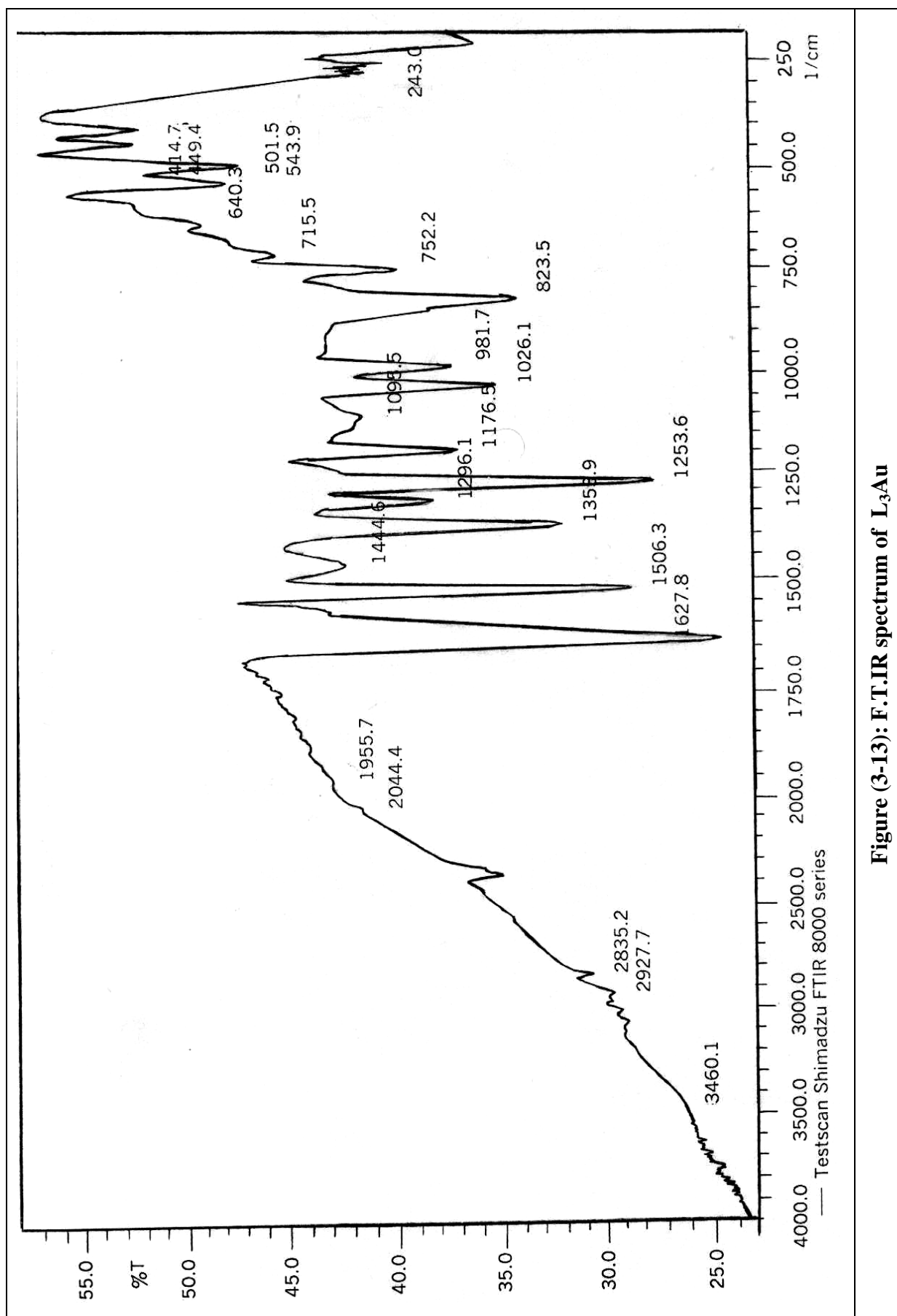


Figure (3-12): F.T.IR spectrum of L₃Pt

Figure (3-13): F.T.I.R spectrum of L₃Au

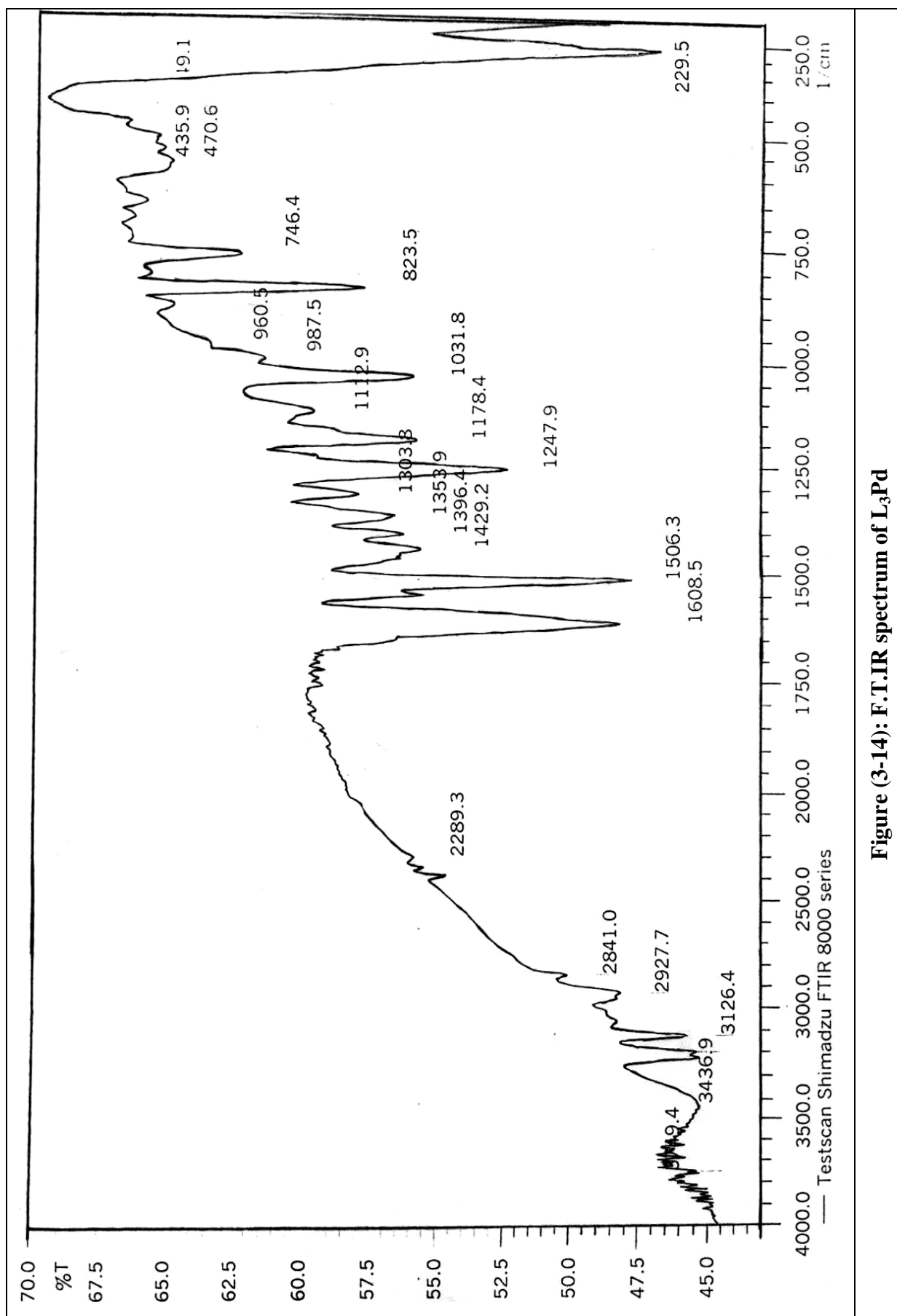


Figure (3-14): F.T.IR spectrum of L₃Pd

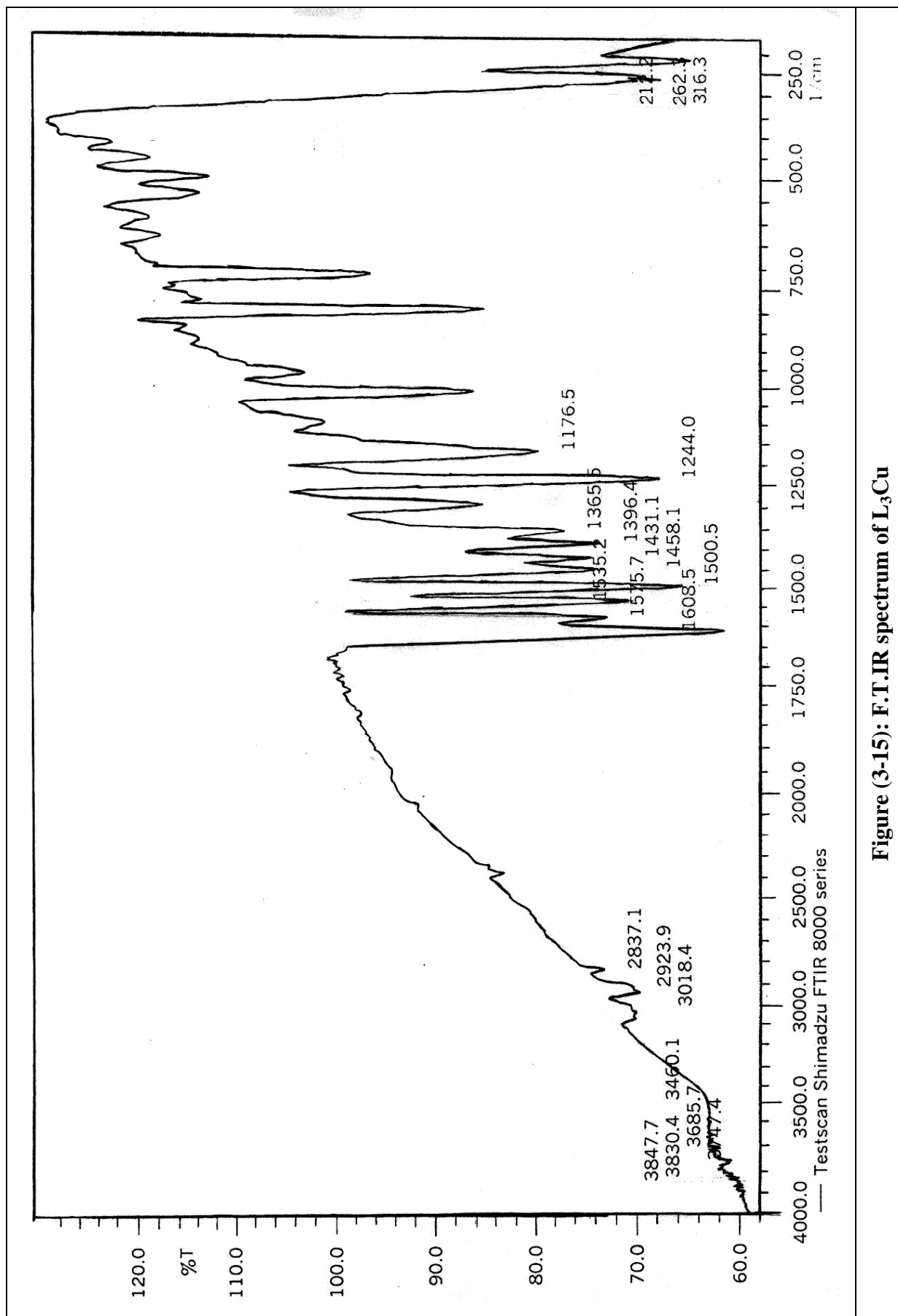


Figure (3-15): F.T.IR spectrum of L₃Cu

3-3 Magnetic Susceptibility Measurements

Magnetic measurements are widely used in studying transition metal complexes⁽¹⁰⁶⁾. The magnetic properties are due to the presence of unpaired electrons in the partially filled d-orbital in the outer shell of these elements. These magnetic measurements give an idea about the electronic state of the metal ion in the complex.

The resultant magnetic moment of an ion is due to both orbital and spin motions⁽¹⁰⁷⁾. Chemically useful information can be obtained by proper interpretation of measured values of magnetic moments.

The magnetic moment is given by the following equation:

$$\mu_{s+L} = \sqrt{4s(s+1) + L(L+1)} \quad \text{B.M.}$$

μ = magnetic moment

S = spin quantum number

L = orbital quantum number

Although detailed determination of the electronic structure requires consideration of the orbital moment, for most complexes of the first transition series the spin-only moment is sufficient, as any orbital contribution is small⁽¹⁰⁸⁾.

$$\mu_s = \sqrt{4s(s+1)} \quad \text{B.M.}$$

$$\mu_s = \sqrt{n(n+2)} \quad \text{B.M.}$$

S = $n \cdot 1/2$, n = number of unpaired electrons

The value of magnetic susceptibility of the prepared complexes at room temperature is calculated using the following equation:

Where:

$$\mu_{\text{eff}} = 2.88 \sqrt{X_A \cdot T} \quad \text{B.M.}$$

$$X_A = X_m + D$$

$$X_m = X_g \cdot M \cdot wt$$

X_g = mass susceptibility

D = Pascals constant

X_m = molar susceptibility

X_A = atomic susceptibility which it's corrected from diamagnetic

μ_{eff} = effective magnetic moment

The values of X_g , X_m , D , and X_A obtained for the present complexes are given in Table (3-4).

Table (3-4): Magnetic properties of the prepared complexes in 298 K.

Complexes	$X_g \times 10^{-6}$	$X_m \times 10^{-6}$	$D \times 10^{-6}$	$X_A \times 10^{-6}$	μ_{eff}	Conductivity ms/cm
L_1Pt	-	-	-	-	Diamag	19.2 (nonconducting)
L_1Au	-	-	-	-	Diamag	17.9 (nonconducting)
L_1Pd	-	-	-	-	Diamag	15.4 (nonconducting)
L_1Cu	0.265	148.22	236.88	385.10	0.95	5.0 (nonconducting)
L_2Pt	-	-	-	-	Diamag	67.4 (conducting 2:1)
L_2Au	2.040	3730.14	431.84	4161.98	3.149	62.3 (conducting 3:1)
L_2Pd	0.1979	285.3	348.8	634.1	1.229	17.2 (non conducting)
L_2Cu	1.146	953.0	306.32	1259.0	1.732	47.8 (conducting 1:1)
L_3Pt	-	-	-	-	Diamag	66.3 (conducting 2:1)
L_3Au	-	-	-	-	Diamag	93.8 (conducting 3:1)
L_3Pd	-	-	-	-	Diamag	72.8 (conducting 2:1)
L_3Cu	2.571	1819.0	160.36	1979.0	2.17	11.4 (nonconducting)

The molar conductance values of all the complexes have been measured in DMSO as a solvent at concentration of $10^{-3}M$ and at room temperature ($25^\circ C$), for determination electrolytic or non-electrolytic nature of the complexes⁽¹⁰⁷⁾.

3-4 Study of the Electronic Spectra of the Prepared Compounds:

3-4-1 Electronic Spectra of the Ligand L_1 , L_2 and L_3 :

Electronic spectra of Schiff bases in (UV-Vis) region have been studied by a number of authors⁽¹⁰⁹⁻¹¹¹⁾. The spectra of the ligands generally exhibit three main peaks: at about 265nm (37735cm^{-1}), 300nm (33333cm^{-1}) and 400nm (25000cm^{-1}). The first and the second peaks are attributed to benzene π - π^* and imines π - π^* transition, respectively. These bands were not significantly affected by chelating. The third band in the spectra of the ligand is assigned to n- π^* transition⁽¹¹²⁾. This band is shifted to a longer wavelength. This shift may be attributed to the donation of the lone pairs of the nitrogen atoms of the Schiff base to the metal ion ($\text{N}\rightarrow\text{M}$)⁽¹¹³⁾.

Figures (3-16), (3-17) and (3-18) show the UV-Vis. Spectra of the new ligands L_1 , L_2 and L_3 . Table (3-5) contains the position and assignment of the absorption bands.

3-4-2 Electronic Spectra of the Complexes:-

A- Platinum (IV) Complexes of L_1 , L_2 , and L_3 ($L_1\text{Pt}$, $L_2\text{Pt}$, $L_3\text{Pt}$):

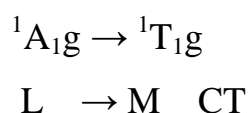
The three complexes of Pt (IV) were diamagnetic as expected^(22,114), the ground state suggesting spin paired octahedral stereochemistry.

The atomic ground state is ^5D . The low spin ground state in an octahedral field is $^1\text{A}_1\text{g}$ referring to $t_2\text{g}^6$ configuration, which give rise to two principle spin allowed transitions whose band envelopes are very sensitive towards certain types of distortion.

Excitation of an electron to the eg orbital yields the configuration $t_2\text{g}^5\text{eg}^1$ which spans $^3\text{T}_1\text{g}+^1\text{T}_1\text{g}+^1\text{T}_2\text{g}+^3\text{T}_2\text{g}$ with the spin-triplet states lying at lower energy than the singlet⁽²²⁾.

Two principles spin allowed absorption bands are to be expected corresponding to transitions from the $^1A_{1g}$ ground state to the $^1T_{1g}$ and $^1T_{2g}$ excited states. In addition, two bands assigned to the spin forbidden singlet-triplet transition may be observed at lower energies than the spin allowed transitions⁽¹¹⁴⁾.

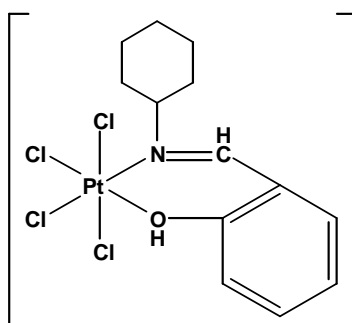
The spectra of the prepared orange platinum complexes, Figures (3-19, 3-23, and 3-27), were shows two bands assigned to the transitions:



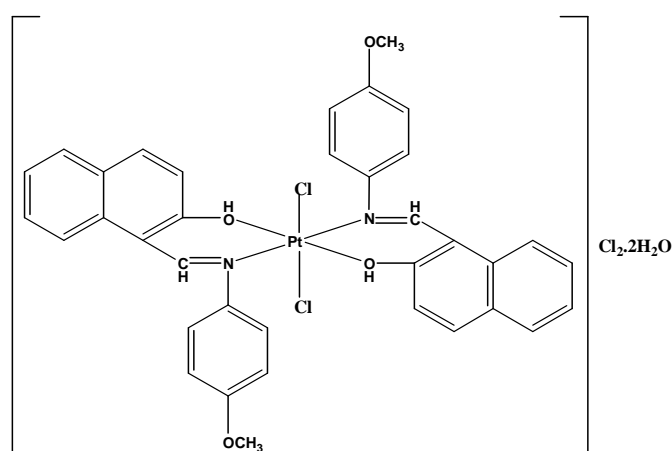
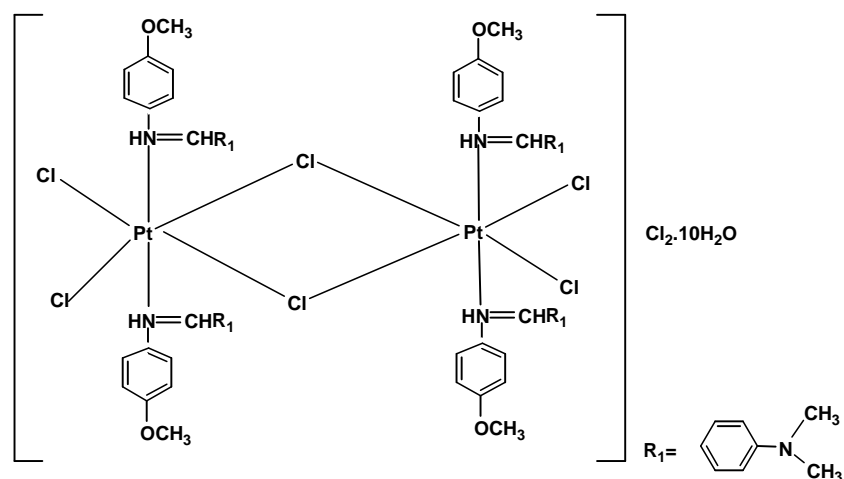
At 464, 293 for L_1Pt , at 436, 333 for L_2Pt , and at 465, 350 for L_3Pt .

Table (3-5) shows the positions and assignments of the absorption bands of L_1Pt , L_2Pt and L_3Pt .

According to these data obtained from C.H.N analysis, and those of the conductivity measurements which show L_1Pt to be non-conductive, L_2Pt and L_3Pt to be conductive, an octahedral geometry around Pt(IV) can be suggested as illustrated below:



L_1Pt



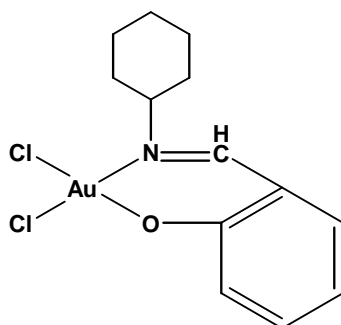
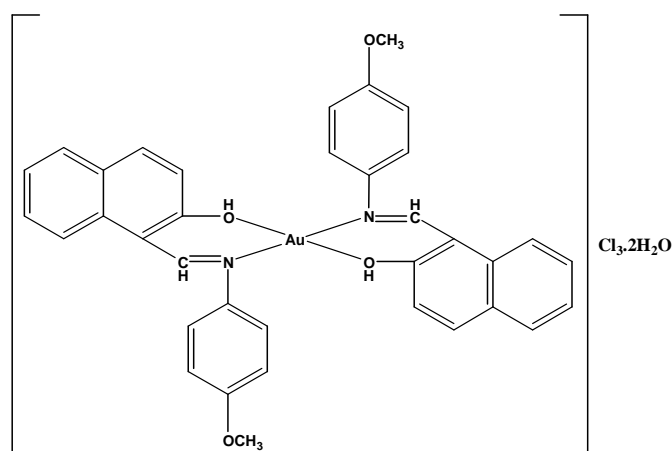
B- Gold (III) Complexes of L_1 , L_2 and L_3 (L_1Au , L_2Au , L_3Au):

The deep red L_1Au and L_3Au complexes were found to be diamagnetic. The diamagnetism of these complexes supports the square planar arrangement of the ligand molecules around the central metal ion⁽¹¹⁵⁾.

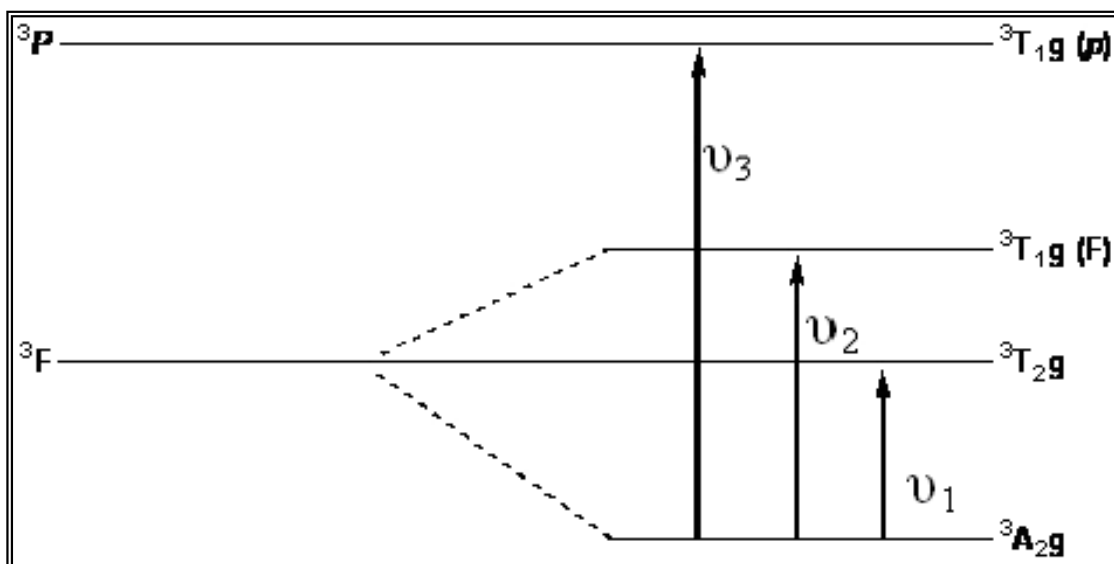
Three spin allowed d-d transitions are anticipated, corresponding to transitions from the three lower lying d levels to the empty $d_{x^2-y^2}$ orbital; two π -electron transitions would be very weak and are neglected. The ground state is $^1A_{1g}$ and the excited states, corresponding to these transitions are $^1A_{2g}$, $^1B_{1g}$ and 1E_g in order of increasing energy⁽¹¹⁴⁾.

The electronic spectra of the L_1Au and L_3Au complexes, Figures (3-20,3-28), showed absorption bands at about 440nm (22727cm^{-1}) and 490nm (20408cm^{-1}), respectively, which may be attributed to $^1A_{1g} \rightarrow ^1A_{2g}$ transitions in a square planar geometry⁽¹¹⁴⁾. The charge transfer bands were appeared around 356nm (28089cm^{-1}), 352nm (28409cm^{-1}) in L_1Au and L_3Au complexes, respectively.

According to these results and those obtained from F.T.IR study, elemental analysis and those of the conductivity measurements, which showed the L_1Au to be non conductive and L_3Au to be conductive, the following structures can be suggested:

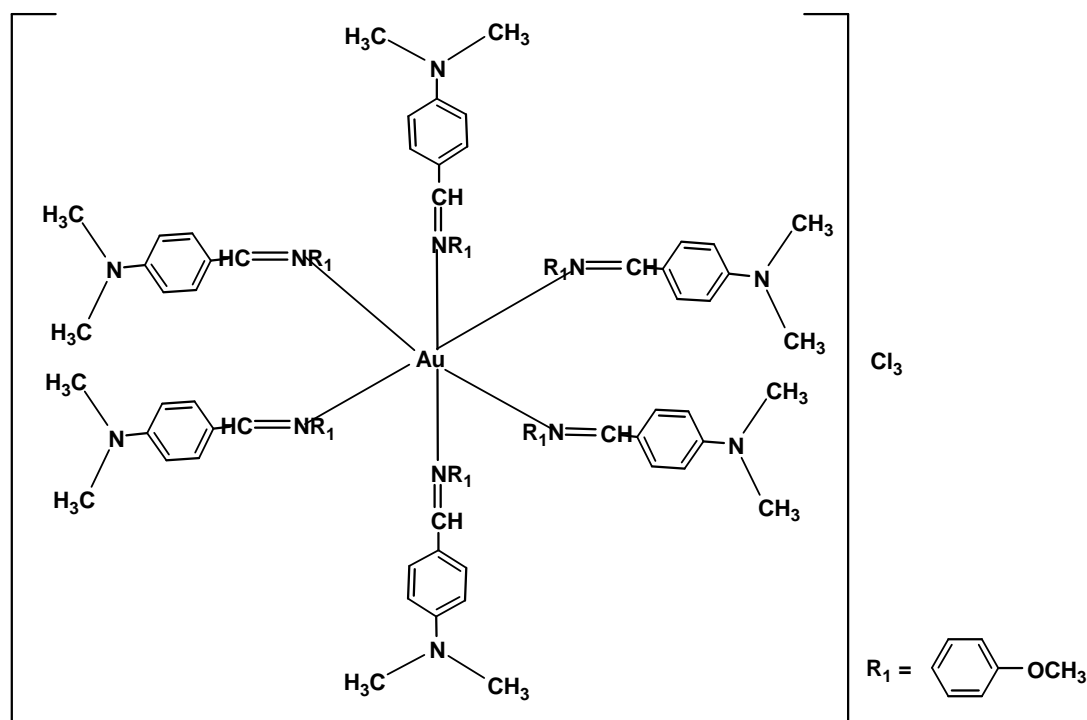
 L_1Au  L_3Au

The brown L_2Au complex, Figure (3-24), showed a weak band at 576nm (17361cm^{-1}) which may assigned to [${}^3A_{2g} \rightarrow {}^3T_{1g}$] transition in octahedral geometry as illustrated in Scheme(3-1)⁽¹¹⁶⁾:



Scheme(3-1): Crystal field splitting of the 3F term of a d^8 ion in O_h field.

The band at 318nm (cm^{-1}) may be due to charge transfer, the paramagnetic (3.149 B.M.) behavior of this complex support the proposed octahedral geometry around gold (III) atom⁽¹¹⁶⁾. According to these results and those obtained from FT.IR Study, elemental analysis and those of conductivity measurements, which showed the L_2Au to be conductive, the following structure can be suggested:



In the electronic spectra of the gold (III) complexes, the bands obtained together with their probable assignments are given in Table (3-5).

C- Palladium (II) Complexes of L_1 , L_2 and L_3 (L_1pd , L_2pd , L_3pd):

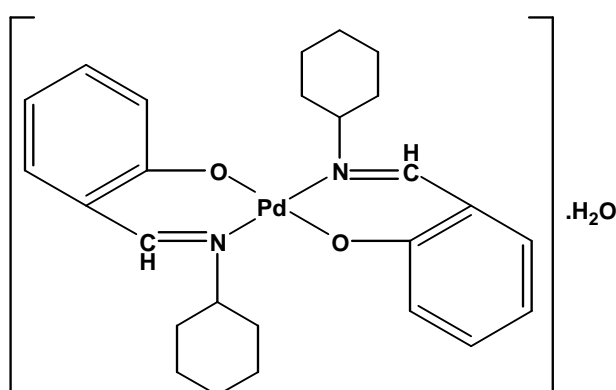
Square complexes of palladium (II) exhibit a broad band in the visible region resolvable into at least two components. Weaker bands are observed on the low energy side of this absorption, whilst several intense bands are observed on the high energy side in the near ultraviolet and ultraviolet region. These last bands are undoubtedly charge transfer in nature⁽¹¹⁴⁾. The ground state for the low spin d^8 system is $^1A_{1g}$. The ligand field excited state are $^1A_{2g}$, $^1B_{1g}$ and 1E_g . Therefore, one should expect three spin allowed transitions in these cases.

In the electronic spectra of L_1pd , L_2pd and L_3pd complexes, two bands were obtained. The first band was a combination of all the three

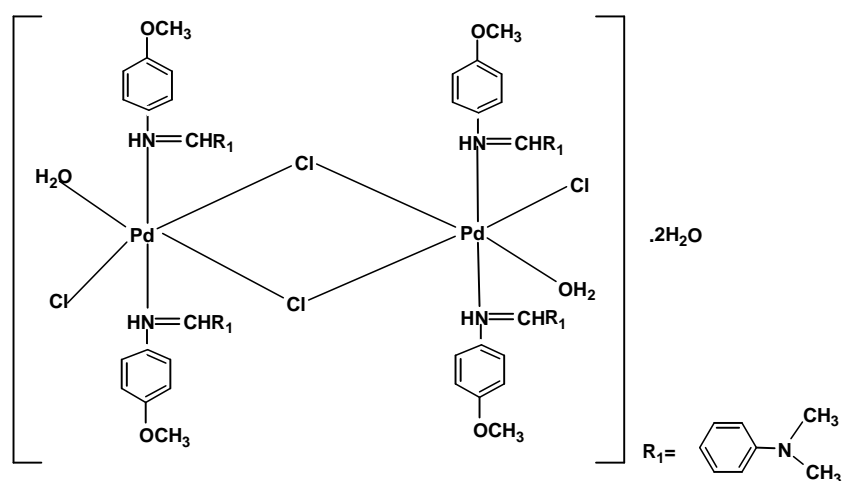
spin-allowed transitions and may be assigned to transitions $^1A_{1g}$, $^1A_{2g}$, $^1B_{1g}$, 1E_g . The second band was a charge transfer band⁽¹⁰⁵⁾.

The bands obtained for the pd(II) complexes together with their probable assignment are given in Table (3-5).

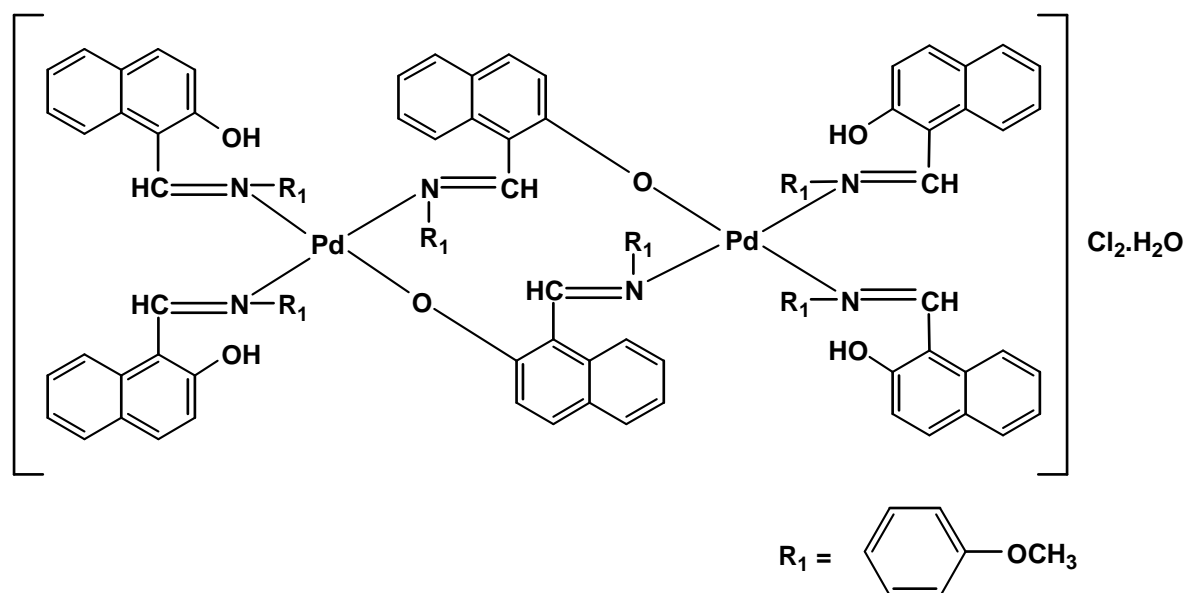
According to these data, and those of the conductivity measurements, this showed the L_1Pd and L_2Pd to be non conductive, while L_3Pd complex to be conductive; the following structural formula can be suggested:



L_1Pd



L_2Pd



L_3Pd

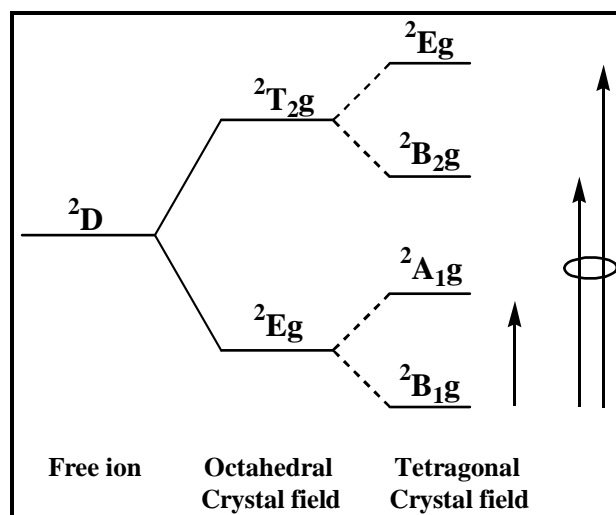
D- Copper (II) Complexes of L_1 , L_2 and L_3 (L_1Cu , L_2Cu , L_3Cu):

All the prepared complexes were brown in color, which suggest a strong field case in all complexes.

L_1Cu , L_2Cu and L_3Cu were all paramagnetic corresponding to one unpaired electron^(32, 90). The observed magnetic moment values of the L_3Cu and L_2Cu were 2.17 and 1.73 B.M., respectively, this can be attributed to spin free (monomeric) copper complex⁽⁹⁰⁾.

The relatively lower values of the magnetic moment for L_1Cu (0.95 B.M.) suggest dimeric structure of the complex ; leading to spin-spin coupling⁽¹¹⁷⁾.

The free ion ground 2D term is expected to split in crystal field according to the following scheme:

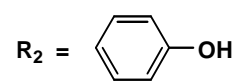
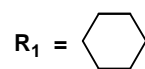
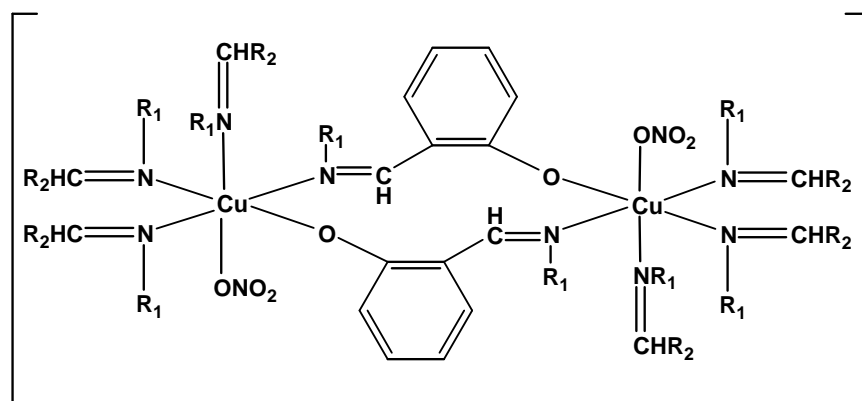


Scheme (3-2): Crystal field splitting of the 2D term of a d^9 ion⁽¹¹⁷⁾.

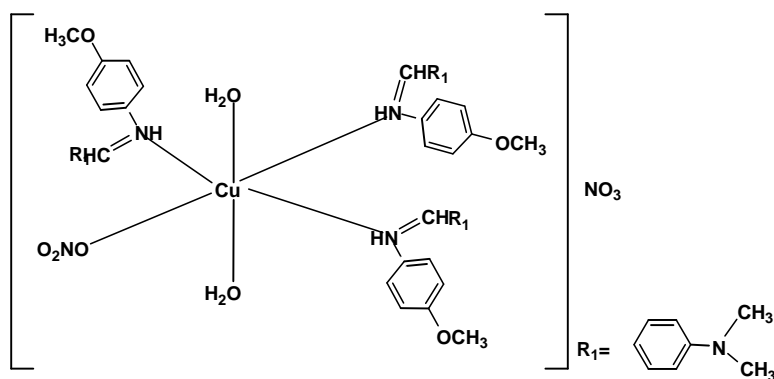
Generally the electronic spectra of copper (II) complexes are difficult to interpret because of the great overlapping of the bands^(117,118). When all the prepared complexes are dissolved in ethanol, the color of the solutions became yellow, which suggest the coordination of the solvent to the vacant axial positions on the copper atoms forming a tetragonally distorted octahedral structures⁽¹¹⁸⁾.

The spectra of L_1Cu , L_2Cu and L_3Cu show broad band in the visible region in the range 450-500nm ($22222-20000\text{ Cm}^{-1}$) which can be assigned as a combination of the transitions ${}^2B_{1g} \rightarrow {}^2A_{1g}$ and ${}^2B_{1g} \rightarrow {}^2E_g({}^2B_{2g})$.

According to the previous elemental analysis, infrared spectra, magnetic measurements, UV-Vis spectra and the results of the conductivity measurement which show L_1Cu and L_3Cu to be non conductive, while L_2Cu to be conductive, the following structures can be suggested:



L_1Cu



L_2Cu

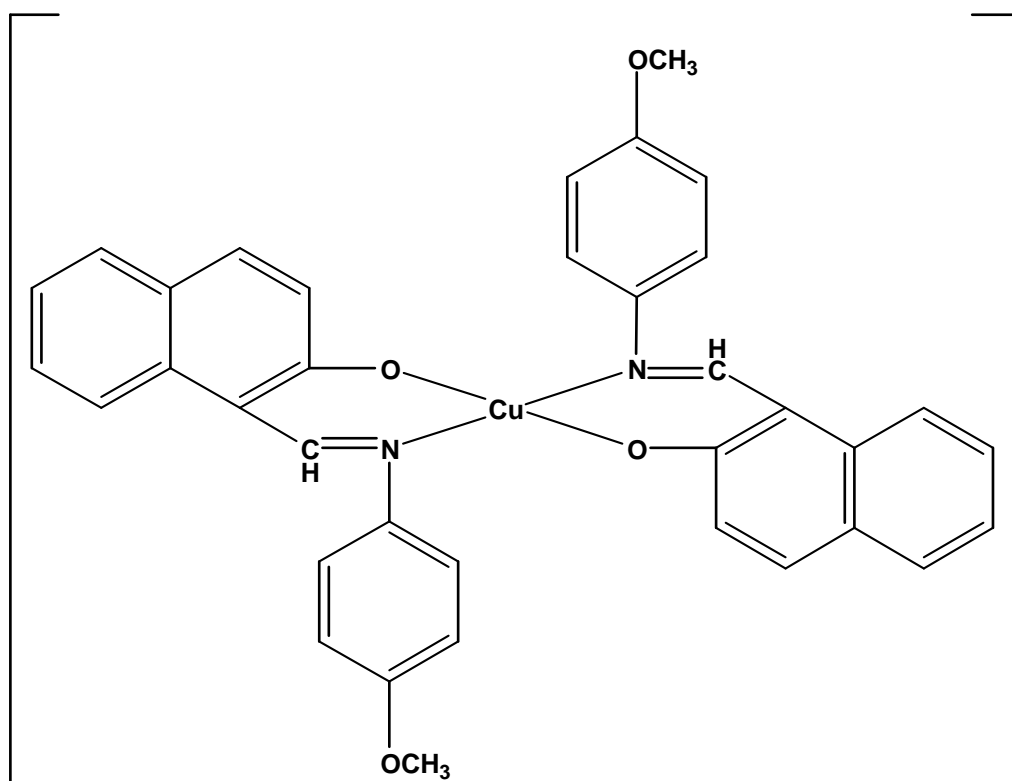
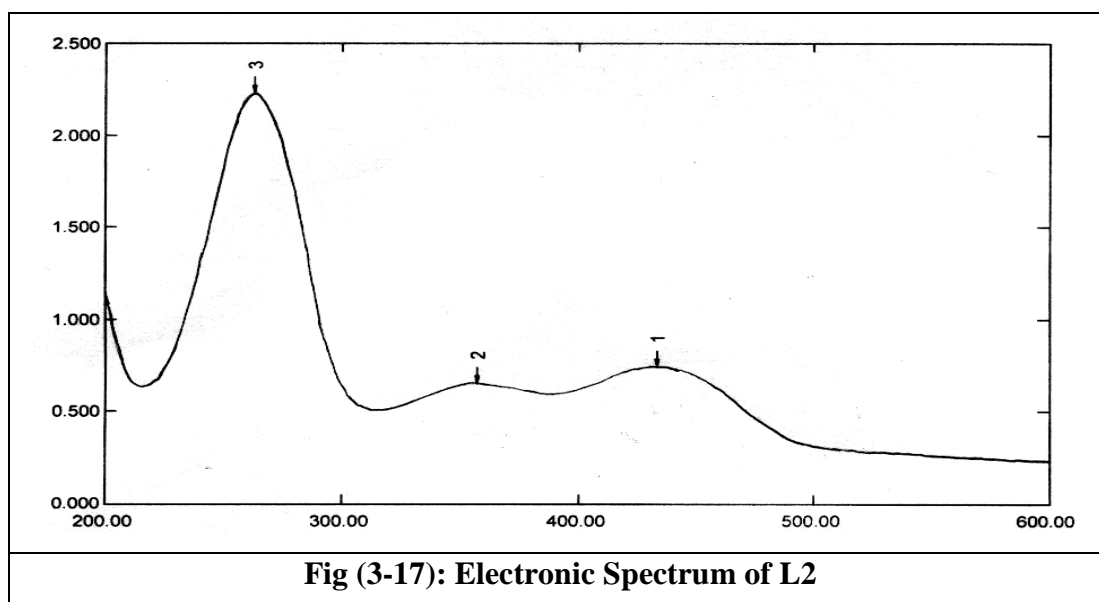
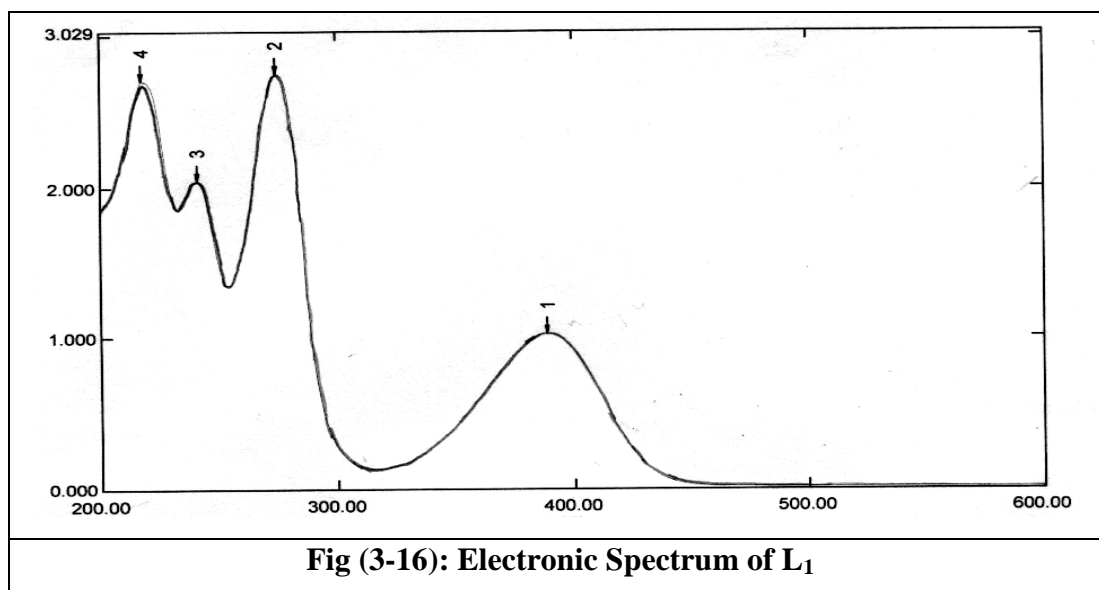
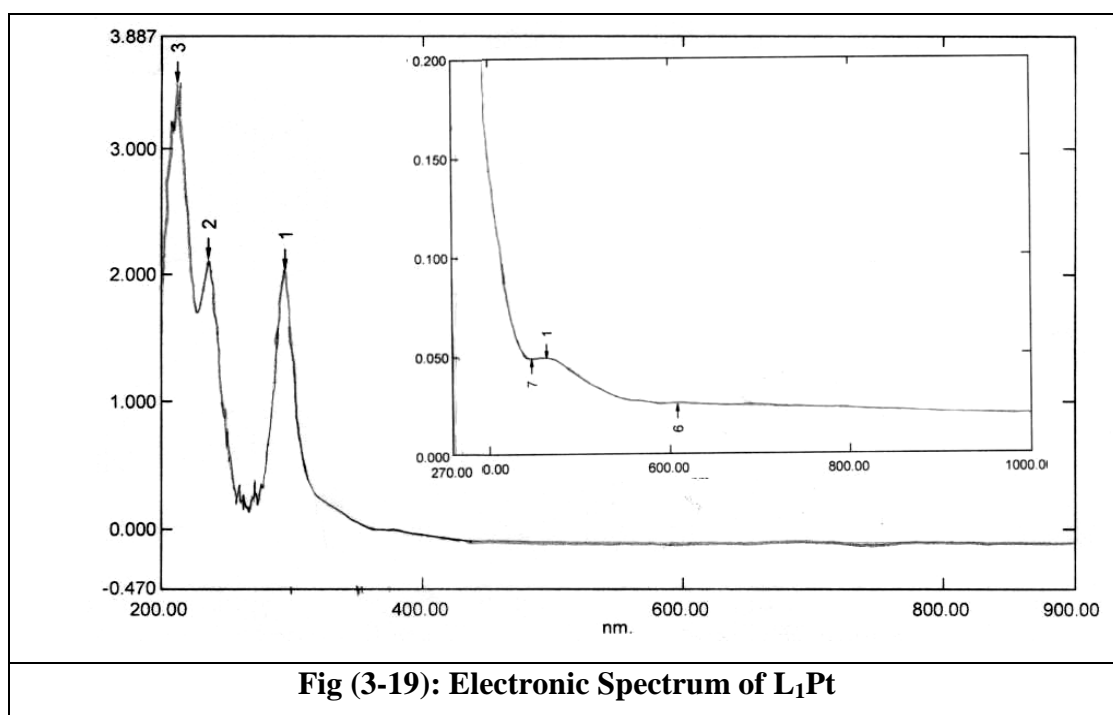
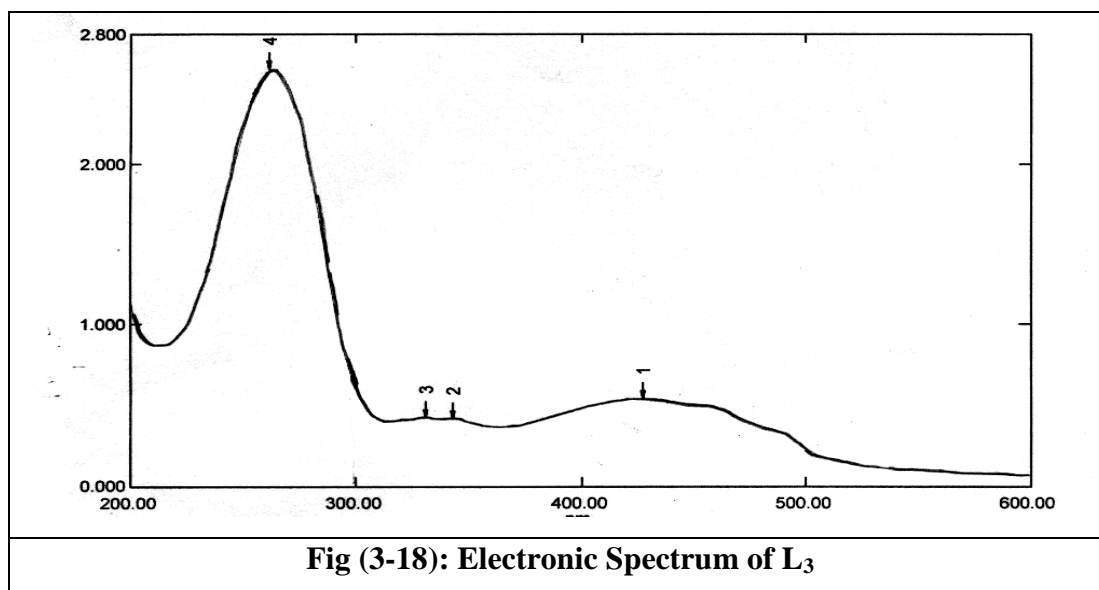
 L_3Cu

Table (3-5): The data of electronic spectra of the prepared compounds.

Compound	Band position, nm	Assignment
L ₁	389	n→π*
	274	π→π* (imino)
	241	π→π*(aromatic)
L ₂	433	n→π*
	357	π→π* (imino)
	262	π→π*(aromatic)
L ₃	427	n→π*
	343	π→π* (imino)
	261	π→π*(aromatic)
L ₁ Pt	464	¹ A _{1g} → ¹ T _{1g}
	293	L →M CT
L ₂ Pt	436	¹ A _{1g} → ¹ T _{1g}
	333	L →M CT
L ₃ Pt	465	¹ A _{1g} → ¹ T _{1g}
	350	L →M CT
L ₁ Au	440	¹ A _{1g} → ¹ A _{2g}
	356	L →M CT
L ₂ Au	576	³ A _{2g} → ³ T _{1g}
	318	L →M CT
L ₃ Au	490	¹ A _{1g} → ¹ A _{2g}
	352	L →M CT
L ₁ Pd	403	¹ A _{1g} → ¹ A _{2g} , ¹ A _{1g} → ¹ E _g , ¹ A _{1g} → ¹ B _{2g}
	325	C.T
L ₂ Pd	385	¹ A _{1g} → ¹ A _{2g} , ¹ A _{1g} → ¹ E _g , ¹ A _{1g} → ¹ B _{2g}
	377	C.T
L ₃ Pd	439	¹ A _{1g} → ¹ A _{2g} , ¹ A _{1g} → ¹ E _g , ¹ A _{1g} → ¹ B _{2g}
	220	C.T
L ₁ Cu	470	² B _{1g} → ² A _{1g} , ² B _{1g} → ² E _g (² B _{2g})
L ₂ Cu	500	² B _{1g} → ² A _{1g} , ² B _{1g} → ² E _g (² B _{2g})
L ₃ Cu	450	² B _{1g} → ² A _{1g} , ² B _{1g} → ² E _g (² B _{2g})





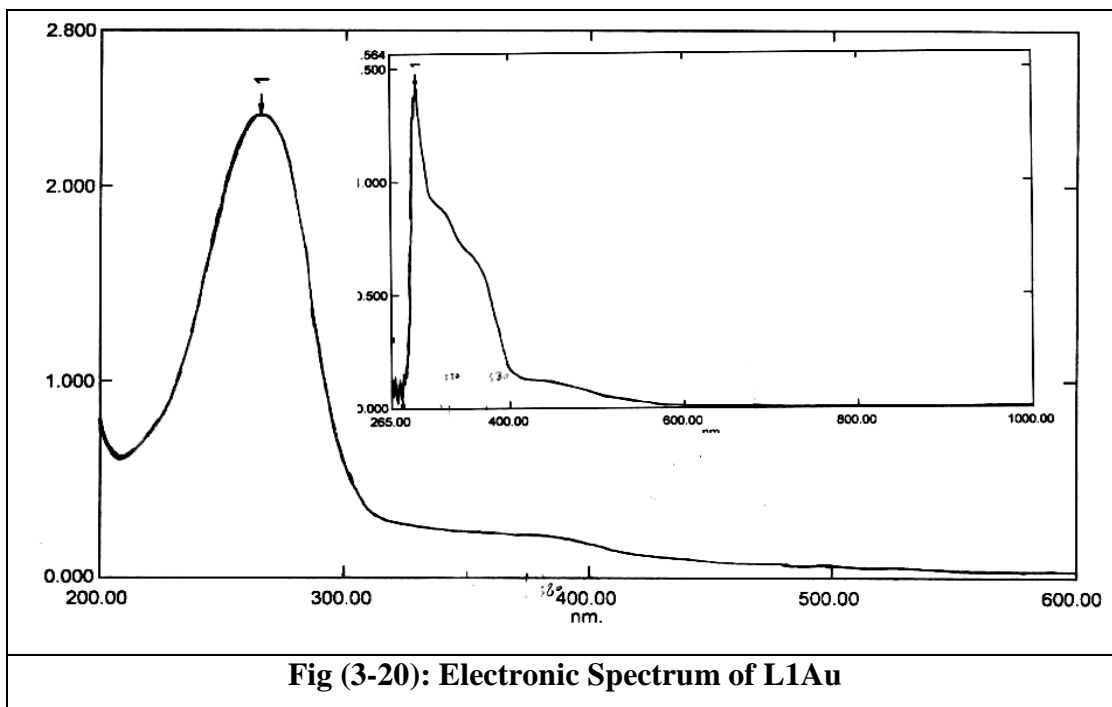


Fig (3-20): Electronic Spectrum of L1Au

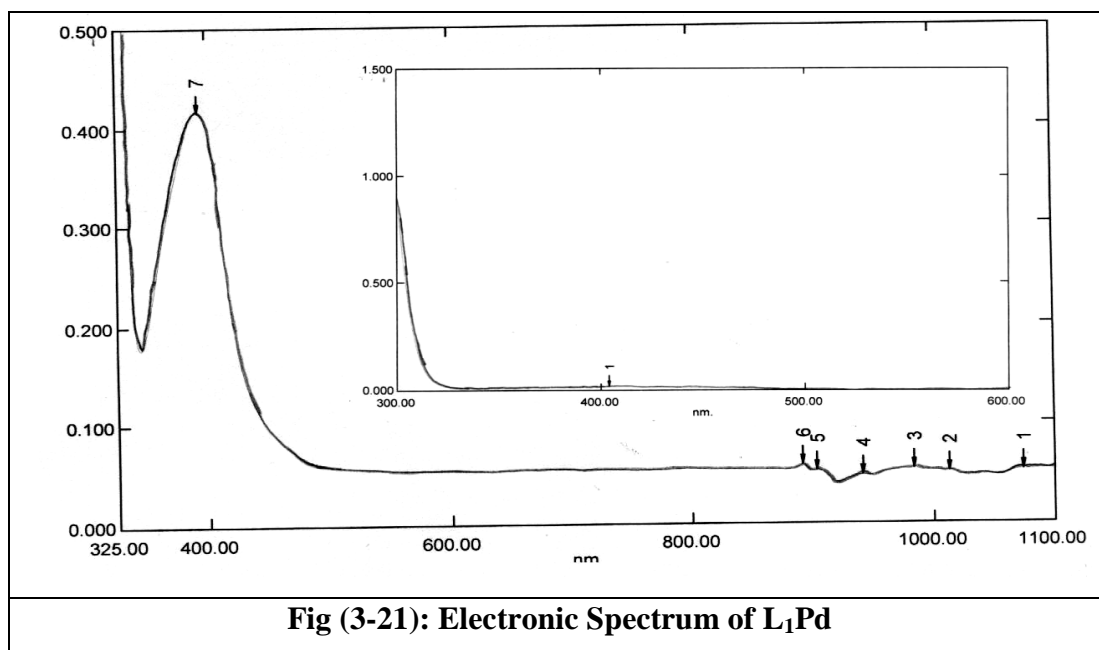
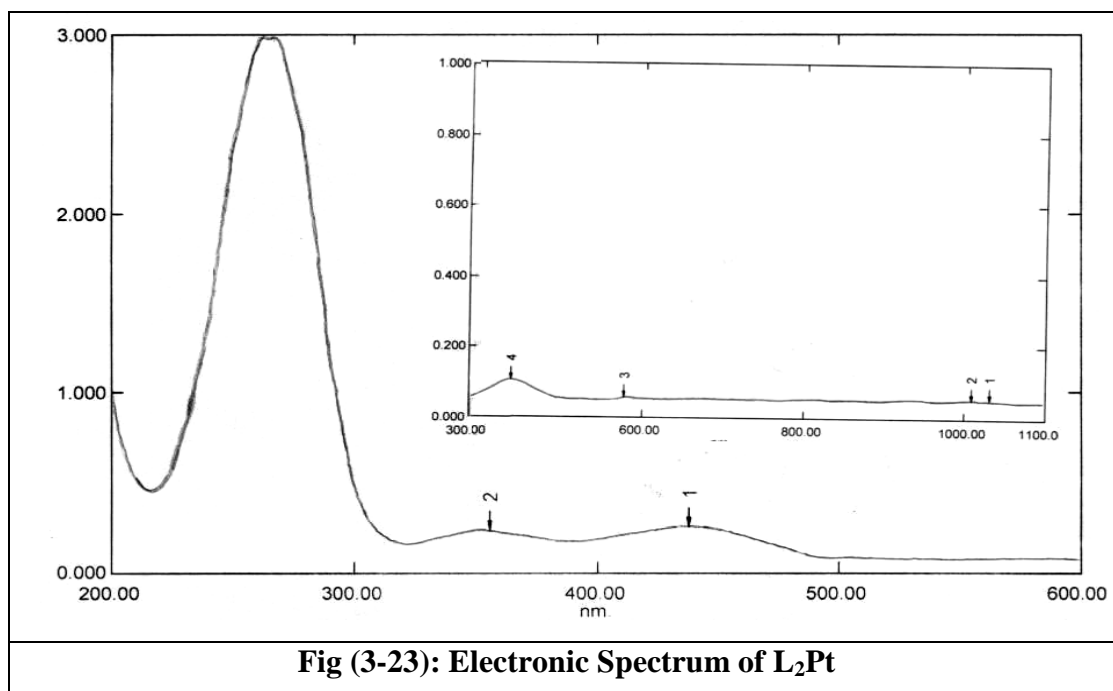
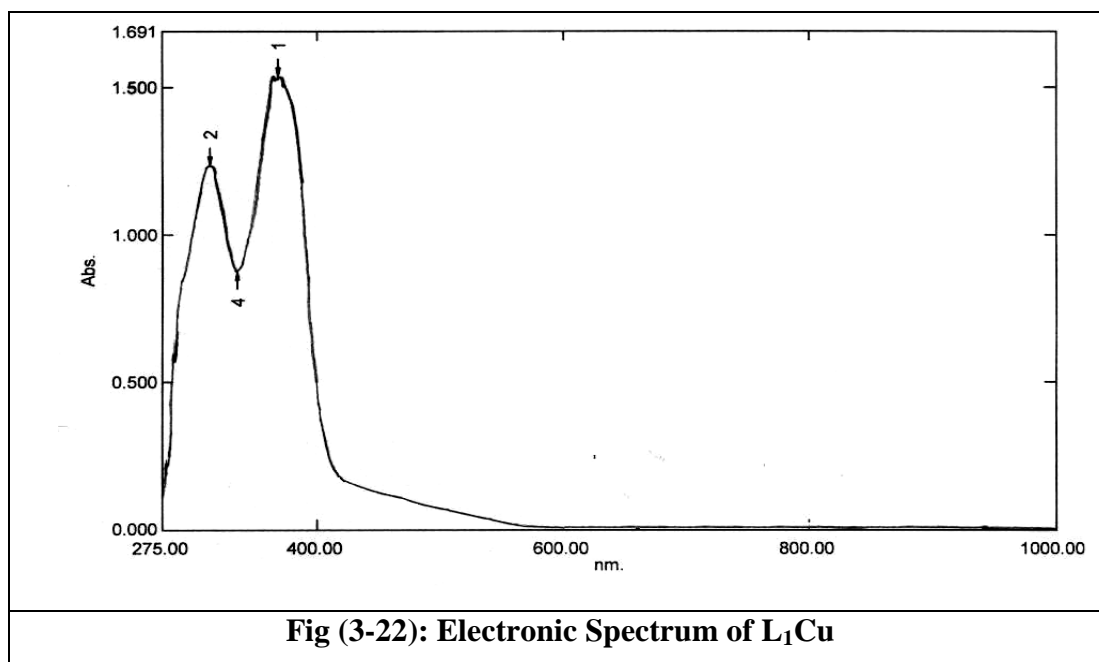
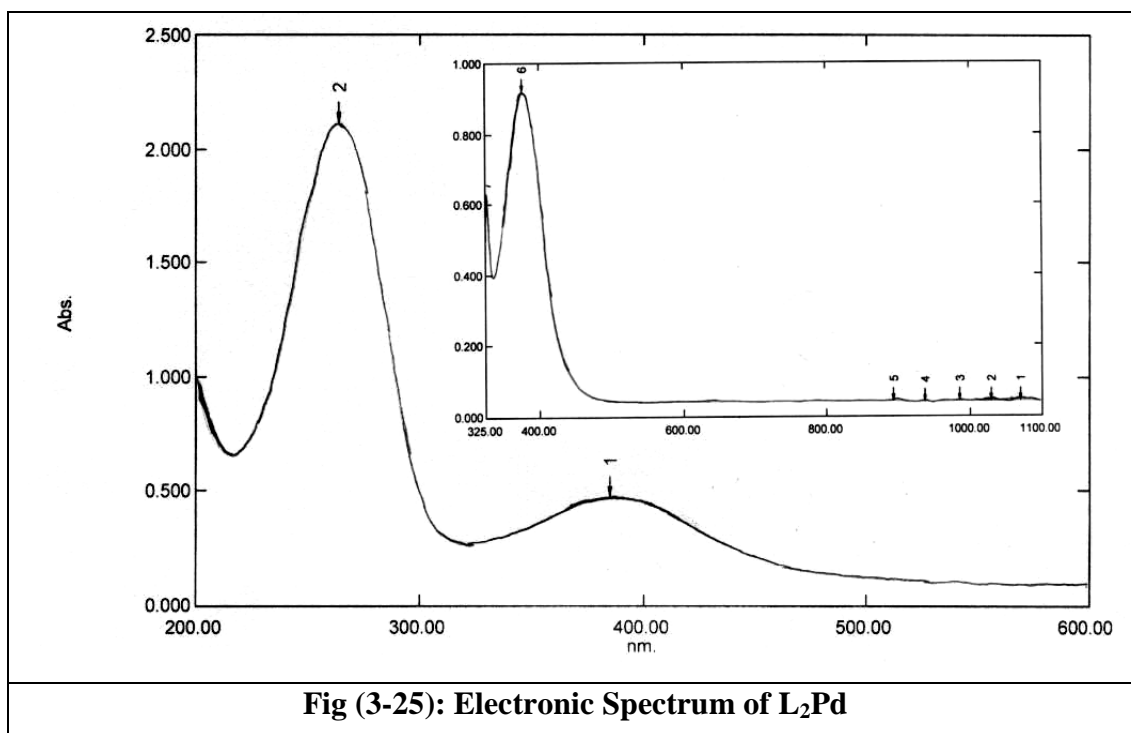
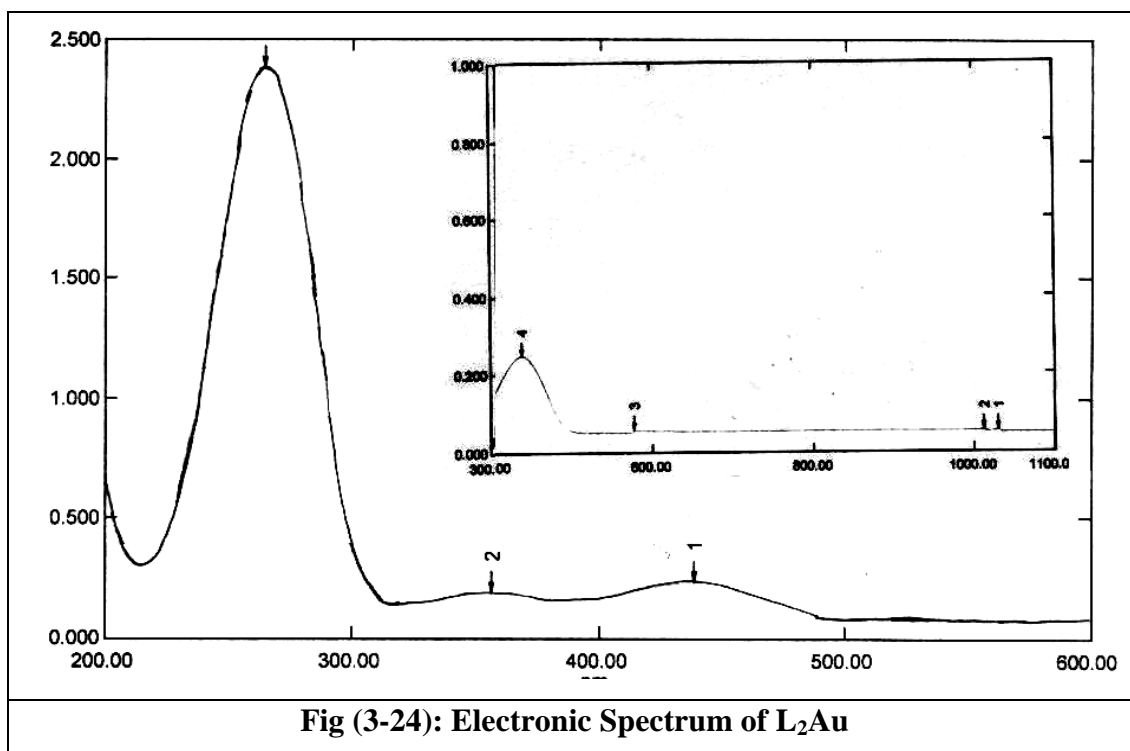
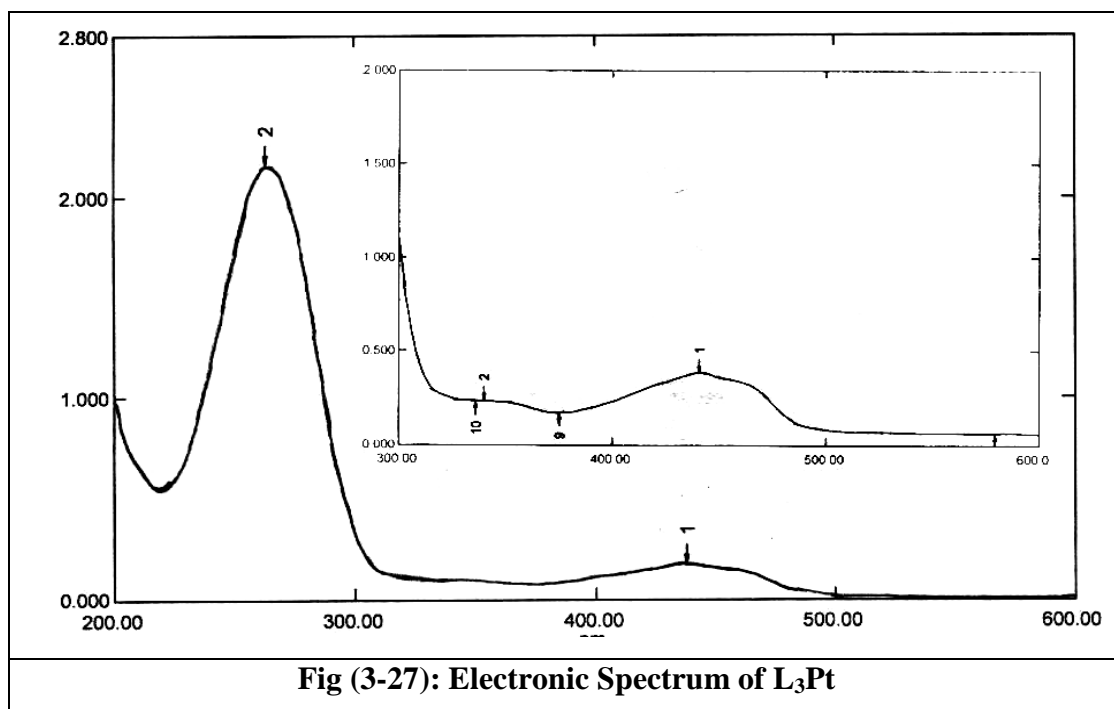
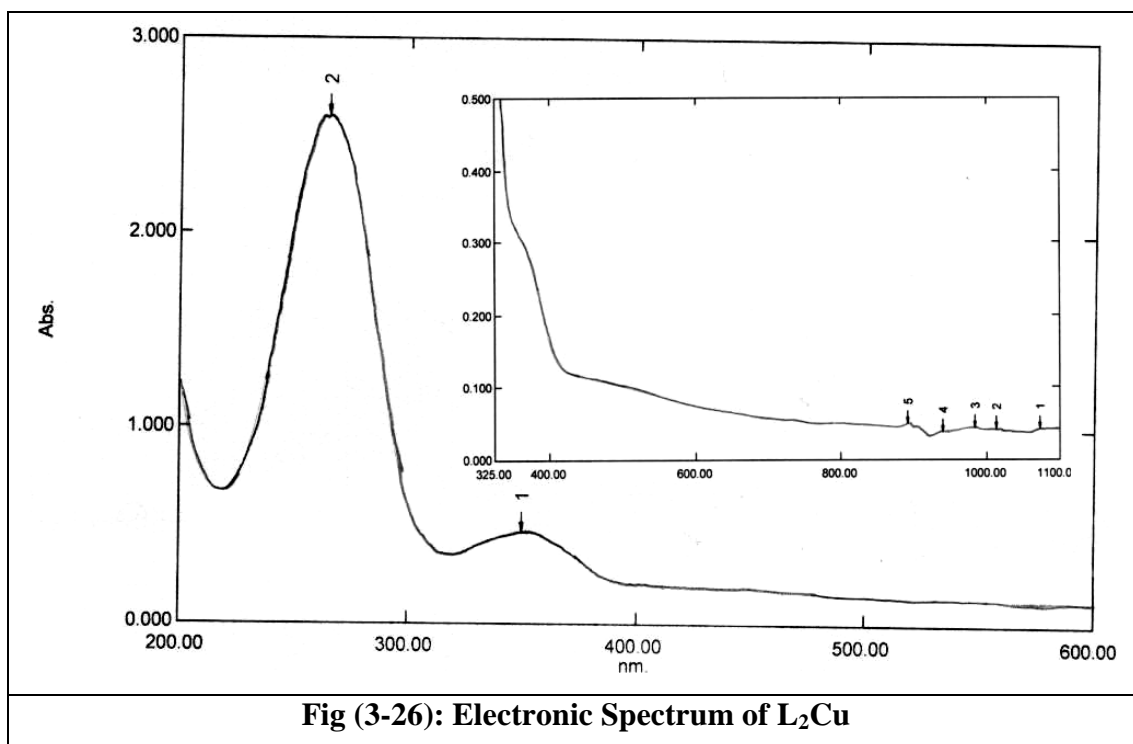
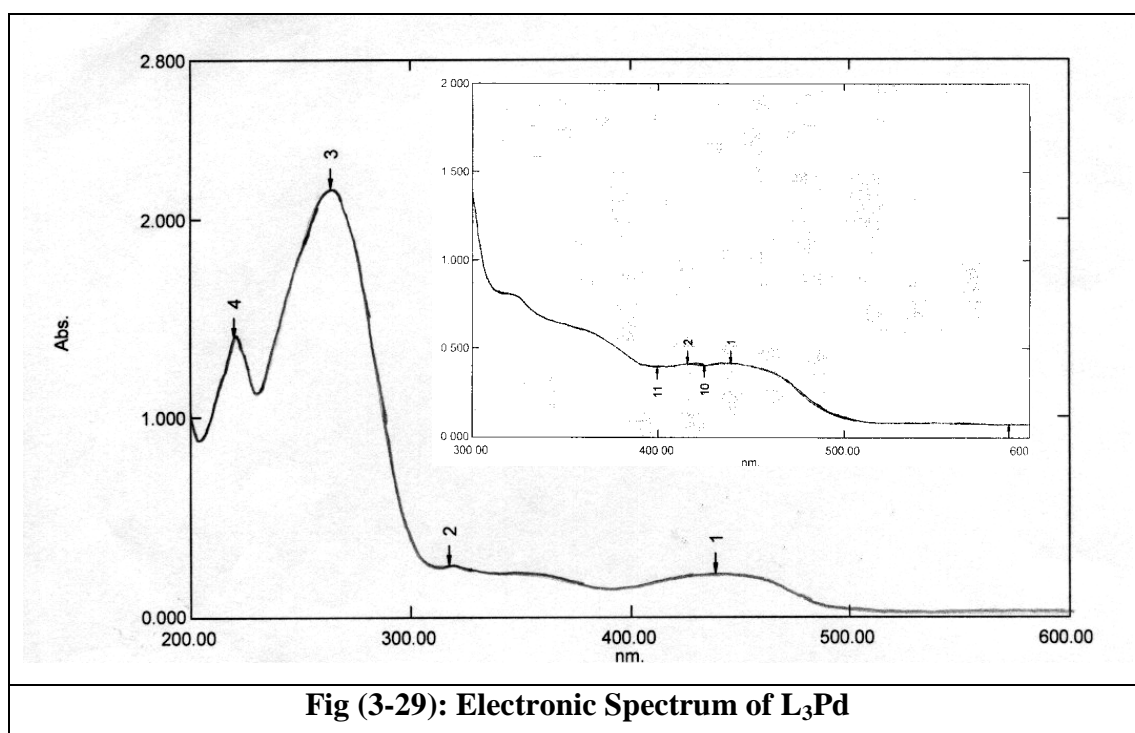
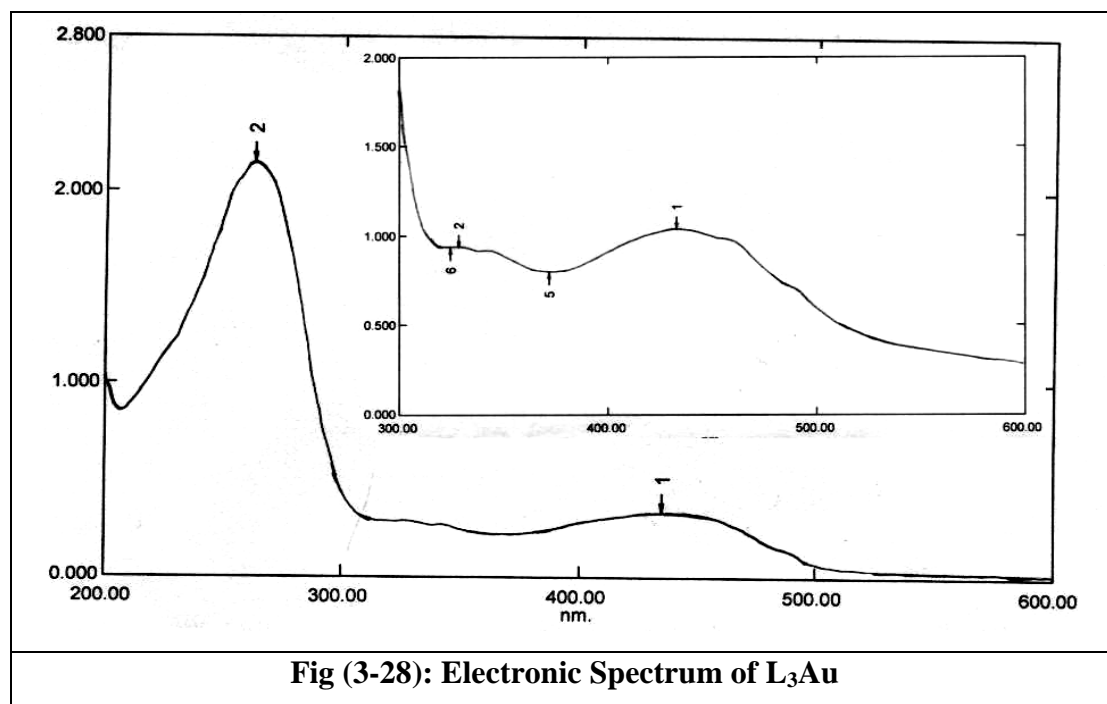


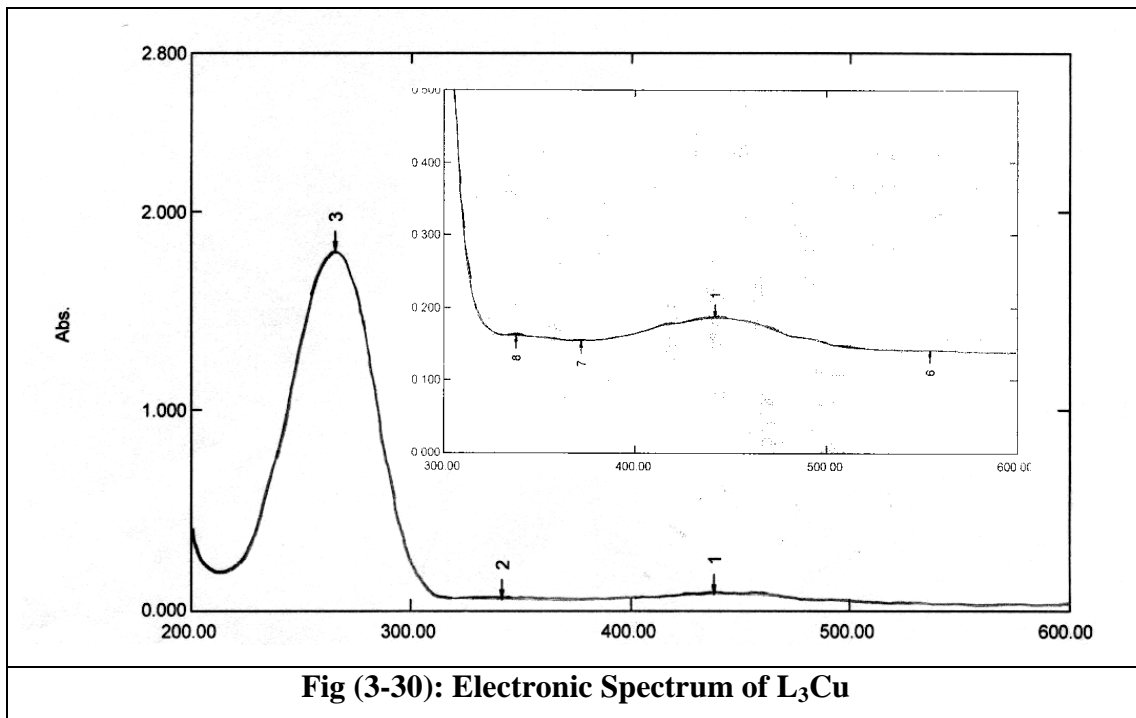
Fig (3-21): Electronic Spectrum of L1Pd











3-5 Glutathione S-transferase Purification:

In order to fully purify the GSTs, a sequence of purification steps have been conducted, these steps include Ion-exchange chromatography by DEAE-Cellulose, CM-cellulose, and gel filtration chromatography by Sephacryl S-200⁽⁷³⁾. GSTs activity, Protein Concentration and Specific Activity were determined for the enzyme in each step⁽¹¹⁹⁾.

3-5-1 Determination of Enzyme Volume for Enzyme Activity Assay:

GSTs activity (2-5-1-2-B) was determined for the supernatant of the crude sample, it has been noticed that 35 μ L is the best volume of crude enzyme which gave the highest absorption at 340nm as shown in Figure (3-31), and this volume was used to measure the enzyme activity in the next steps of purification.

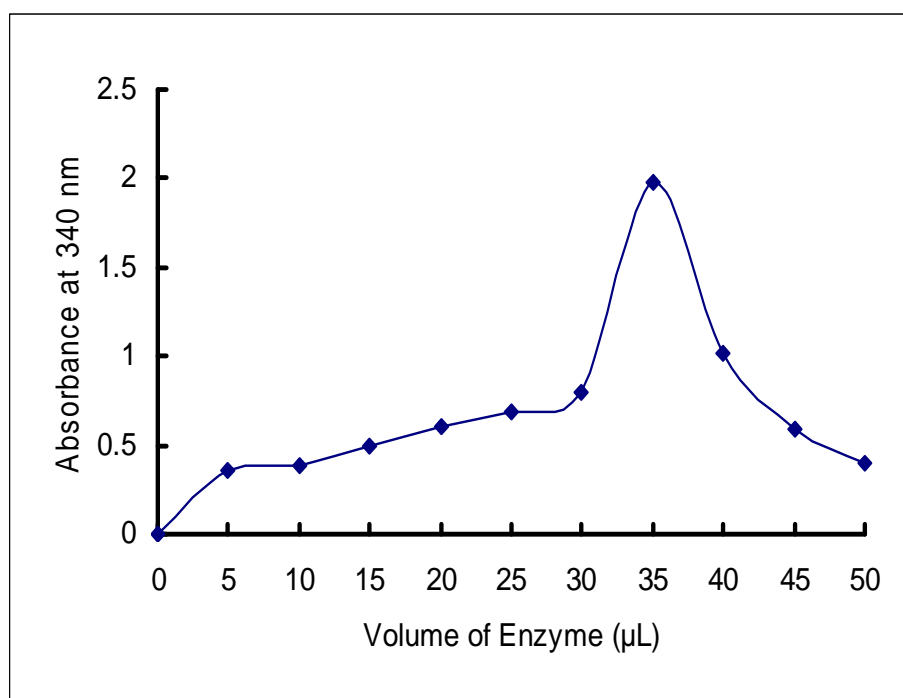


Figure (3-31): Standard curve of enzyme activity at different volumes after 300 seconds.

3-5-2 Crude Extract:

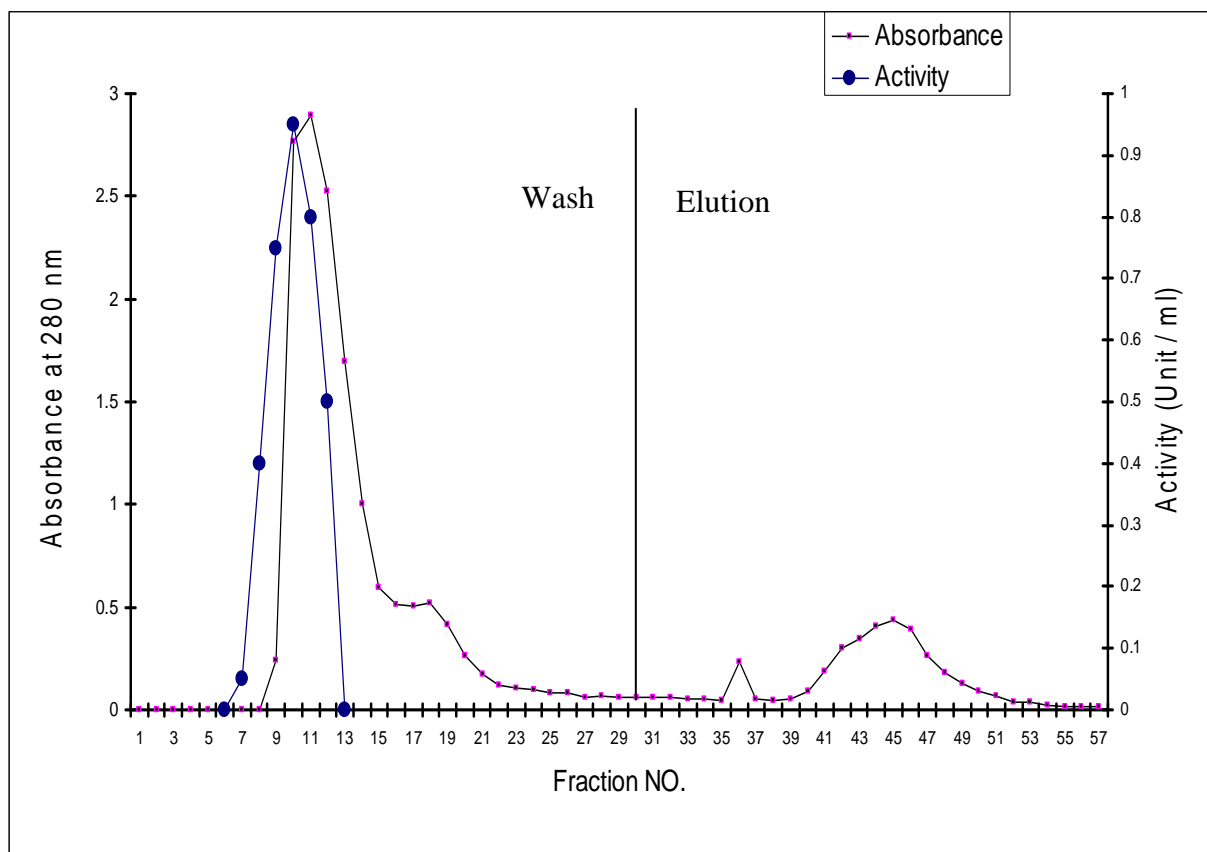
After determining GSTs activity (2-5-1-2-B) and protein concentration (2-5-3-2-6) for the supernatant of the crude sample, it had been found that the crude sample had demonstrated a specific activity of 2.977×10^{-3} U/mg protein with fold (1) and 100% over all yield, as shown in Table (3-6).

3-5-3 Purification by Ion Exchange Chromatography:

A- DEAE-Cellulose:

The first step in Purification of GSTs was done by using ion exchange chromatography using DEAE-Cellulose column⁽¹²⁰⁾, after being dialyzed. Figure (3-32) shows the protein peaks obtained from ion exchange chromatography using DEAE-Cellulose and it reflects the presence of three proteins by reading the absorbance at (280nm).

Estimation of GSTs activity (2-5-1-2-B) in all eluted protein peaks showed that the first peak contain GSTs activity. While the second and third peaks, which appeared after addition of 0.2M NaCl in the same buffer, contain no GSTs activity. Thus DEAE-Cellulose column retained about 80% of the applied protein whereas enzyme activity, as assayed by 1-chloro-2, 4-dinitrobenzene, was not adsorbed⁽⁷³⁾. The fractions of the first peak were then all collected and after determining GSTs activity (2-5-1-2-B) and protein concentration (2-5-3-2-6), it was found that the partially purified enzyme had demonstrated a specific activity of 4.450×10^{-3} U/mg protein with 2.219 purification folds and 96.45% over all yields, as shown in Table (3-6).



Figure(3-32): Purification of crude GSTs on DEAE-Cellulose column (30X2.5cm). the column was eluted by using 10mM tris buffer (pH 8.0), then eluted by using gradient of 10mM tris buffer (pH8.0) containing 0.2M NaCl, at flow rate of (50ml/hour).

B- CM-Cellulose:

The second step in the purification of GSTs was done by ion exchange chromatography using CM-Cellulose column. The results shown in Figure (3-33), indicate that after washing with (150 ml) of phosphate buffer (10mM) (pH 6.7) (buffer C), two protein peaks were observed by reading the absorbance at (280 nm). Plotting (260ml) gradient of phosphate buffer (400mM) (pH 6.7) (buffer D), two further protein peaks were obtained. Estimation of the GSTs activity (2-5-1-2-B) in all protein peaks showed that the first couple washing peaks contains

no GSTs activity, while GSTs activity for the second couple was found to be concentrated in the second peak fractions. Therefore the fractions of the second peak of couple two were collected and after determining GSTs activity (2-5-1-2-B) and protein concentration (2-5-3-2-6), it had been found that the partially purified enzyme had demonstrated a specific activity of (74×10^{-3} U/mg protein) with (30.142) purification folds and yield of GSTs of (64.59%)., as shown in Table (3-6).

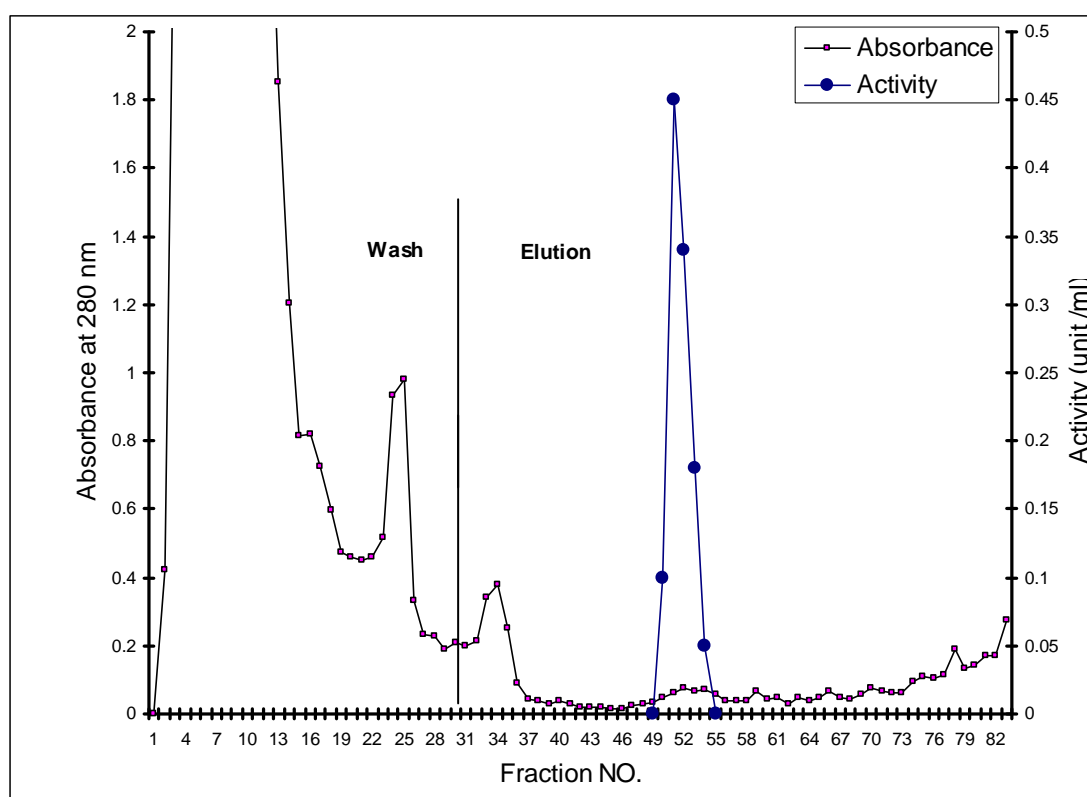


Figure (3-33): Purification of GSTs on CM-Cellulose column (30X2.5cm). The column was eluted by using 10mM phosphate buffer (pH 6.7), then eluted by using gradient of 400mM phosphate buffer (pH 6.7), at flow rate of (50ml/hour).

3-5-4 Purification by Gel Filtration Chromatography:

Partially purified GSTs represented by the collected fractions from step B above were subjected to further purification using gel filtration column⁽¹²¹⁾. By reading the absorbance at (280nm), two major protein peaks were observed as shown in Figure (3-34).

Estimation of the GSTs activity in the two peaks showed that the first one contains no GSTs activity, and it was found to be concentrated in the second one. The fractions of the second peak were then collected and after determining GSTs activity (2-5-1-2-B) and protein concentration (2-5-3-2-6) it had been found that the purified enzyme had demonstrated a specific activity of 1250×10^{-3} U/mg protein with purification folds 512.295 and 56.43% over all yields, as shown in Table (3-6).

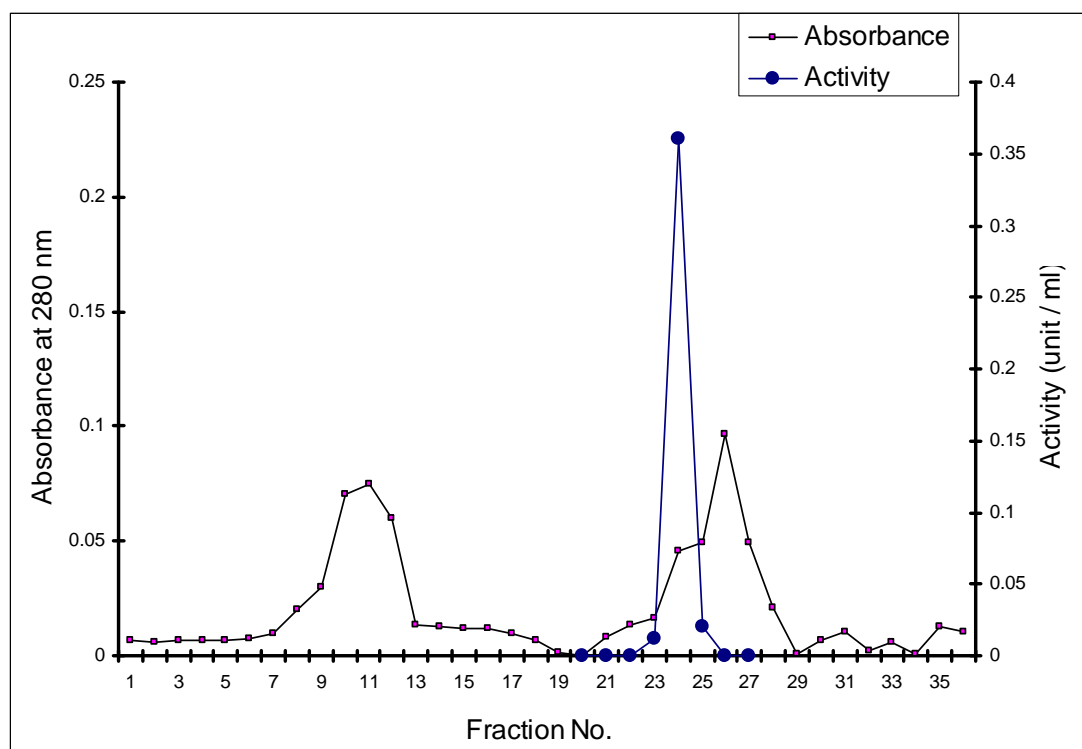


Figure (3-34): Purification of GSTs on Sephacryl S-200 column (63X2cm). Eluent: 0.1M phosphate buffer (pH 6.7), at a flow rate of (30ml/hour).

Table (3-6): Purification steps of Glutathione S-transferase.

Purification Step	Vol. (ml)	Activity (U/ml) X10 ⁻³	Protein Conc. (mg/ml)	Specific Activity (U/mg)X10 ⁻³	Total Activity (U)X10 ⁻³	Purification fold	Yield (%)
Crude Extract	50	1.329	0.446	2.977	66.45	1	100
Ion exchange Chromatography (DEAE- Cellulose)	34	1.885	0.346	5.45	64.09	2.219	96.45
Ion exchange Chromatography (CM-Cellulose)	20	2.146	0.029	74	42.92	30.142	64.59
Gel Filtration (Sephacryl S-200)	10	3.75	0.003	1250	37.5	512.29	56.43

3.5.5 Test of GSTs Purity and its Molecular Weight Determination

The purity of the purified GSTs was determined by polyacrylamide gel electrophoresis under denatured conditions. The purified enzyme preparation showed only single protein band on the gel after staining with commassie brilliant blue R-250, indicating the probability of reaching the apparent homogeneity of purification process Figure (3-35). The location of the protein band on the gel could be as a result of the low molecular weight of the protein, since the electrophoresis mobility of protein in the gel essentially depends on the molecular weight of the protein in addition to its net charge⁽¹²²⁾, this low molecular weight was determined by comparison with standard protein of known molecular weight.

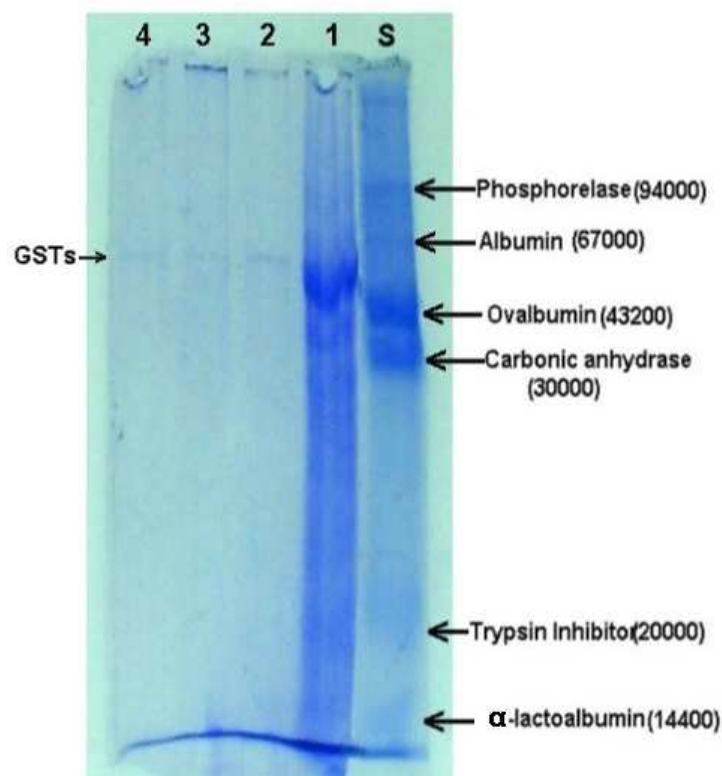


Figure (3-35): Shows the electrophoresis of GSTs enzyme taking from mouse liver in acrylamide gel in presence of SDS and mercapto ethanol and determining the molecular weight of purified enzyme.

The standard curve Figure (3-36) of standard proteins in acrylamide gel in presence of SDS, was used to calculate the molecular weight of the enzyme by electrophoresis method. The molecular weight obtained was 50000 Dalton.

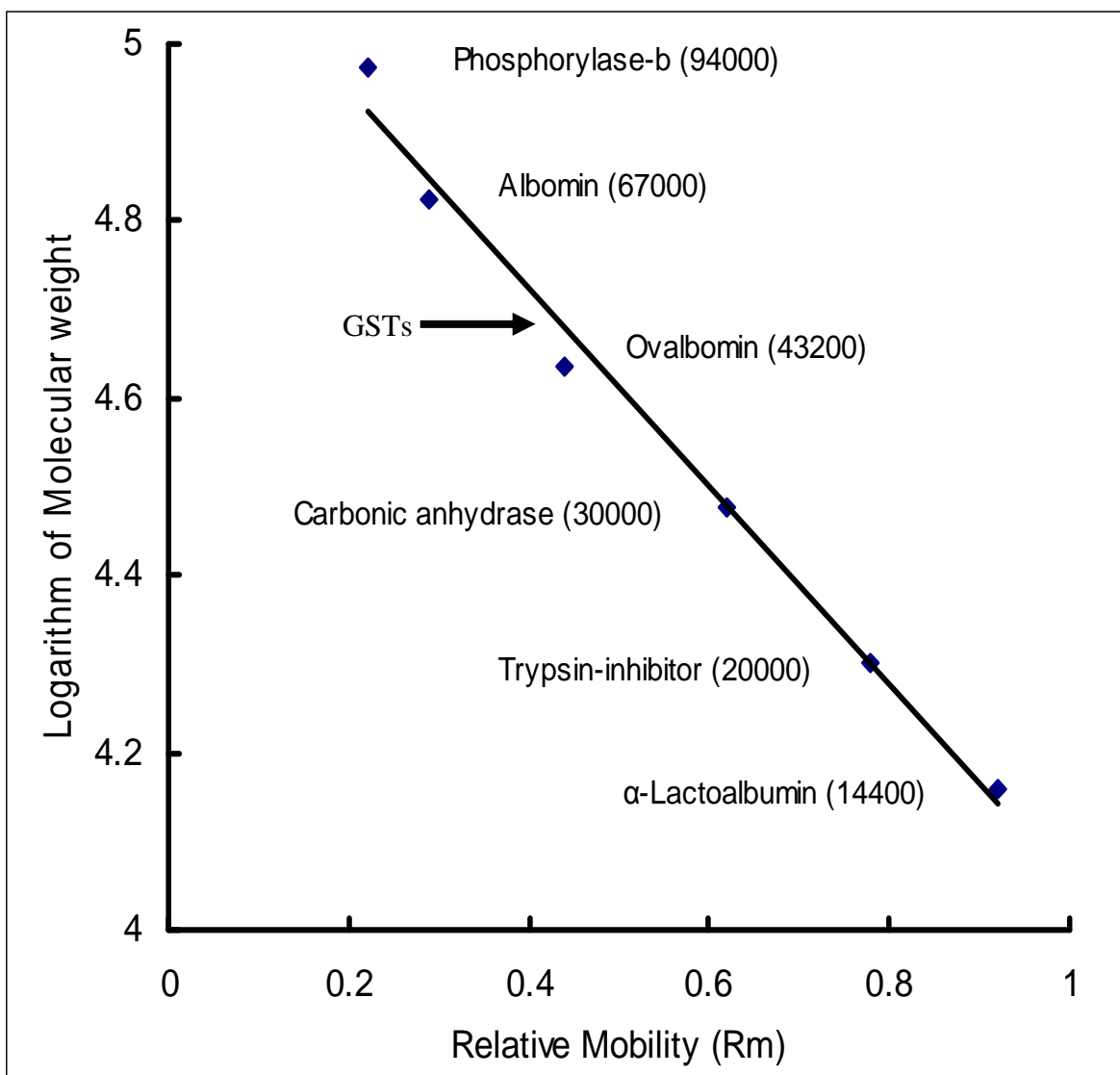


Figure (3-36): Molecular weight determination for purified GSTs extracted from rat liver, using gel filtration chromatography on Sephacryl S-200 column

3-6 Study of the Conjugation Process:

3-6-1 Determination of λ_{max} for the Glutathione Conjugate:

The λ_{max} , which was chosen to follow the interaction process between GSH and CDNB, was that characteristic for the conjugate and not found in the spectra of CDNB or GSH alone, as seen in Figures (3-46, 3-47). The value of this maximum wavelength was found to be at 340 nm for the conjugate. Which was compatible with that reported earlier⁽⁶³⁾.

The selected λ_{max} for studying the conjugation between GSH and the metal complexes was that characteristic for the metal complex itself, which depend on the type of the complex.

3-6-2 Kinetic Studies:

Accurate absorbance measurements of known concentration of starting compound and of the resulting product allowed the absorbance change, ΔA to be obtained for each compound. This value was necessary for each compound. It is converted to the rate of reaction ($\Delta A \cdot \text{min}^{-1}$).

The following bimolecular rate equation for the conjugation reaction was established:

$$r = k_2 [\text{compd.}] [\text{GSH}]$$

Where r is the initial rate of reaction, k_2 is second order rate constant, $[\text{compd.}]$ is the initial concentration of the tested compound and $[\text{GSH}]$ is the initial concentration of GSH.

In this study, initial rates of reaction were obtained in phosphate buffer (as mentioned in chapter 2) at 30°C. The concentration of the tested compounds was [1.0mM] and that of GSH [1.0mM], values of k_2 in $\text{mol}^{-1} \cdot \text{L} \cdot \text{min}^{-1}$ were calculated for each complex using the rate equation above.

3-6-3 Study of the Interaction between GSH and the Substrates:

3-6-3-1 CDNB-substrate

CDNB was chosen as a standard substrate since it was reported^(63,93) to be good general one for spectroscopic assay of GSTs activity, and found to conjugate by the enzyme to GSH through electrophilic-nucleophilic reaction.

The rate and rate constant of the conjugation reaction between CDNB and GSH, under the previously established conditions, in the absence and presence of the enzyme, are shown in Table (3-7) and Figure (3-37).

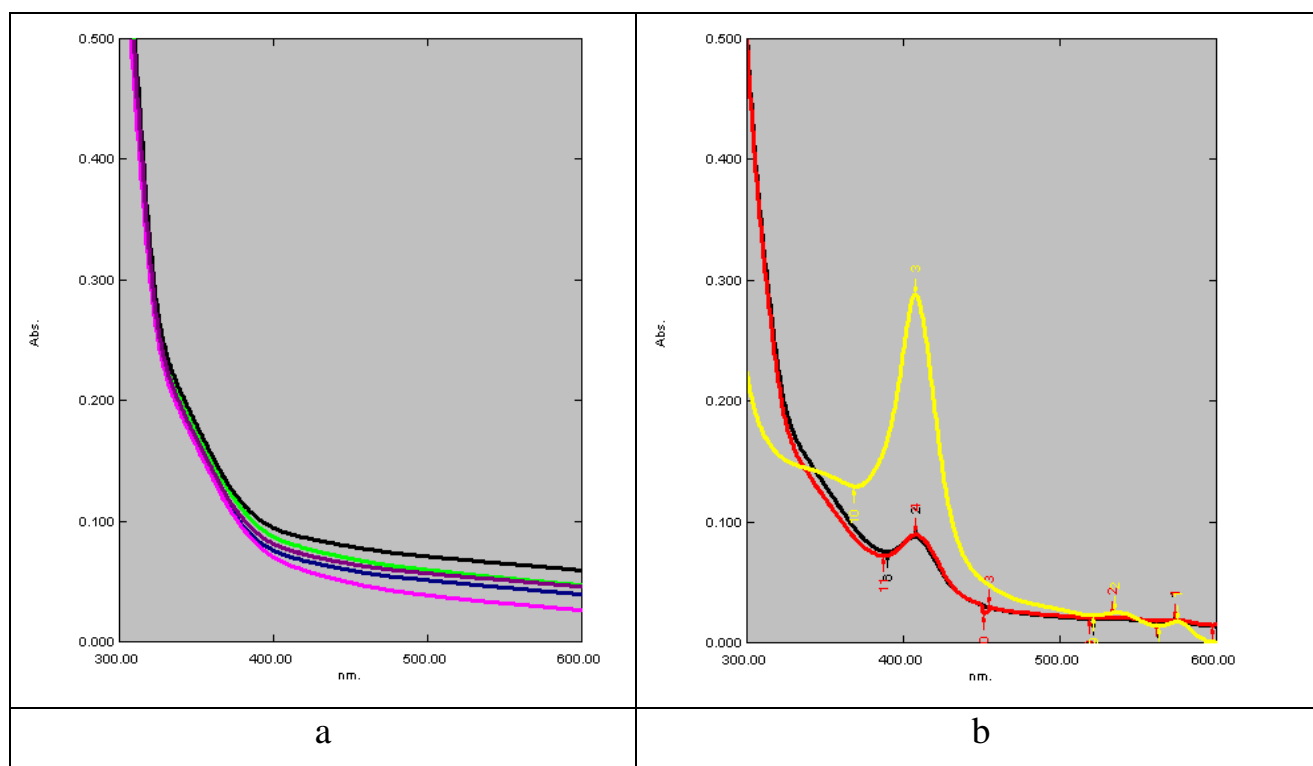


Figure (3-37): Change of absorbance for the conjugation reaction between GSH and CDNB with time in the absence (a) and presence (b) of enzyme.

The results show that the rate constant for the enzymatic reaction was 10 times than of the nonenzymatic rate.

3-6-3-2 Metal complexes as substrates:

A study of the new pt(IV), Au(III), Pd(II) and Cu(II) complexes of aromatic Schiff bases of expected anti-tumor activity was undertaken to establish whether a particular complex could react with GSH under physiological conditions, and therefore whether it's a potential substrate for GSTs. Figures (3-38)-(3-45) show the absorbance changes with times for the conjugation reactions.

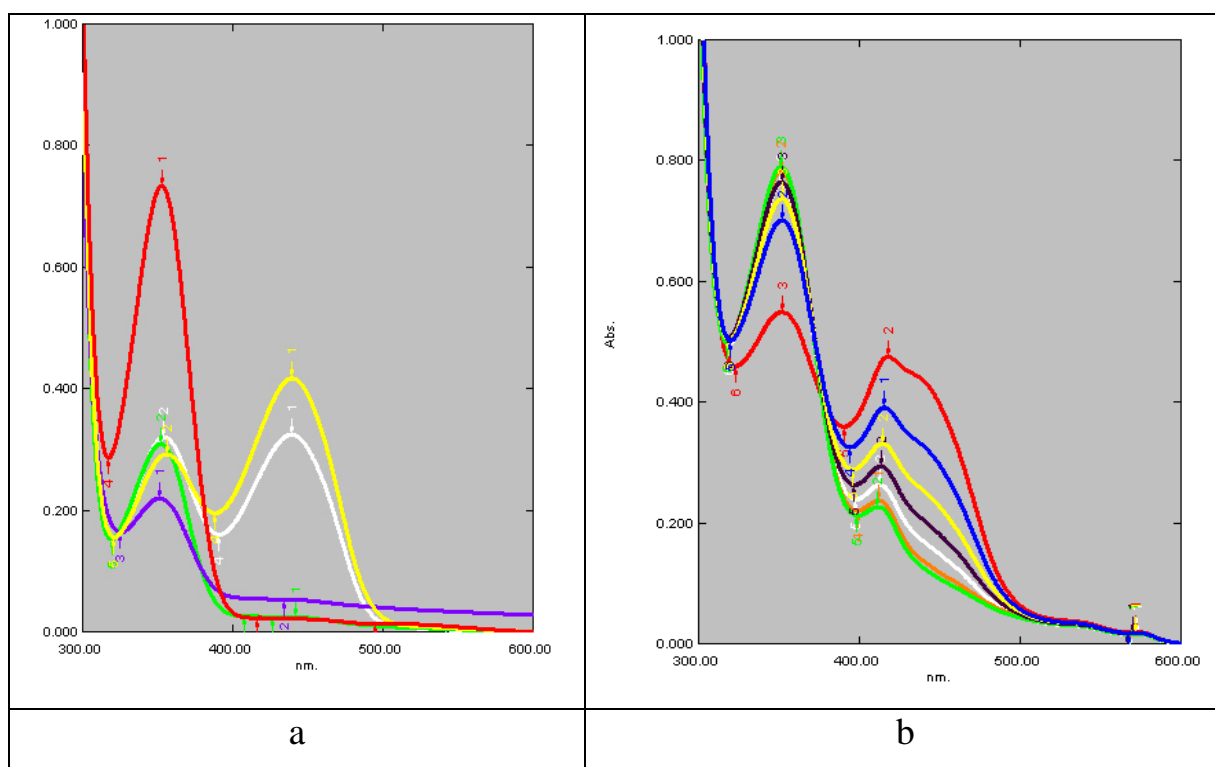


Figure (3-38): Change of absorbance for the conjugation reaction between GSH and L₂Pt with time in the absence (a) and presence (b) of enzyme.

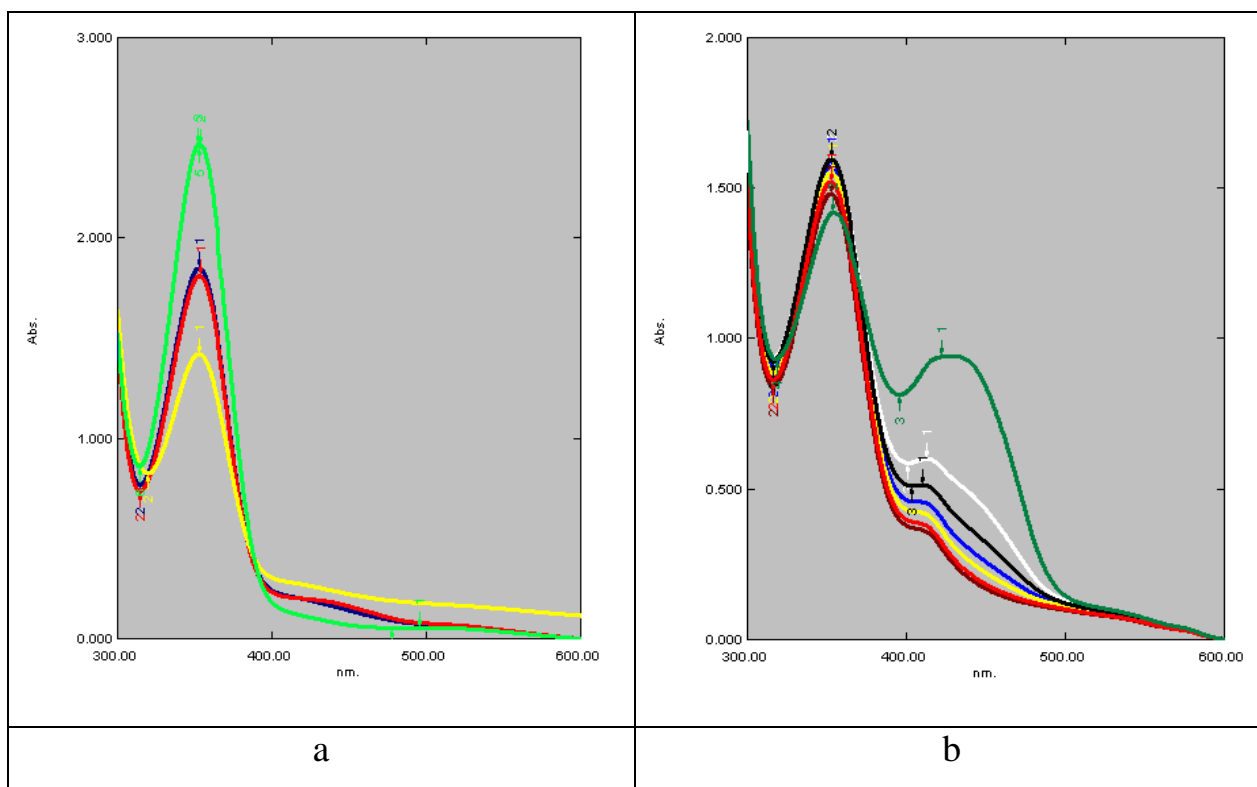


Figure (3-39): Change of absorbance for the conjugation reaction between GSH and L_2Au with time in the absence (a) and presence (b) of enzyme.

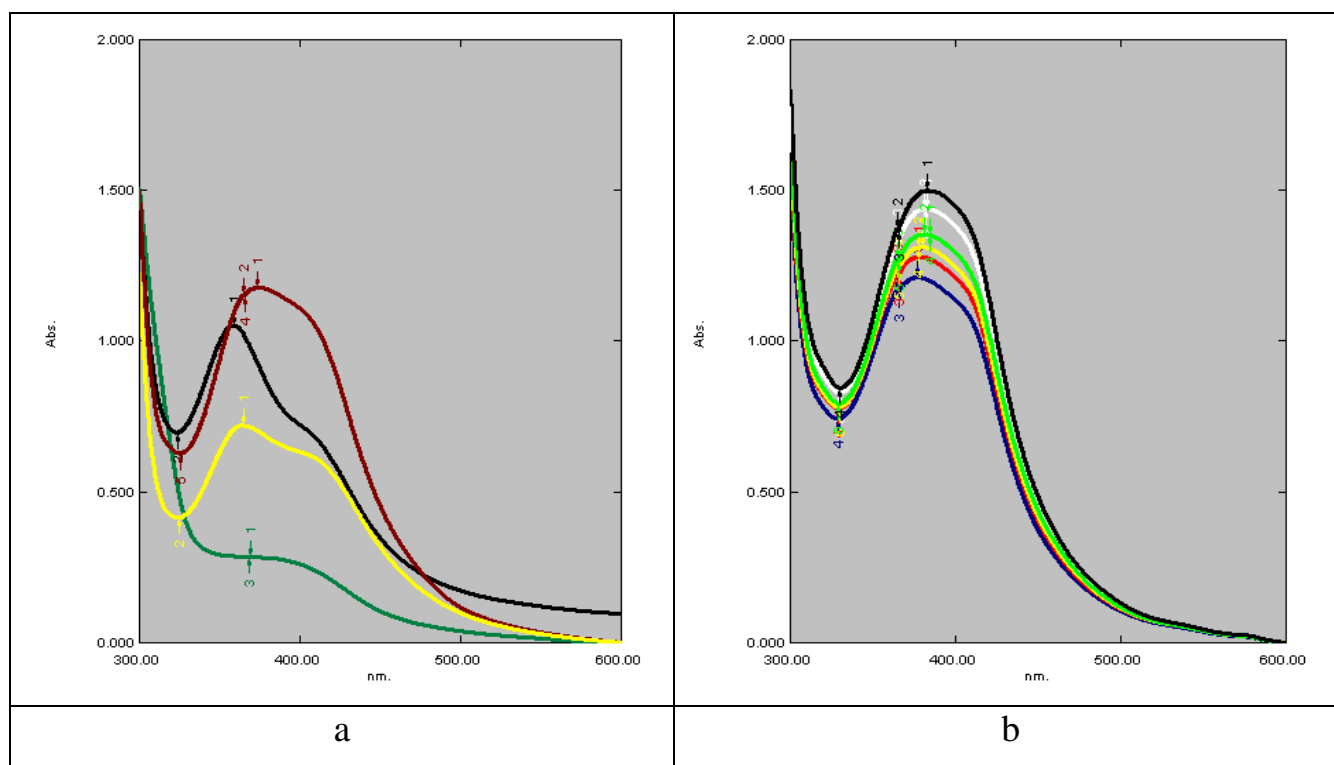


Figure (3-40): Change of absorbance for the conjugation reaction between GSH and L_2Pd with time in the absence (a) and presence (b) of enzyme.

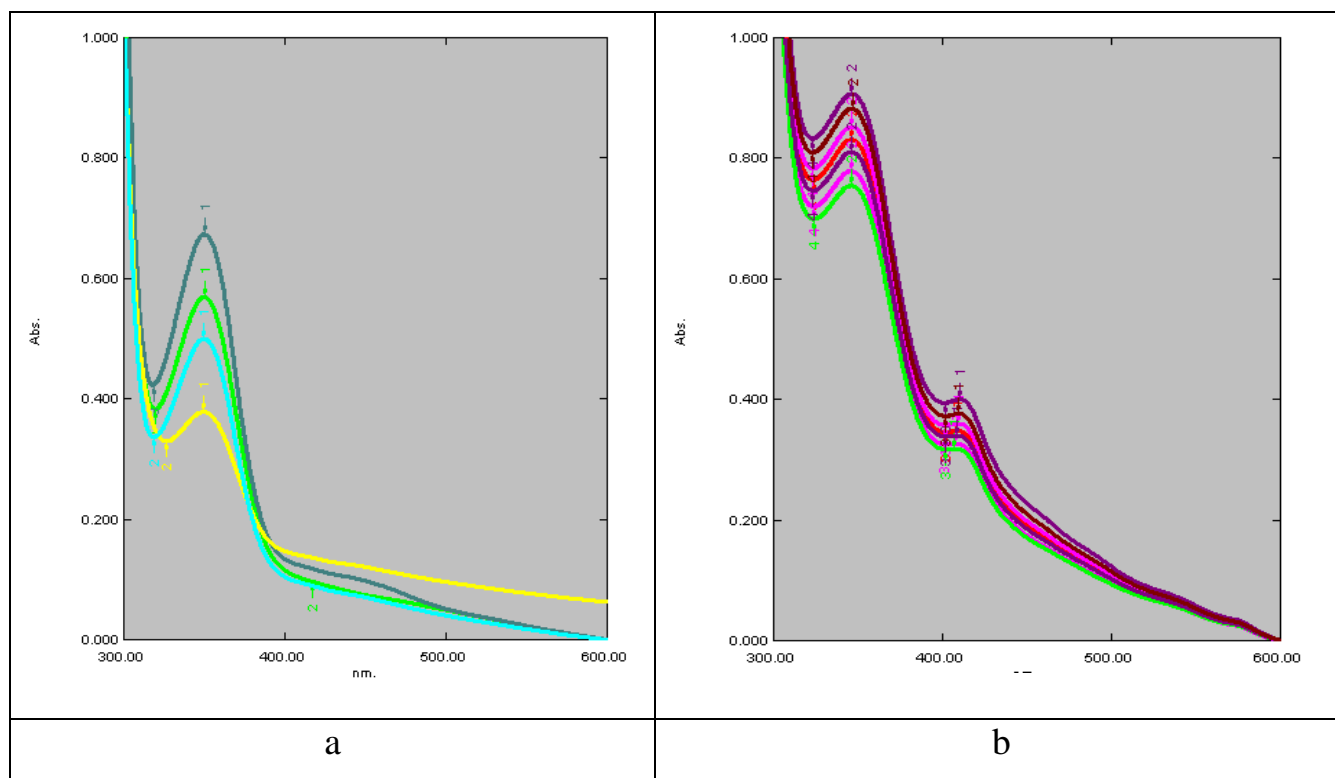


Figure (3-41): Change of absorbance for the conjugation reaction between GSH and L₂Cu with time in the absence (a) and presence (b) of enzyme.

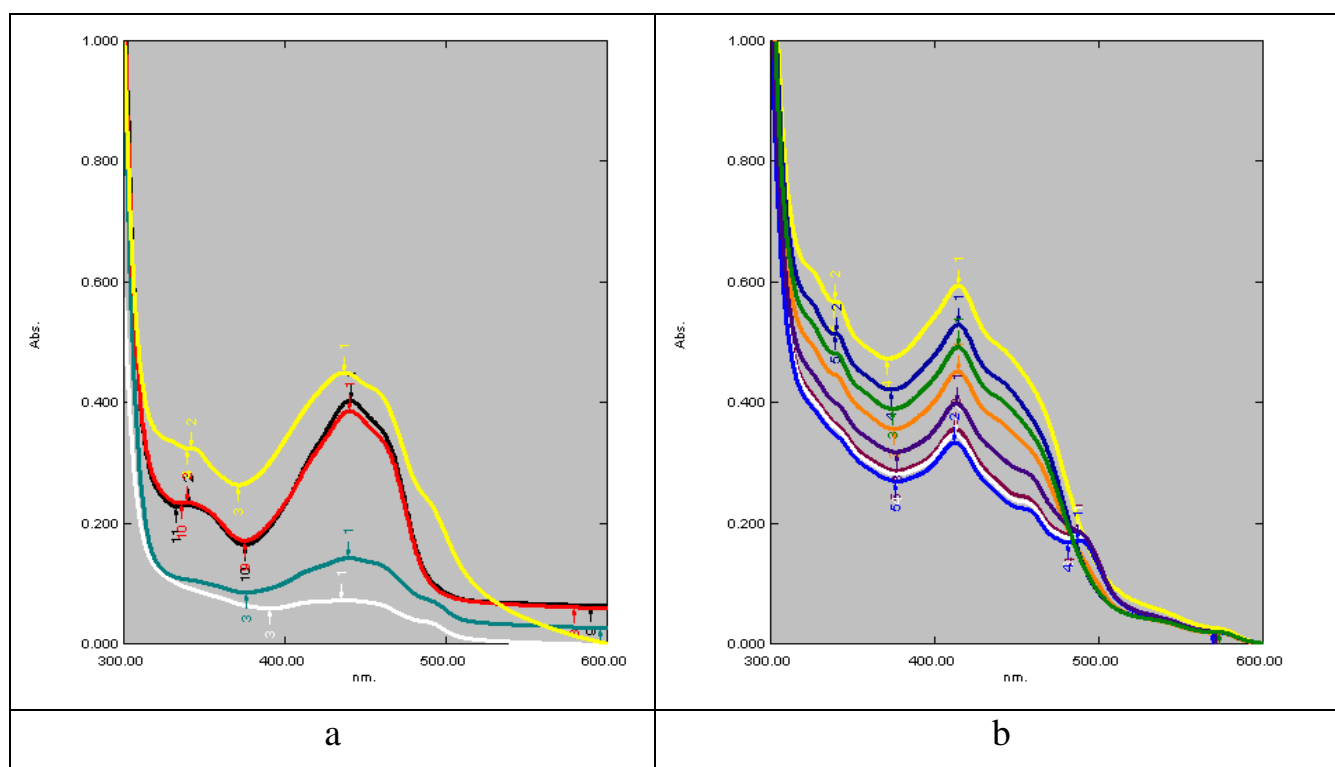


Figure (3-42): Change of absorbance for the conjugation reaction between GSH and L₃Pt with time in the absence (a) and presence (b) of enzyme.

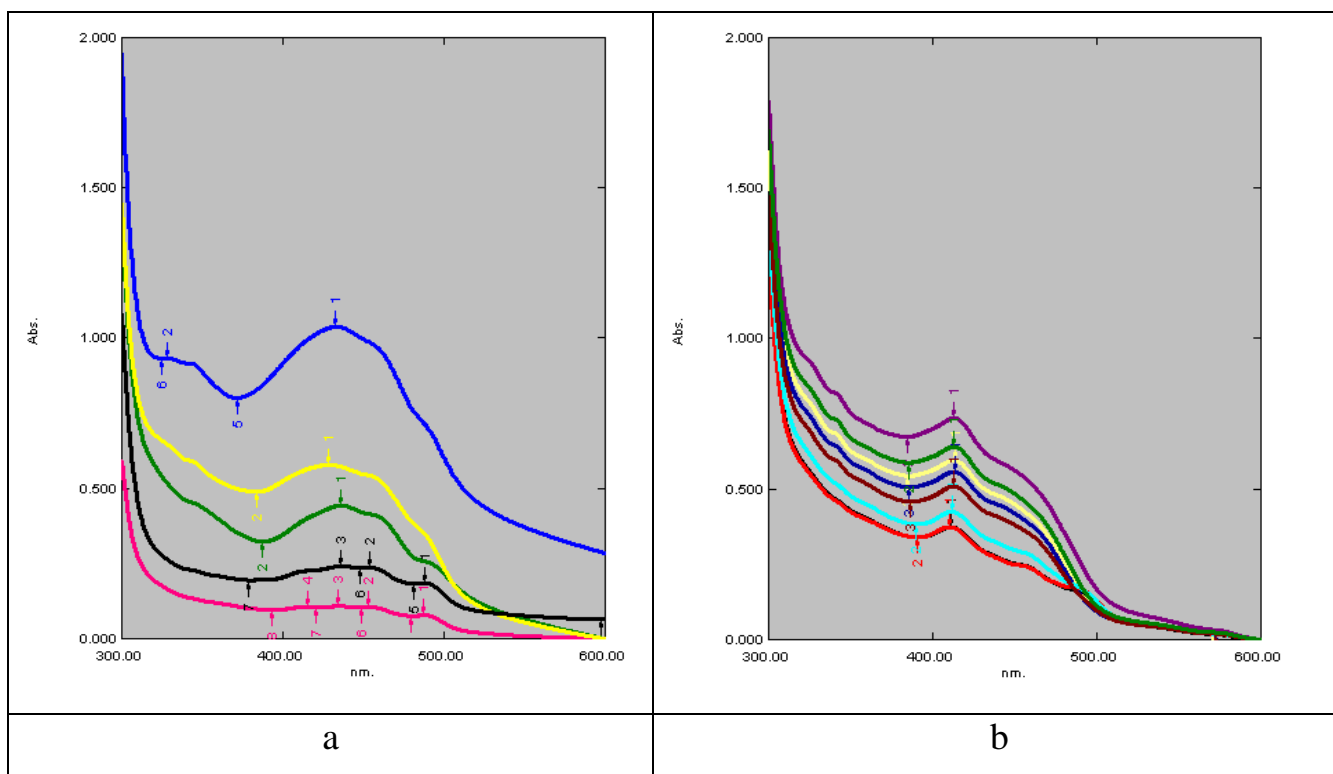


Figure (3-43): Change of absorbance for the conjugation reaction between GSH and L₃Au with time in the absence (a) and presence (b) of enzyme.

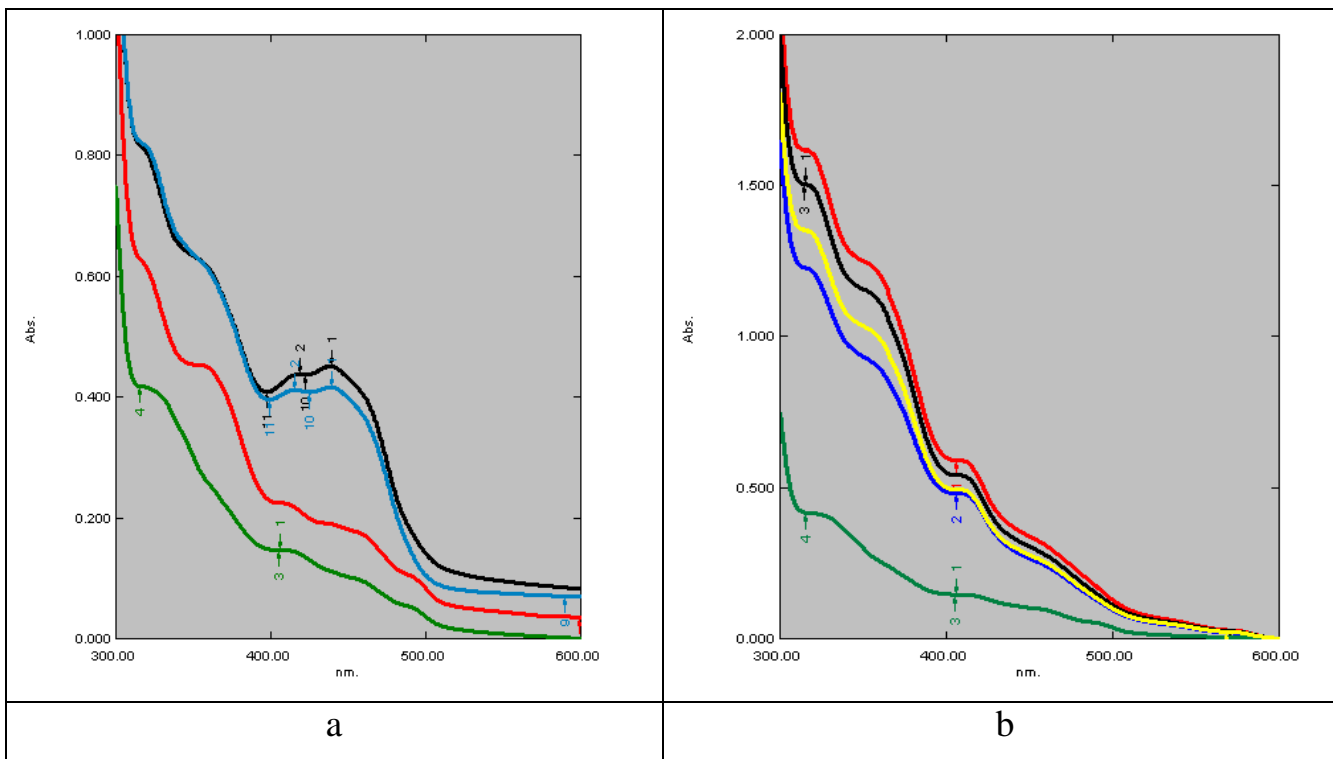


Figure (3-44): Change of absorbance for the conjugation reaction between GSH and L₃Pd with time in the absence (a) and presence (b) of enzyme.

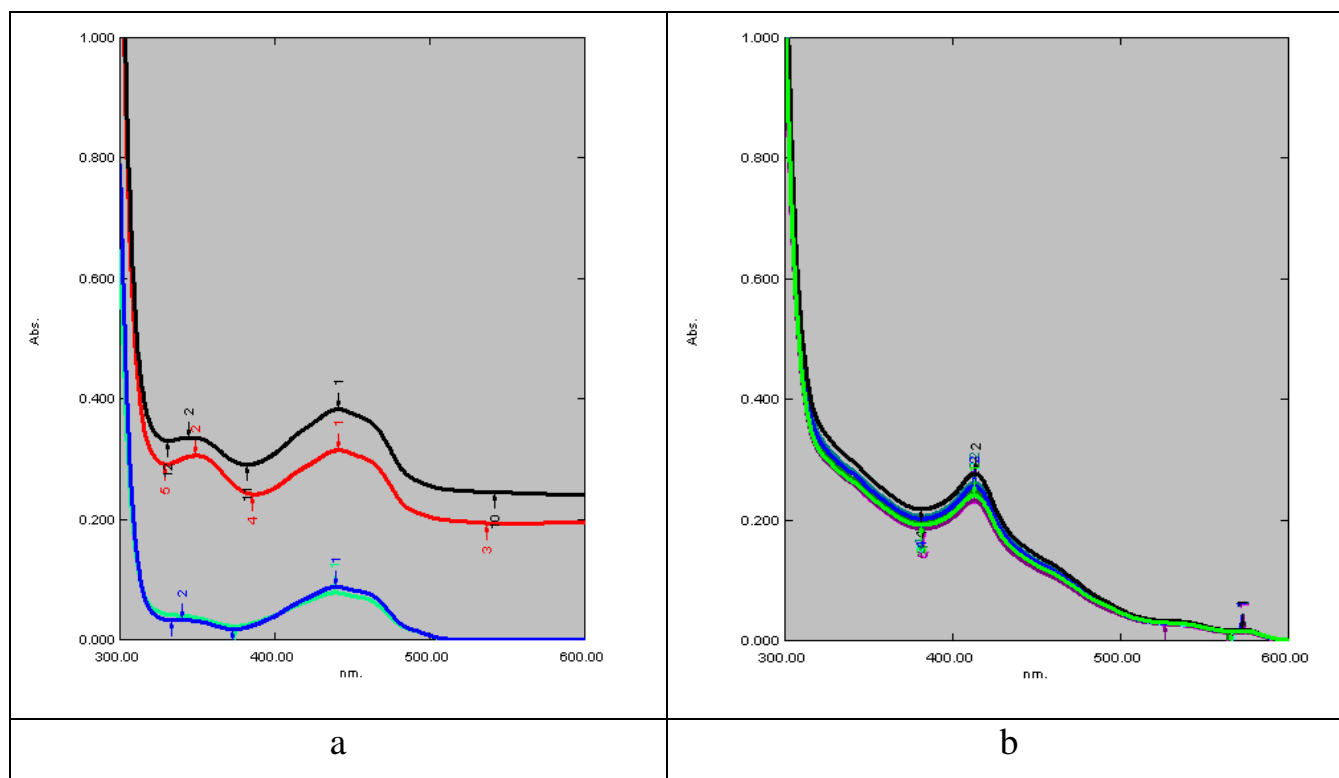


Figure (3-45): Change of absorbance for the conjugation reaction between GSH and L_3Cu with time in the absence (a) and presence (b) of enzyme.

For the present work the slow nonenzymatic rate of reaction (measured as the absorbance change per minute) for each complex was converted into a bimolecular rate constant K_2 , as shown in table (3-7). It also records the corresponding data for the rapid enzymatic reactions under the same conditions.

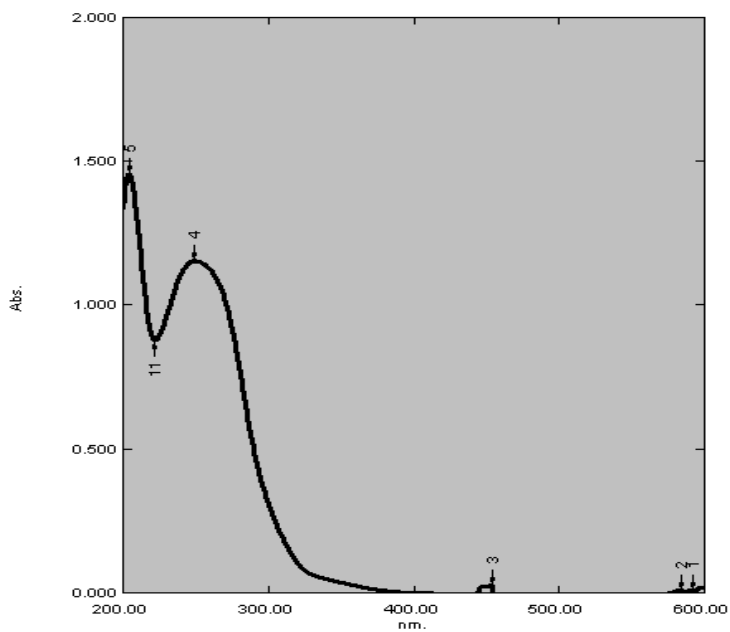


Figure (3-46): Electronic Spectrum of CDNB

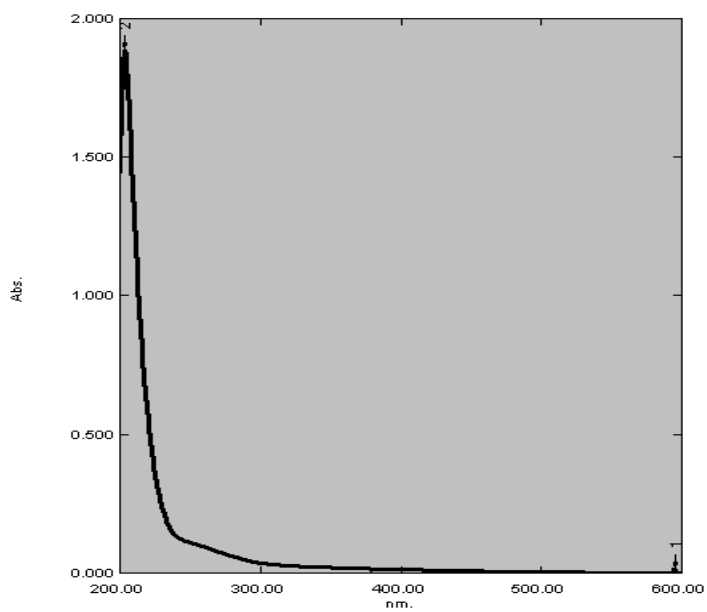


Figure (3-47): Electronic Spectrum of GSH

Table (3-7): The kinetic data for the enzymatic and non-enzymatic reactions

Compound	Non-enzymatic reaction		Enzymatic reaction		Fold
	Rate constant K_2	Fold A	Rate constant K_2	Fold A	
CDNB	666	1	6666.6	1	10
L3Cu	211.80	0.317	1500	0.225	7.08
L2Cu	204.86	0.307	5066	0.759	24.72
L2Pt	250.41	0.376	8000	1.200	31.94
L3Pt	261.11	0.391	8300	1.245	31.78
L3Pd	235.41	0.353	8733.3	1.310	37.09
L2Pd	604.86	0.901	9900	1.485	16.36
L3Au	645.83	0.968	10866	1.629	16.82
L2Au	727.08	1.909	20400	3.060	28.05

Fold A = K of compound / K of CDNB

Fold B = K of enzymatic reaction / K of non-enzymatic reaction

Reactivity of these complexes can be arranged according to the decrease in their k_2 value for enzymatic reaction as follows:



Taking these data in consideration, the following observations can be concluded:

- 1) Gold complexes were of highest K_2 enzymatic values, i.e. of highest reactivity toward GSH.
- 2) Copper complexes were of lowest K_2 enzymatic values, i.e. of lowest reactivity toward GSH.

3) All the studied complexes accepted copper complexes show higher reactivity than the standard CDNB substrate.

4) The charged complexes, i.e. of L_2Au , L_3Au , , L_3Pd , L_3Pt L_2Pt and L_2Cu were of higher reactivity than the neutral complexes, i.e. L_2Pd and L_3Cu , this finding reflects the type of the postulated mechanism of reaction between the nucleophilic glutathione (GS^-) thiolate ion^(93,123) and the electrophilic substrate.

So by this work a number of new substrates can be recorded for GSTs.

Suggestions for further work:

- 1) Complete characterization of the prepared complexes using GC-Mass, NMR and Thermal analysis.
- 2) Study of the side effects of the new complexes and the determination of Minimum Inhibitory Concentration (MIC).
- 3) Study of the antitumor activity, using Cell-line technique, of the new complexes.
- 4) Study of the conjugation reaction products, in order to investigate conjugation mechanism.

Chapter two**Materials and Methods****2-1 Instrumentation:**

1. Infrared Spectrophotometer: The infra-red spectra of the prepared compounds were recorded using:

FT.IR 8300 Fourier Transform Infrared Spectrophotometer of *SHIMADZU*, in the range at wave number (4000-200) cm^{-1} , using CsI as disk.

2. Ultraviolet-Visible Spectrophotometer: The electronic spectra of the prepared compounds were obtained using: *SHIMADZU* UV-Vis-160A ultraviolet spectrophotometer and using 1 cm quartz cell in the range at wavelength (200-1100) nm.

3. Melting Points: The melting points of the prepared compounds were obtained using *Gallenkamp M. F. B. 600 F* Melting Point Apparatus.

4. Magnetic Susceptibility Measurements: The magnetic susceptibility values of the prepared complexes were obtained at room temperature using Magnetic Susceptibility Balance of *Bruke Magnet B.M.6, England*.

5. pH Meter 3305/Jenway/Germany.

6. Refrigerated High Speed Centrifuge/Sanyo/U.K.

7. Vacuum Oven / GallenKamp / Germany.

8. Sensitive Electric Balance, Sartorius, Germany.

9. Magnetic Stirrer/Jlassco/India.

10. Electrophoresis/Bio-Rad/U.S.A.

11. Vacuum Pump/Charles Austen/England.

12. Vortex/Kunkel Gmbhucokg/England.

13. Pump /Mcro Tube Pump /England.

14. Ultrafiltration Cell Model 8200 / nmicon / U.S.A.

15. Conductometer WTW/Germany.

16. C.H.N analyzer of College of Science/Cairo University/Egypt

2-2 Chemicals: The chemicals used in this work were of highest available purity and used as supplied without further purification, other chemicals were prepared as described below; cyclohexylamine was purified by distillation under normal pressure (B.P. 145°C).

2-2-1 Chemicals Supplied:

Table (2-1): Specification supplied chemicals

Chemicals	Purity %	Company
Absolute ethanol	99.99	BDH
Acetic acid	99	BDH
Acetone	99	BDH
Acrylamide	99	BDH
Ammonium persulfate	98	LKB
Bis-acrylamide	97	BDH
Bovine Serum Albumin	99.9	Sigma
Bromo Phenol Blue	90	BDH
Chloroauric acid	51 (Au)	BDH
1-Chloro-2,4-dinitrobenzene	98	Fluka
Chloroform	98	BDH
Chloroplatinic acid mono-hydrate	40 (Pt)	GPR
CM-Cellulose	98	BDH
Coomassie Brilliant Blue G-250	90	BDH
Coomassie Brilliant Blue R-250	90	BDH
Copper nitrate	99	Fluka
Cyclohexylamine	99	BDH
DEAE-Cellulose	99	Merk
Diethyl ether	90	Fluka
4-Diethylamino benzaldehyde	99	Readel-Dehean
Dimethyl sulfoxide	99	Fluka
Dipotassium hydrogen orthophosphate	99	BDH

EDTA	98	Fluka
Gold plates	100	
Glutathione	96	Sigma
Glycerol	98	BDH
Hydrochloric acid	37	BDH
2-Hydroxy naphthaldehyde	98	BDH
2-Hydroxy benzaldehyde	98	BDH
Methanol	99.9	BDH
4-Methoxy aniline	99	Fluka
Nitric acid	70	BDH
Palladium (II) chloride anhydrous	60 (Pd)	Fluka
Potassium dihydrogen orthophosphate	99.9	BDH
Potassium hydroxide	98	BDH
Sephacryl S-200		Pharmacia Fine Chemical
Sucrose	99	BDH
Sulfuric acid	98	BDH
TEMED	99	BDH
4-Toluene sulfonic acid	99	BDH
Trichloro acetic acid	98	BDH
Tris	98	BDH

2-2-2 Preparation of the Starting Materials:

A- Preparation of Chloroauric Acid Mono-hydrate:

A 0.1g piece of gold (5.102×10^{-4} mol) is dissolved in a mixture of 0.5 ml of concentrated (12M) hydrochloric acid and 0.13 ml of concentrated nitric acid (16M). The mixture was heated to 90°C hasten the process somewhat, aqua regia was added occasionally to maintain a constant volume. The mixture was allowed to stand at room temperature until all the gold has been dissolved. The resulting solution was evaporated to about 0.1 ml, 0.3 ml of concentrated hydrochloric acid was added, and the evaporation was repeated⁽⁶⁵⁾.

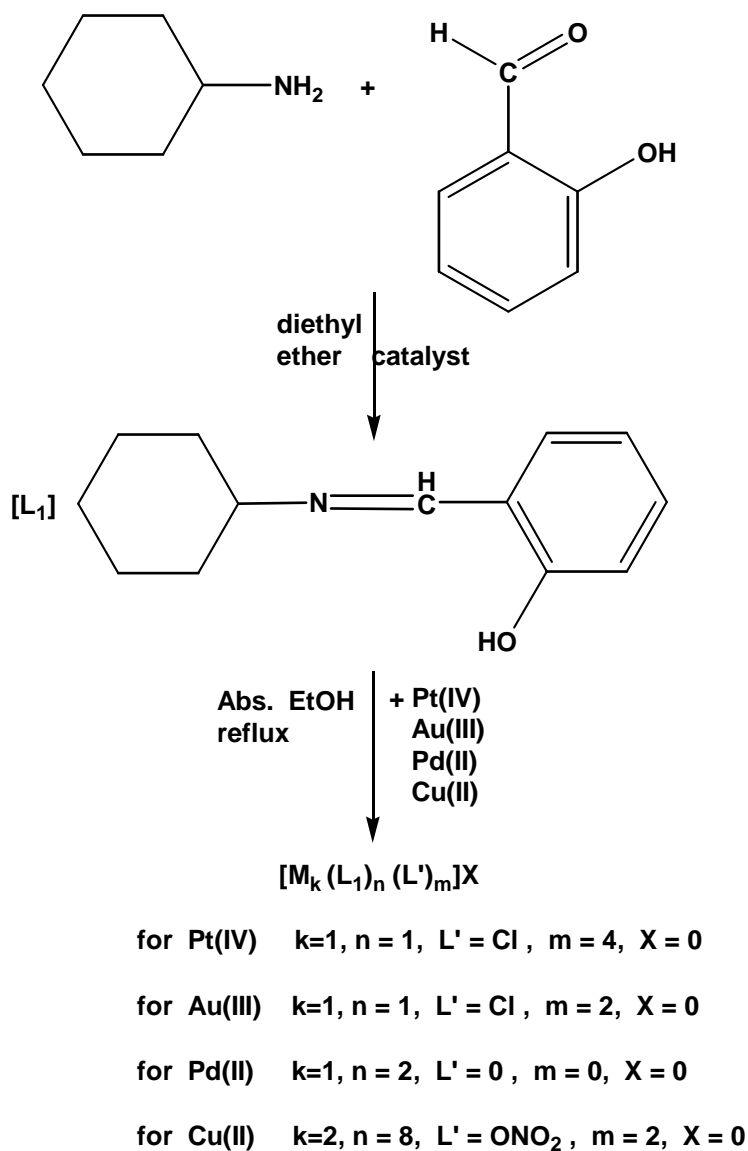
B- Preparation of trans- [Pd(DMSO)₂Cl₂]:

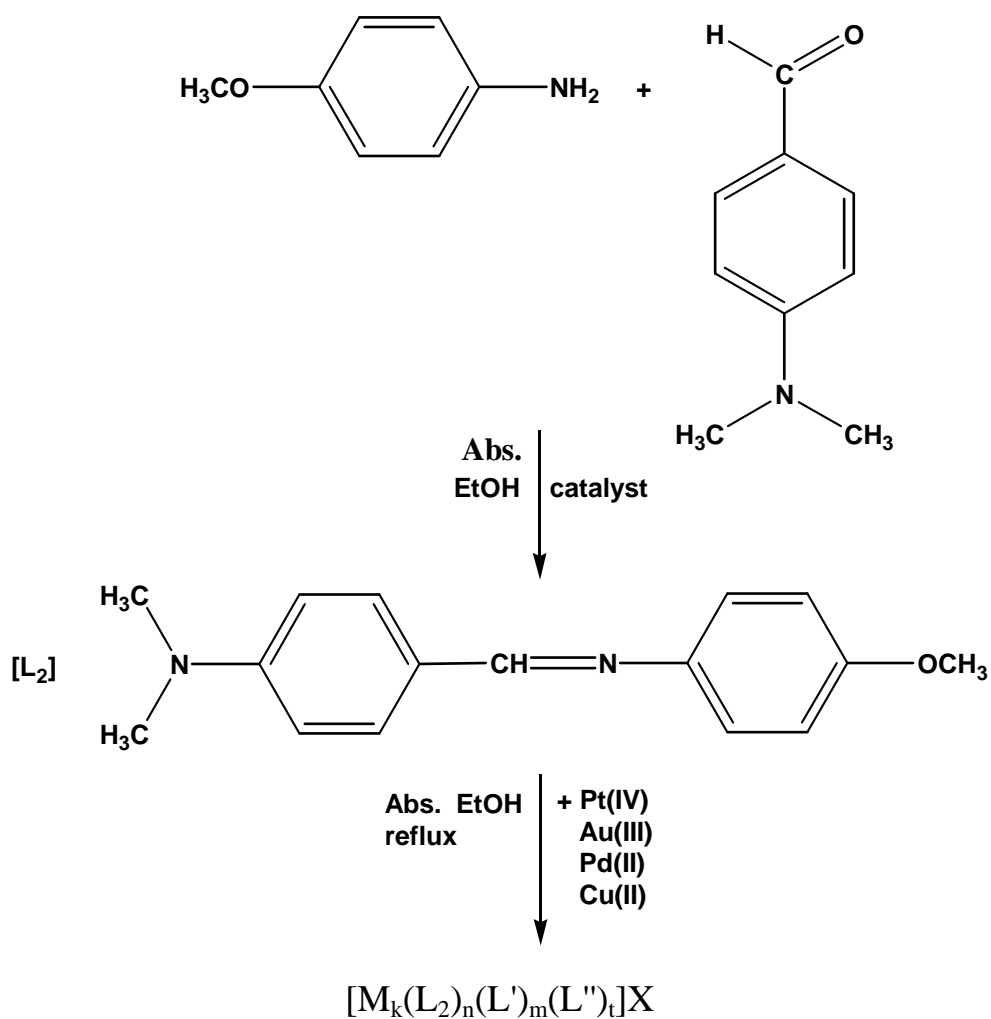
The neutral palladium sulfoxide complex was prepared by dissolving 0.25g of PdCl₂ in 5 ml of dimethyl sulfoxide (DMSO) at 50°C. The DMSO complex was precipitated upon addition of anhydrous ether with stirring. The complex was dried in vacuum for 5 hr⁽⁶⁶⁾.

2-3 Preparation of Ligands:

The new ligands were prepared by a modification of the reported method⁽⁶⁷⁻⁷⁰⁾. Scheme (2-1) shows the reaction steps.

Scheme (2-1): Shows the reaction pathway used to prepare the ligand L₁, L₂ and L₃ and their respective metal complexes.



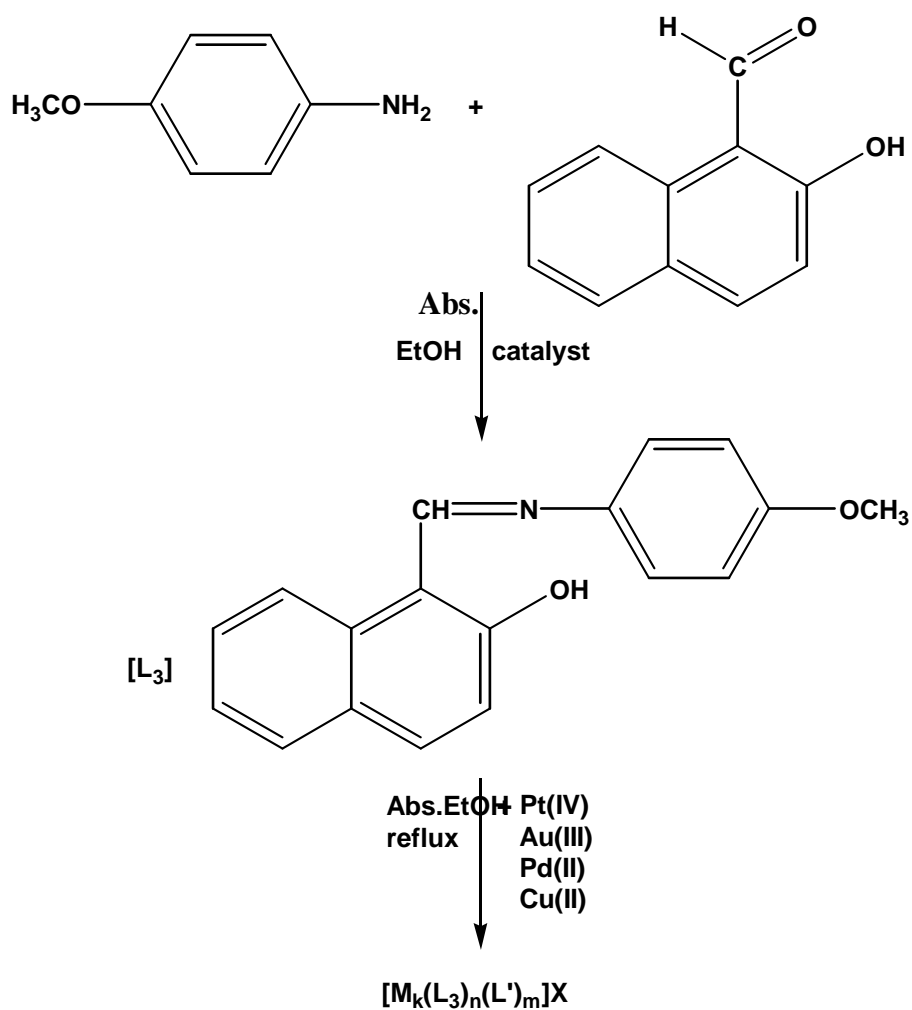


for Pt(IV) $k=2, n=4, L' = Cl, m=6, L''=0, t=0, X = Cl$

for Au(III) $k=1, n=6, L' = 0, m=0, L''=0, t=0, X = Cl$

for Pd(II) $k=2, n=4, L' = Cl, m=4, L''=H_2O, t=2, X = 0$

for Cu(II) $k=1, n=3, L' = ONO_2, m=1, L''=H_2O, t=2, X=NO_3$



for Pt(IV) $k=1, n=2, L'=Cl, m=2, X=Cl$

for Au(III) $k=1, n=2, L'=0, m=0, X=Cl$

for Pd(II) $k=2, n=6, L'=0, m=0, X=Cl$

for Cu(II) $k=1, n=2, L'=0, m=0, X=0$

2-3-1 Preparation of 2-[(cyclohexylimino)methyl]phenol(L₁):

A solution of 0.01 mole (1.15 ml) of cyclohexylamine was slowly added to a solution of 0.01 mole (1.06 ml) of salicylaldehyde, to it *p*-toluene sulfonic acid was added in small portions as catalyst^(71,72). The mixture was diluted with 20 ml of dry diethyl ether. The solution was refluxed for 2 h at 30-40°C, and then the solvent was removed under vacuum. A yellow viscous liquid was obtained with 89.65% yield^(30,70).

2-3-2 Preparation of N[4(dimethylamino)benzylidene]-N-(4-methoxyphenyl)amine(L₂):

The Schiff base (L₂) was prepared by dissolving 0.01 mole (1.232g) of the *p*-methoxy aniline in 40 ml of absolute ethanol, to the resulting solution 0.01 mole (1.77g) of 4-dimethyl amino benzaldehyde, dissolved in 50 ml of absolute ethanol, was added. The resulting solution was mixed with the addition of few drops (2-3) of glacial acetic acid as catalyst⁽³⁴⁾. After stirring, the reaction mixture was heated for two hours at 50°C, the solution was cooled and the precipitate was collected by filtration. The precipitate was washed several times using diethyl ether, then with ethanol, followed by recrystallization in ether and drying at 50°C in vacuum oven for 1 hour⁽³⁰⁾.

2-3-3 Preparation of 1-[(4-methoxyphenylimino)methyl]-2-naphthol (L₃):

L₃ was prepared by dissolving 0.01mole (1.72g) of 2-hydroxy naphthaldehyde in absolute ethanol, 3 drops of glacial acetic acid was added as catalyst⁽³⁴⁾, followed by slow addition of 0.01mole (1.232g) of *p*-methoxy aniline dissolved in absolute ethanol. The mixture was stirring for 30 min at 50°C and agitated for 24 hour at room temperature; the

solution was cooled and the resulting precipitate was collected by filtration. The precipitate was washed several times with ethanol followed by recrystallization in diethyl ether and drying at 50°C overnight in vacuum oven⁽³⁰⁾.

2-4 Preparation of the Complexes:

2-4-1 Metal Complexes of L₁

A) The Platinum (IV) Complex (L₁Pt):

A solution of H₂PtCl₆.H₂O 2mmole (0.856g) was added drop wise to the original ligand 4mmole (0.812g) in absolute ethanol, the addition took 5min. The mixture was refluxed for 2 hours at 60°C. After cooling to room temperature the precipitate was filtered and recrystallized from ethanol, orange bright crystals were formed.

B) The Gold Complex (L₁Au):

A solution of H_{Au}Cl₄ 2mmole (0.71g) was added drop wise to the original ligand 4mmole (0.811g) in absolute ethanol, the red solution was formed, the mixture was placed in ice bath for 20 min until the precipitate was formed, then it was filtered off, washed several times with absolute ethanol and recrystallized by ethanol and dried under vacuum at 50°C. The yield was deep red powder.

C) The Palladium Complex (L₁Pd):

A solution of [Pd(DMSO)₂Cl₂] 2mmole (0.666g), dissolved in 5 ml absolute ethanol was added drop wise to the original ligand (L₁), 4mmole (0.807g) dissolved in absolute ethanol. The mixture was refluxed for 1 hour at 60°C. After cooling the solution the precipitate was filtered off,

washed several times with absolute ethanol then recrystallized by diethyl ether. A yellowish-green fine crystalline powder was obtained.

D) Copper (II) Complex (L_1Cu):

4 mmole (0.812g) of L_1 was dissolved in minimum amount of absolute ethanol (15 ml), to which drops of aqueous solution of potassium hydroxide (1%) was added, followed by the addition of 2mmole (0.465g) of the copper nitrate dissolved in minimum amount of absolute ethanol (10 ml). The mixture was refluxed for 2 hours at 60°C. After cooling to room temperature, the precipitate was filtered off, and washed several times with diethyl ether and recrystallized from hot diethyl ether and dried under vacuum at 50°C. A bright deep reddish-brown powder was obtained.

2-4-2 Complexes of (L_2) and (L_3) (L_2Pt-L_3Cu):

A general method was followed for the preparation of metal complexes of (L_2) and (L_3), which can be described below:

To a solution of 4 mmole of L_2 /or L_3 in appropriate amount of absolute ethanol, a 2 mmole of the metal salt (described in table 2-2) dissolved in minimum amount of absolute ethanol, was added. The mixture was warmed for 5 min. then refluxed for 2 hours to complete the reaction. The products were washed several times with absolute ethanol and recrystallized from hot ethanol. Fine crystalline powders were obtained with different colors depending on the type of the metal salt as described in Table (2-2).

Table (2-2): Schiff base, metal salt and purification solvent of prepared complexes.

Complex	Schiff base	Metal salt	Purification solvent
L ₁ Pt	L ₁	H ₂ PtCl ₆ .H ₂ O	ethanol
L ₁ Au	L ₁	HAuCl ₄	ethanol
L ₁ Pd	L ₁	[Pd(DMSO) ₂ Cl ₂]	diethyl ether
L ₁ Cu	L ₁	Cu(NO ₃) ₂ .3H ₂ O	diethyl ether
L ₂ Pt	L ₂	H ₂ PtCl ₆ .H ₂ O	ethanol
L ₂ Au	L ₂	HAuCl ₄	ethanol
L ₂ Pd	L ₂	[Pd(DMSO) ₂ Cl ₂]	ethanol
L ₂ Cu	L ₂	Cu(NO ₃) ₂ .3H ₂ O	ethanol
L ₃ Pt	L ₃	H ₂ PtCl ₆ .H ₂ O	ethanol
L ₃ Au	L ₃	HAuCl ₄	ethanol
L ₃ Pd	L ₃	[Pd(DMSO) ₂ Cl ₂]	ethanol
L ₃ Cu	L ₃	Cu(NO ₃) ₂ .3H ₂ O	ethanol

2-5 Isolation and Purification of Glutathione S-transferase from Rat Liver

2-5-1 Assay Method

Principle: Enzyme activity during purification was determined spectrophotometrically at 340nm by measuring the formation of the conjugate of glutathione (GSH) and 1-chloro-2,4-dinitrobenzene (CDNB)⁽⁶³⁾.

2-5-1-1 Solutions:

1) Buffer A- potassium phosphate buffer (0.1M) (pH=6.5).

This solution was prepared by mixing 42ml of (0.1M K₂HPO₄) with 91ml of (0.1M KH₂PO₄). The pH of the final solution was 6.5.

2) Glutathione (GSH) (20mM):

It was prepared by dissolving 0.03g GSH in 5ml of buffer A above.

3) 1-Chloro 2,4-dinitrobenzene (CDNB) (20mM):

It was prepared by dissolving 0.02g CDNB in 5ml of ethanol 95%.

2-5-1-2 Procedure:

A) Determination of enzyme volume:

To a one ml cuvette was added 850-895μl of buffer A, 50μl of 20mM GSH and 50μl of 20mM CDNB. The reaction, which was carried out at 30°C, was started by addition of a suitable amount of enzyme (5-50μl); the final volume was 1ml. The reaction was monitored spectrophotometrically by the increase in absorbance at 340nm ($\epsilon = 9.6 \text{ mM}^{-1}\text{cm}^{-1}$) Figure (3-31). Correction for the spontaneous activity was made by subtracting the rate in the absence of enzyme⁽⁵⁶⁾.

B) Determination of enzyme activity:

The same steps above (2-5-1-2-A) were done using 865 μl of buffer A and 35μl of enzyme.

2-5-2 Definition of Unit and Specific Activity:

A unit of enzyme activity was defined as the amount of enzyme that catalyzes the formation of 1 μ mol of S-2, 4-dinitrophenylglutathione per minute at 30°C using 1mM concentration of GSH and CDNB⁽⁶³⁾. A specific activity was defined as enzyme activity (units) per milligram of protein⁽⁵⁶⁾.

2-5-3 Determination of Protein concentration:

2-5-3-1 Solutions:

a) Bovine Serum Albumin Stock Solution:

Bovine Serum Albumin (BSA) stock solution was prepared by dissolving 10mg of BSA in 10ml of phosphate buffer (0.05M) (pH 7)⁽⁷³⁾.

b) Sodium hydroxide(1M):

It was prepared by dissolving 4g of NaOH in 50ml distilled water, and then diluted to 100ml with distilled water.

c) Commassie Brilliant Blue G-250⁽⁷⁴⁾:

This dye was prepared by dissolving 100mg of Commassie Brilliant Blue G-250 in 50ml of ethanol 95%, and then 100ml of orthophosphoric acid 85% was added. The volume was then completed in volumetric flask to 1000ml with distilled waster.

2-5-3-2 Procedure:

Protein concentration determination was performed as follows ⁽⁷⁴⁾:

- 1) Several dilutions of standard protein (BSA) (2.5, 5, 7.5, 10, 12.5, 15, 20 μ g/ml) were prepared from BSA stock solution (2.5.3.1 a) in the same buffer using 20 μ l of each concentration for each dilution.
- 2) 50 μ l from 1M NaOH (2.5.3.1 b) was added to each dilution.
- 3) Then 1ml of Commassie Brilliant Blue G-250 (2.5.3.1 c) was added to each dilution and left to stand for 2min at room temperature.

- 4) The absorbance at 595nm was measured: the blank was prepared from 0.1ml of the buffer and 1ml of the dye reagent.
- 5) A standard curve was plotted between the amounts of protein corresponding absorbance of the standard protein. The protein concentration of unknown samples was calculated from the standard curve Figure (2-1).
- 6) The same steps were done using 20 μ l of the sample.

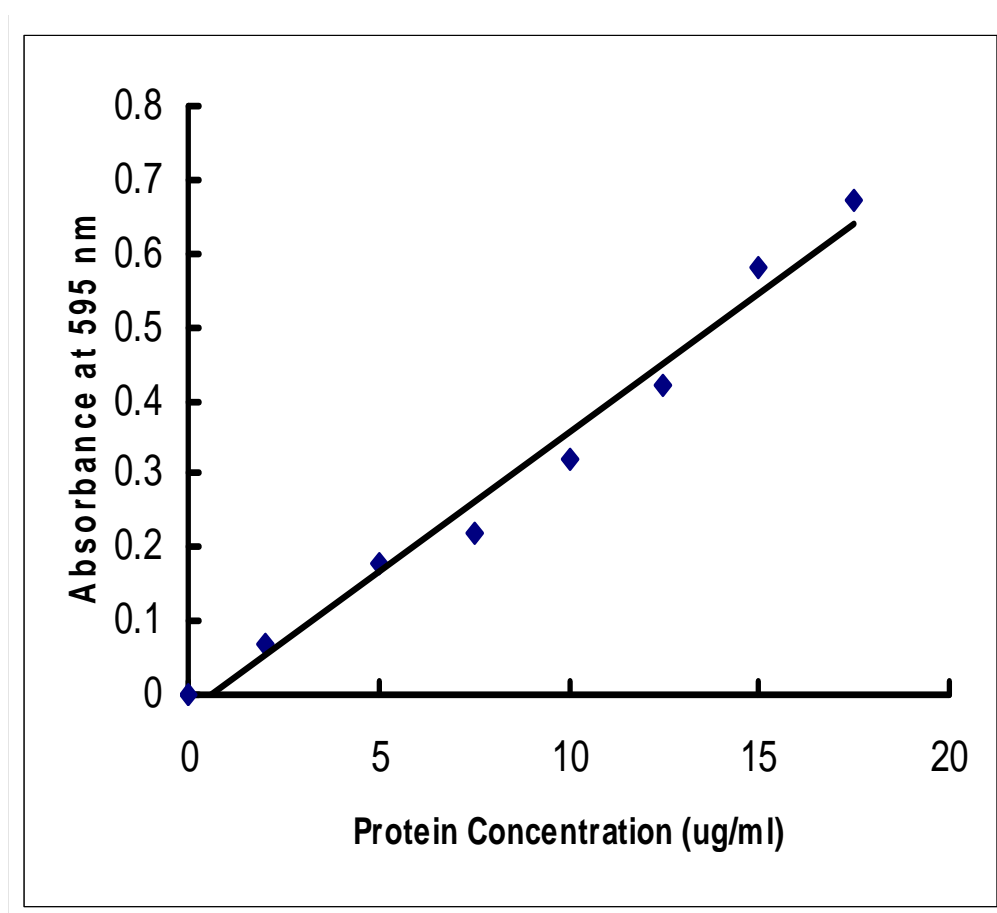
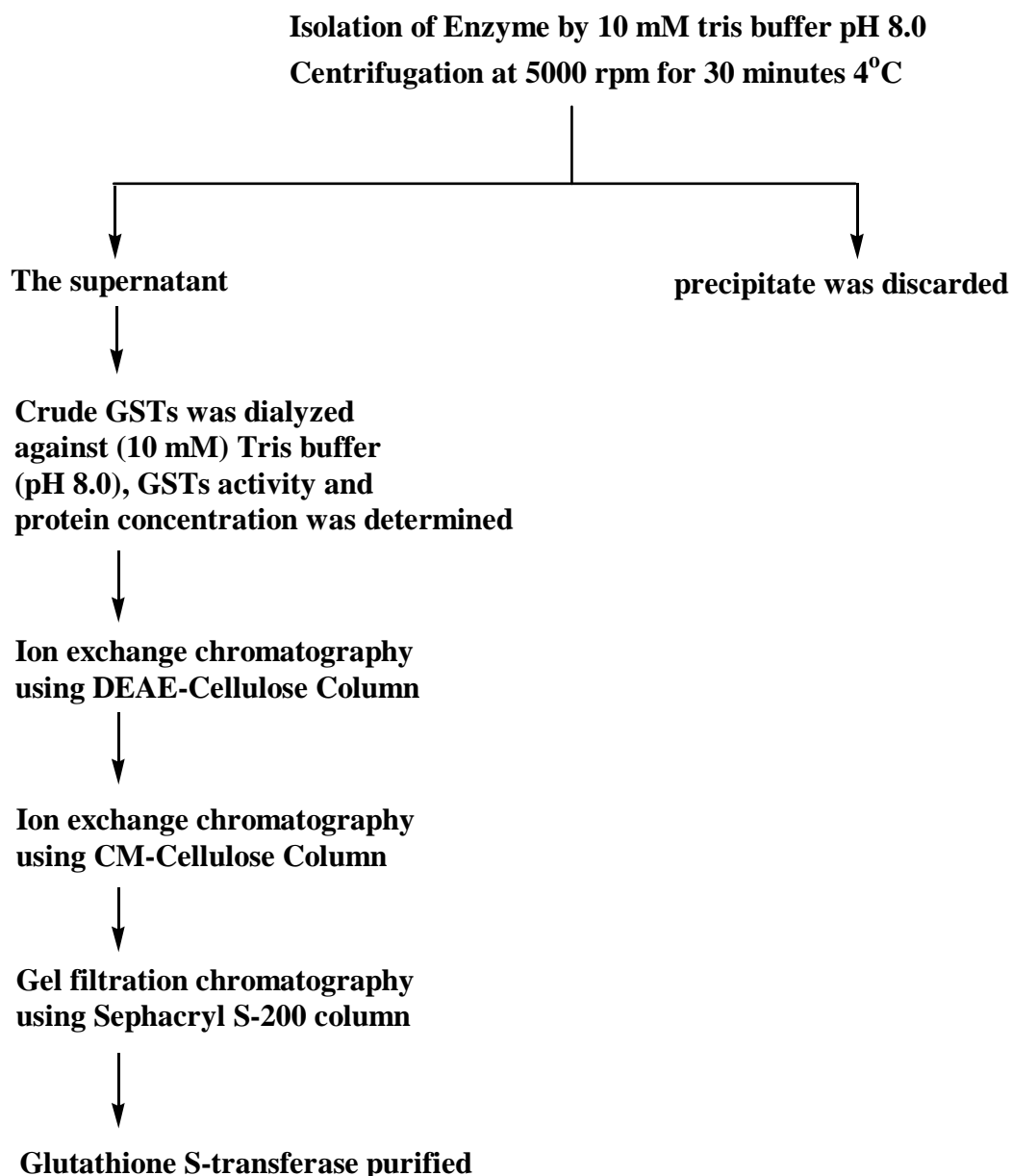


Figure (2-1): Standard protein curve.

2-5-4 Isolation and Purification Procedure:

The purification steps were performed at 5°C the procedure was dimensioned for two rat liver (14-20 g) as shown in Scheme (2-2).

Scheme (2-2): The isolation and purification of GSTs from Rat liver.



2-5-4-1 Preparation of Cytosol Fractions:***2-5-4-1-1 Solutions:*****a) Tris-solution (10mM):**

It was prepared from dissolving 0.15g of Tris-chloride in 100ml distilled water.

b) HCl (10mM):

It was prepared from dilution of 1ml of concentrated HCl to 100ml by distilled water.

c) Buffer B- Tris buffer (10mM) (pH=8.0):

It was prepared by mixing 93.2ml of Tris-chloride (a) with 50ml of HCl solution (b), the pH of the prepared buffer solution was 8.0.

2-5-4-1-2 Procedure:

Rat liver (17g) was cut into small pieces and homogenized in 10 mM ice-cold buffer B (3ml/g liver) in a blender. The homogenate was filtrated through 2 layers of gauze to remove connective tissue. The homogenate was centrifuged at 5,000 rpm for 1 hour. The resulting supernatant was then centrifuged for 30 minute. The cytosol fraction was obtained, and stored at $-20^{\circ}\text{C}^{(63)}$.

2-5-5 Purification Procedures:

The purification was made through the following three steps:

2-5-5-1 Ion Exchange Chromatography by DEAE-Cellulose:

2-5-5-1-1 Solutions:

- a) Sodium chloride (0.25M).
- b) Hydrochloric acid (0.25M).
- c) Sodium hydroxide (0.25M).
- d) Buffer B- Tris buffer (10mM) (pH 8.0).

2-5-5-1-2 Preparation of the Ion Exchanger DEAE-Cellulose:

The ion exchanger diethylaminoethyl cellulose (DEAE-cellulose) was prepared according to the manufacturing company (Whatman) as described below⁽⁷⁵⁾.

DEAE-Cellulose (25g) was suspended in (100 ml) of distilled water and left for 2 hours to get swelled. The floating flakes were removed away from the solution until the upper layer was cleared, then filtered through buchner funnel with Whatman No. 1 filter paper under vacuum. The precipitate was suspended in (500 ml) of (0.25 M) NaCl (2-5-5-1-1 a) under vacuum, then washed several times with distilled water. A (500 ml) of (0.25 M) HCl (2-5-5-1-1 b) was passed through the precipitated exchanger under vacuum and washed several times with distilled water. The exchanger was suspended also with (0.25 M) NaOH solution (2-5-5-1-1 c) and washed several times with distilled water. The DEAE-Cellulose was suspended in (10 mM) Tris-HCl buffer B (pH 8.0) (2-5-5-1-1 d) until the pH of the exchanger was reached (8.0). The DEAE-Cellulose was packed into the column (30X2.5cm), and then the

column was equilibrated with the same buffer overnight with a flow rate (50ml/ hour).

2-5-5-1-3 Procedure⁽⁶³⁾:

Crude GSTs was dialyzed against (10mM) Tris-HCl buffer B (pH 8.0) then 34ml of this sample was loaded onto the column carefully until passed the exchanger. Then (150ml) of (10mM) Tris-HCl buffer B was added, then (150 ml) of a gradient from (10mM) Tris-HCl buffer to (10mM) Tris buffer containing 0.2M NaCl was added. Fractions of (5ml) were collected in test tubes. The absorbance in each fraction was measured spectrophotometrically at 280nm, fractions of the protein peaks were assayed for GSTs activity (2-5-1-2-B) and Protein concentration (2-5-3-2-6). Fractions containing enzymatic activity were collected, and stored at 5°C for further purification.

2-5-5-2 Ion Exchange Chromatography by CM-Cellulose:

2-5-5-2-1 Solution¹:

- a) Sodium chloride 0.25M.
- b) Sodium hydroxide 0.25M.
- c) Hydrochloric acid 0.25M.
- d) Buffer C- phosphate buffer (10mM) (pH 6.7).
- e) Buffer D- Phosphate buffer (400mM) (pH 6.7).

2-5-5-2-2 Preparation of the Ion Exchanger CM-Cellulose:

The ion exchanger was prepared according to the manufacturing company (whatman) as described follows⁽⁷⁵⁾.

CM-Cellulose (25g) was suspended in (100 ml) of distilled water and left for 2 hours to precipitate. The floating flakes were removed away from the solution until the upper layer was cleared, then filtered through

buchner funnel with whatman No. 1 filter paper under vacuum.

The precipitate was suspended in (500 ml) of (0.25 M) NaCl (2-5-5-2-1 a) under vacuum, then washed several times with distilled water. A (500 ml) of (0.25 M) NaOH (2-5-5-2-1 b) was passed through the precipitated exchanger under vacuum and washed several times with distilled water. The exchanger was suspended also with (0.25 M) HCl solution (2-5-5-2-1 c) and washed several times with distilled water. The CM-Cellulose was suspended in (10 mM) buffer C (pH 6.7) (2-5-5-2-1 d) until the pH of the exchanger was reached (6.7). The CM-Cellulose was packed into the column (30X2.5cm), and then the column was equilibrated with the same buffer overnight.

2-5-5-2-3 Procedure:

The sample (20ml) was loaded onto the column carefully until passed the exchanger. Then (150 ml) of phosphate buffer (10mM) (pH 6.7) Buffer C (2-5-5-2-1 d) was added, protein was eluted by using (260 ml) of a gradient from (10 mM) to (400 mM) phosphate buffer (pH 6.7) buffer D (2-5-5-2-1 e). Fractions of (5 ml) were collected in test tubes. The absorbance in each fraction was monitored spectrophotometrically at 280nm, fractions of the protein peaks were assayed for GSTs activity (2-5-1-2-B) and protein concentration (2-5-3-2-6). Fractions containing enzymatic activity were collected, and concentrated by ultrafiltration⁽⁷⁶⁾.

2-5-5-3 Gel Filtration Chromatography on Sephacryl S-200 Column:

2-5-5-3-1 Materials and Solutions:

- a) Buffer E- phosphate buffer (0.1 M) (pH 6.7).
- b) Sephacryl S-200.

2-5-5-3-2 Preparation of Gel Filtration Column:

Sephacryl S-200 column (63X2 cm) was prepared and packed according to the instruction of the manufacturing company (Pharmacia Fine Chemical)⁽⁷⁷⁾. The column was equilibrated with (0.1 M) phosphate buffer (pH 6.7) buffer E (2-5-5-3-1 a), at a flow rate of (60ml/hour).

2.5.5.3.3 Procedure^(78,79):

A sample (10 ml) of partially purified GSTs was added to the Sephacryl S-200 column, carefully using pasture pipette. Elution of protein was done with the application of (200ml) phosphate buffer (0.1M) (pH 6.7). Fractions of (5 ml) were collected in test tubes. The absorbance in each fraction was monitored spectrophotometrically at 280nm, fractions of the protein peaks were assayed for GSTs activity (2-5-1-2-B) and Protein concentration (2-5-3-2-6). Fractions containing enzymatic activity were collected.

2-5-6 Polyacrylamide Gel Electrophoresis under Denatured Conditions:

In order to test the purity and to determine the molecular weight of the GSTs obtained from the gel filtration step, protein polyacrylamide gel electrophoresis was performed for the purified enzyme^(73, 80).

2-5-6-1 Solutions:

a) Resolving Gel Buffer Solution (1.5 M Tris-HCl):

This solution was prepared by dissolving 18.2g of Tris-HCl in 80ml of distilled water. The pH was adjusted to 8.8 by 1M of HCl solution and the volume was then completed to 100ml.

b) Stacking Gel Buffer Solution (0.5M):

This solution was prepared by dissolving 6g of Tris-Base in distilled water and the pH was then adjusted to 6.8 using 1M HCl. The volume was then completed to 100ml in volumetric flask.

c) Sodium Dodecyl Sulfate Solution (10%)

This solution was prepared by dissolving 10g of SDS in distilled water, and the volume was then completed to 100ml.

d) Reservoir Buffer Solution:

This solution was prepared by dissolving 3g of Tris-Base with 14.4g of glycine in 800ml of distilled water. pH was adjusted to 8.3 by 1M HCl solution, 10 ml of (10%) SDS solution was then added and the volume was then completed to 1000ml by distilled water.

e) Acrylamide Bisacrylamide Solution (30%):

This solution was prepared by dissolving 30g of acrylamide and 0.8g bisacrylamide in 80ml of distilled water then the volume was completed to 100ml and kept in dark bottle.

f) Bromophenol Blue (0.5%)⁽⁸¹⁾:

This dye was prepared by dissolving 0.5g of bromophenol blue in 100ml of distilled water. Mixed until completely dissolved.

g) Stock Sample Buffer:

It was prepared by mixing 4.3ml of distilled water, 1.2ml of stacking gel buffer, 2ml of 10% SDS solution, 2g of sucrose and 0.5 ml of 0.5% bromophenol blue solution.

h) Ammonium Persulfate Solution (10%):

This solution was prepared freshly by dissolving 1g of ammonium persulfate in 10ml of distilled water.

i) *N,N,N,N Tetra methyl ethylene diamine (TEMED)***j) Fixing Solution:**

This solution composed of 40% methanol and 10% Trichloro acetic acid (TCA). It was prepared by dissolving 100g of TCA in 500ml distilled water, 400ml of ethanol was added and the volume was then completed to 1000ml by distilled water.

k) Enzyme Solution:

It was prepared by mixing 250 μ l of (0.2mg/ml) of GSTs solution with 250 μ l of stock sample solution in test tube, 25 μ l of mercapto ethanol was added, and it heated to boiling point in a water bath for 5 min, then it was cooled to room temperature.

l) Standard Proteins Solution:

They were prepared by dissolving the following standard proteins Table (2-3) in the concentration of (10 μ g/100 μ l of stock sample buffer).

Table (2-3): Molecular weight of standard proteins

Standard protein	Molecular weight (Dalton)
Phosphorylase	94000
Albumin	67000
Ovalbumin	43000
Carbonic anhydrase	30000
Trypsin inhibitor	20000
α -Lactalbumin	14400

m) Coomassie Brilliant Blue R-250:

10ml of 70% of PCA was diluted to 200ml by distilled water, then 0.8g of dye dissolved in it, the solution was mixed for 1 hour, then filtered and kept in dark bottle.

n) Distaining Solution:

This solution composed of 40% methanol and 10% acetic acid. It was prepared by mixing acetic acid, methanol and distilled water in a ratio 1:4:5, respectively.

2-5-6-2 Procedure:

A) Resolving Gel:

Resolving gel (7.5%) was prepared by mixing 2.5ml of acrylamide bisacrylamide (2-5-6-1 e), 4.85ml of distilled water, 2.5ml of resolving gel buffer(2-5-6-1 a), and 0.1 ml of 10% SDS (2-5-6-1 c) the solution was degassed for 10 min. using a vacuum pump, then 50 μ l of 10% ammonium persulphate solution (2-5-6-1 h) and 5 μ l of TEMED were added to the degassed solution and mixed gently. Using Pasteur pipette, the separating gel was transferred to Polyacrylamide gel electrophoresis slab gel, using another pipette, the top of the gel was covered with isobutyl alcohol. The gel was then allowed to polymerize for 1 hour at room temperature.

B) Stacking Gel:

Stacking gel was prepared by mixing 1.3ml of acrylamide-bisacrylamide solution (2-5-6-1 e), 2.5 ml of stacking gel buffer (2-5-6-1 b), 6.1ml of distilled water and 0.1ml of 10% SDS solution (2-5-6-1 c). The solution was then degassed for 10 min. using a vacuum pump. 50 μ l of 10% ammonium persulfate solution (2-5-6-1 h) and 5 μ l TEMED were then added and mixed gently. The stacking gel was then transferred slowly over the separating gel, the top of the gel was covered with isobutyl alcohol. The gel was then allowed to polymerize for about 1 hour at 25°C.

C) Electrophoresis:

The slab gel was submerged in the reservoir buffer (2-5-6-1 d) and 50 μ l of 40 μ g/ml enzyme solution (2-5-6-1 k) was loaded on the gel surface.

The power supply was connected and run at 2 mA/tube of constant current until the tracking dye enter the separating gel, and then the current was increased to 5 mA.

The total run time for the gel was about 4 hours. Then, polyacrylamide gels were removed from the slab gel and placed separately in plate.

Gels were immersed in fixing solution (2-5-6-1 j) for 30 min, fixing solution was then poured off and the gels were immersed in the staining solution (Coommassie Brilliant Blue R-250) for 3 hours.

Then staining solution was poured off and the gel was immersed with destaining solution (2-5-6-1 n) to remove the unbound stain.

The destaining process continued until blue bands of protein were obtained. Gels were stored in 7% acetic acid solution.

To determine the molecular weight of Glutathione S-transferase enzyme, The distance of the bromophenol blue dye transfer from the top of the gel to the center of the dye band was measured,

Also the distance from the top of the gel to the center of separated standard protein bands was measured. The relative mobility (R_m) was calculated for each protein according to the following equation:

$$\text{Relative mobility } (R_m) = \text{distance of protein} / \text{distance of bromophenol blue dye}$$

The relation between R_m and log molecular weight of the standard protein was drawn, then the molecular weight of the enzyme was determined by using the R_m value of the enzyme from the standard curve.

2-6 Interaction of GSH with Prepared Complexes and Standard Substrate:

2-6-1 Solutions:

1) Phosphate buffer (0.1M) (pH 6.7):

It was prepared by dissolving (13.609 gm) of KH_2PO_4 in (1000 ml) of distilled water; pH was adjusted to (6.7) using dilute solution of NaOH.

2) Glutathione (GSH) (1mM): It was prepared by dissolving (0.0922 gm) of GSH in (10 ml) of (0.1M phosphate buffer).

3) 1-chloro2,4-dinitro benzene (CDNB) (1mM): It was prepared by dissolving (0.0182 gm) of CDNB in (3ml) of absolute ethanol.

4) The prepared complexes (1mM): It was prepared by dissolving a suitable weight, corresponding to 1mM of each complex in 5ml of acetone.

2-6-2 General Procedure for Studying the Interaction Process in the Absence and Presence of the Enzyme:

The standard substrate, CDNB, of 1mM was dissolved in absolute ethanol. The resulting solution (0.1ml) was added to 3ml of 0.1M phosphate buffer and the spectrum was measured, the spectrum of GSH was also measured at the same concentration and conditions. 0.1ml of 1mM glutathione was added and the spectrum was measured for the product of interaction at one hour time intervals for three hours, then after twenty four hours.

The same procedure was followed using 1mM of each complex (which was dissolved in acetone) instead of CDNB as substrate mimics.

The procedure was repeated using 0.02ml of the purified Glutathione S-transferase as catalyst, and the spectrum was measured at 5 minute intervals for fifteen minutes, then after half hour.

CONTENTS

		Page
List of Tables		vi
List of Figures		vii
List of Schemes		ix
List of Abbreviations and Symbols		ix
CHAPTER ONE: INTRODUCTION		
1-1	Biomedical Inorganic Chemistry	1
1-2	Chemotherapy	2
1-3	New Metal Complexes as Potential Therapeutics	2
1-3-1	Platinum Complexes	3
1-3-2	Palladium Complexes	6
1-3-3	Gold Complexes	7
1-3-3-1	History of Gold as a Therapeutic Agent	8
1-3-3-2	Gold (III)	9
1-3-3-3	Overview of Gold Drugs	9
1-3-3-4	<i>in vivo</i> Chemistry of Gold Drugs	11
1-3-3-5	Mechanism of Action	12
1-3-4	Copper Complexes	13
1-3-4-1	Biochemistry of Copper	13
1-3-4-2	Copper Anti-Cancer Agent	13
1-4	Schiff Bases	14
1-4-1	Schiff Bases as Ligands in Biologically Important Complexes	16
1-5	Glutathione	18
1-5-1	Structure and Functions of GSH	18
1-5-2	Some Examples of Detoxifying Function of GSH	21
1-5-3	Glutathione Depletion	23
1-6	Glutathione S-Transferase (GSTs)	24
1-6-1	Role of GSTs in Enzymic Detoxification	24
1-6-2	Classification of GSTs	27
1-6-3	Crystal Structures of GSTs	28
1-7	Aim of the Work	31
CHAPTER TWO: METATERIALS AND METHODS		
2-1	Instrumentation	32
2-2	Chemicals	33
2-2-1	Chemicals Supplied	33
2-2-2	Preparation of the Starting Materials	35
2-3	Preparation of Ligands	36
2-4	Preparation of Complexes	40
2-4-1	Metal Complexes of L₁	40
2-4-2	Complexes of L₂ and L₃	41
2-5	Isolation and Purification of Glutathione S-Transferase from	43

	rat liver	
2-5-1	Assay Method	43
2-5-2	Definition of Unit and Specific Activity	44
2-5-3	Determination of Protein Concentration	44
2-5-4	Isolation and Purification Procedure	46
2-5-4-1	Preparation of Cytosol Fractions	47
2-5-5	Purification Procedure	48
2-5-5-1	Ion Exchange Chromatography by DEAE-Cellulose	48
2-5-5-2	Ion Exchange Chromatography by CM-Cellulose	49
2-5-5-3	Gel Filtration Chromatography on Sephacryl S-200 Column	51
2-5-6	Polyacrylamide Gel Electrophoresis under Denatured Conditions	52
2-6	Interaction of GSH with Prepared Complexes and Standard Substrate	57
CHAPTER THREE: RESULTS AND DISCUSSION		
3-1	Preparation and Physical Properties of the Prepared Complexes	58
3-2	Infrared Spectra of the Prepared Complexes	61
3-2-1	Spectra of Ligand (L₁) and Their Metal Complexes	62
3-2-2	Spectra of Ligand (L₂) and Their Metal Complexes	64
3-2-3	Spectra of Ligand (L₃) and Their Metal Complexes	66
3-3	Magnetic Susceptibility Measurements	85
3-4	Study of the Electronic Spectra of the Prepared Compounds	87
3-4-1	Electronic Spectra of the Ligand L₁, L₂ and L₃	87
3-4-2	Electronic Spectra of the Complexes	87
3-5	Glutathione S-Transferase	107
3-5-1	Determination of Enzyme Volume for Enzyme Activity Assay	107
3-5-2	Crude extract	108
3-5-3	Purification by Ion Exchange Chromatography	108
3-5-4	Purification by Gel Filtration Chromatography	111
3-5-5	Estimate GSTs Purity and Determination its Molecular Weight	112
3-6	Study of the Conjugation Process	115
3-6-1	Determination of λ_{max} for the Glutathione Conjugate	115
3-6-2	Kinetic Studies	115
3-6-3	Study of the Interaction Between GSH and the Substrates	116
3-7	Suggestion for Further Work	125
	References	126

List of Tables

Table	Page
1-1 Some types of Schiff bases and their biological activities	17
1-2 Some useful classification criteria for GSTs	28
2-1 Specification supplied chemicals	33
2-2 Schiff base, metal salt and purification solvents of prepared complexes	42
2-3 Molecular weight of standard proteins	54
3-1 The Physical data of the prepared complexes	59
3-2 Describes, Symbols, Molecular formula and Names of the prepared ligands and complexes	60
3-3 Number of the most bands of FT.IR to prepared ligands and their complexes in (cm⁻¹)	69
3-4 Magnetic properties of the prepared complexes in 298K	86
3-5 The data of electronic spectra of the prepared complexes	98
3-6 Purification steps of glutathione S-transferase	112
3-7 The kinetic data for the enzymatic and non-enzymatic reactions	122

List of Figures

Figure	Page
1-1 Cisplatin[<i>cis</i> -diaminedichloroplatinum(II)]	3
1-2 The cellular uptake of cisplatin and its targets	5
1-3 Platinum(II) complexes in world wide clinical use	6
1-4 Periodic Table of the elements showing metals derived from active antitumor complexes	7
1-5 Some representative gold(I) thiol complexes of medical interest	10
1-6 The structure of (dihydroxy(2,2'-bipyridyl) gold (III) ion [Au(bipy)(OH) ₂] ⁺ PF ₆ ⁻	11
1-7 The structure of [Au(bipy-H)(OH)] ⁺ PF ₆ ⁻	11
1-8 Glutathione synthesis and forms	19
1-9 The structure of glutathione	20
1-10 The mercapturic pathway	22
1-11 Domain structures of GSTs subunits	30
2-1 Standard curve of protein	45
3-1 FT.IR spectrum of L ₁	70
3-2 FT.IR spectrum of L ₁ Pt	71
3-3 FT.IR spectrum of L ₁ Au	72
3-4 FT.IR spectrum of L ₁ Pd	73
3-5 FT.IR spectrum of L ₁ Cu	74
3-6 FT.IR spectrum of L ₂	75
3-7 FT.IR spectrum of L ₂ Pt	76
3-8 FT.IR spectrum of L ₂ Au	77
3-9 FT.IR spectrum of L ₂ Pd	78
3-10 FT.IR spectrum of L ₂ Cu	79
3-11 FT.IR spectrum of L ₃	80
3-12 FT.IR spectrum of L ₃ Pt	81
3-13 FT.IR spectrum of L ₃ Au	82
3-14 FT.IR spectrum of L ₃ Pd	83
3-15 FT.IR spectrum of L ₃ Cu	84
3-16 Electronic spectrum of L ₁	99
3-17 Electronic spectrum of L ₂	99
3-18 Electronic spectrum of L ₃	100
3-19 Electronic spectrum of L ₁ Pt	100
3-20 Electronic spectrum of L ₁ Au	101
3-21 Electronic spectrum of L ₁ Pd	101
3-22 Electronic spectrum of L ₁ Cu	102
3-23 Electronic spectrum of L ₂ Pt	102

3-24 Electronic spectrum of L₂Au	103
3-25 Electronic spectrum of L₂Pd	103
3-26 Electronic spectrum of L₂Cu	104
3-27 Electronic spectrum of L₃Pt	104
3-28 Electronic spectrum of L₃Au	105
3-29 Electronic spectrum of L₃Pd	105
3-30 Electronic spectrum of L₃Cu	106
3-31 Standard curve of enzyme activity at different volumes after 300 seconds.	107
3-32 Purification of crude GSTs on DEAE-Cellulose column (32X3.5cm)	109
3-33 Purification of GSTs on CM-Cellulose column (32X3.5cm)	110
3-34 Purification of GSTs on Sephacryl S-200 column (63X2cm)	111
3-35 The electrophoresis of GSTs enzyme taking from mouse liver	113
3-36 Molecular weight determination for purified GSTs extracted from rat liver	114
3-37 Change of absorbance for the conjugation reaction between GSH and CDNB	116
3-38 Change of absorbance for the conjugation reaction between GSH and L₂Pt	117
3-39 Change of absorbance for the conjugation reaction between GSH and L₂Au	118
3-40 Change of absorbance for the conjugation reaction between GSH and L₂Pd	118
3-41 Change of absorbance for the conjugation reaction between GSH and L₂Cu	119
3-42 Change of absorbance for the conjugation reaction between GSH and L₃Pt	119
3-43 Change of absorbance for the conjugation reaction between GSH and L₃Au	120
3-44 Change of absorbance for the conjugation reaction between GSH and L₃Pd	120
3-45 Change of absorbance for the conjugation reaction between GSH and L₃Cu	121
3-46 Electronic spectrum of CDNB	122
3-47 Electronic spectrum of GSH	122

List of Schemes

	Scheme	Page
1-1	General preparation steps for the preparation of Schiff bases	14
1-2	Overview of enzymic detoxification	26
2-1	The reaction pathway used to prepare the ligand L₁, L₂ and L₃ and their respective metal complexes.	36
2-2	The isolation and purification of GSTs from Rat liver.	46
3-1	Crystal field splitting of the ³F term of a d⁸ ion in Oh field	91
3-2	Crystal field splitting of the ²D term of a d⁹ ion	95

References:

1. G.T. Spiro, "Metal Ion Activation of Dioxygen", **2**, (1980).
2. E. Frieden, *J. Chem. Educ.*, **65**, 917, (1985).
3. Z. Guo and P. J. Sadler, *Angew. Chem. Int. Ed.*, **38**, 1513, (1999).
4. H. Sigal, "Metal Ion in Biochemical Systems", Marcel Dekker, Inc., (1985).
5. Wilson and Griswold's, "Text Book of Organic Medical and Pharmaceutical Chemistry", 10th ed., 255, (1998).
6. NV. Lyubimova, SV. Topchieva, SG. Averinova, AV. Kashkadaeva, VA . Gorbunova, SV. Shiryaev and NE. Kushlinskii, *Bull. Exp. Biol. Med.*, **130 (9)**, 886, (2000).
7. P.J. Sadler, C. Muncie and M. A. Shipman, "Biological Inorganic Chemistry: Structure & Reactivity", (2005).
8. C.X. Zhang and S.J. Lippard, *Current Opinion in Chemical Biology*, **7**, 481, (2003).
9. P.P.Lippard and S.J. *In Encyclopedia of cancer*, J.R.Bertino, Ed.Academic Press: San Diego, CA, **1**, 392, (1997).
10. M. Galanski, V. B. Arion, M. A. Jakupec and B. K. Keppler, *Current Pharmaceutical Design*, **9**, 2078, (2003).
11. S. P.Fricker, "Metal Compounds in Cancer Therapy", (1994).
12. D. L. JAMES, Ph. D. Thesis, McMaster University, Canada (1996).
13. R. A. Al-Mahdi, Ph. D. Thesis, Al-Nahrain University, Iraq (2004).
14. L.Messori, F.Abbate, G.Marcon, P.Orioli, M.Fontani, E.Mini, T.Mazzei, S.Carotti, T.O Connell and P.Zanello, *J.Med.Chem.*, **43**, 3541, (2000).
- 15.RG.Buckley, AM.Elson, SP.Fricker, GR.Henderson, BRC.Theobald, RV.Parish, BP.Howe and LR.Kelland, *J. Med. Chem.*, **39**, 5208, (1996).
16. G.Marcon, S.Carotti, M.Coronello, L.Messori, E.Mini, P.Orioli, T.Mazzei, MA.Cinellu and G.Minghetti, *J.Med.Chem.*, **45**, 1672, (2002).

References

17. J. H. Green and Dowons, *J. Clin. Path.*, **7**, 322, (1986).
18. M.F.Khan, M.Ashfaq and G.M.Khan, *Online Journal of Biological Sciences*, **2(3)**, 145, (2002).
19. M. H. Al-Qaissy, Ph. D. Thesis, Saddam University, Iraq (2001).
20. X.Tai, X. Yin, Q. Chen and M.Tan, *Molecules*, **8**, 439, (2003).
21. H. H. Al-HMEDAWI, M. Sc. Thesis, Baghdad University, Iraq (2003).
22. G. P. Pokhariyal and S. K. Sharma, *J. Indian Chem. Soc.*, **LVIII**, 1199, DECEMBER (1981).
23. U. Casellato, P. Guerriero, S.Tamburini and P.A.Vigato, *Inorganic Chimica Acta*, **119**, 75, (1986).
24. F. H. Urena, N. A. Cabeza, M.N.Carretero and A.L.Chamorro, *Acta. Chim. Slov.*, **47**, 481, (2000).
25. G. V. Karunakar, N. R. Sangeetha, V.Susila and S.Pal, *J. Coord. Chem.*, **50**, 51, (2000).
26. A. Syamal and B. K. Gupta, *J. Indian Chem. Soc.*, **LVIII**, 413, April (1981).
27. A. Syamal and K. S. Kale, *J. Indian Chem. Soc.*, **LVIII**, 186, February (1981).
28. A. Syamal and B. K. Gupta, *J. Indian Chem. Soc.*, **LVIII**, 911, September (1981).
29. J. A. Goodwin, L. J. Wilson, D.M.Stanbury and R.A.Scott, *Inorganic Chemistry*, **28(1)**, 42, (1989).
30. M. M. Abd-Elzaher, *Journal of the Chinese Chemical Society*, **48**, 153, (2001).
31. N.Raman, Y. P.Raja and A.Kulandaisamy, *Indian Acad. Sci.*, **113(3)**, 183, June (2001).
32. B. A. Jani, R.K. Kohli and P.K.Bhattacharya, *J. Indian Chem. Soc.*, **LVIII**, 18, January (1981).

References

33. B. A. Jani and P. K. Bhattacharya, *J. Indian Chem. Soc.*, **LVIII**, 207, March (1981).
34. Z. N. J. Al-Zubaidy, M. Sc. Thesis, Al-Nahrain University, Iraq (2004).
35. F. A. Hassan, M. Sc. Thesis, Al-Nahrain University, Iraq (2002).
36. S. S. Tewari, M. I. Husain and G. C. Srivastava, *J. Indian Chem. Soc.*, **LVIII**, 214, March (1981).
37. M. Agrawal, S. B. Bansal and O. P. Singhal, *J. Indian Chem. Soc.*, **LVIII**, 200, February (1981).
38. A. Echevarria, M.D.Nascimento, V. Geronimo, J. Miller and A. Giesbrecht, *J. Braz. Chem. Soc.*, **10(1)**, 60, (1999).
39. R. Sharma, S. Awasthi, P. Zimniak and Y. C. Awasthi, *Acta. Biochimica Polonica*, **47(3)**, 751, (2000).
40. C.LU. Shelly, *The FASEB Journal*, **13**, 1196, (1999).
41. L. Deleve and N. Kaplowitz, *Pharmacol. Ther.*, **52**, 287, (1991).
42. W. Wang and N. Ballatori, *Pharmacological Reviews*, **50(3)**, 335, September, (1998).
43. E. Boyland and LF. Chasseaud, *Adv Enzymol.Rrelat. Areas Mol. Biol.*, **32**, 173, (1969).
44. H. Sun, S. C. Yan and W. S. Cheng, *European Journal of Biochemistry*, **267(17)**, 5450, September (2000).
45. C.Chen and S.Liao, *Journal of Neurochemistry*, **85(2)**, 443, April (2003).
46. L. H. Lash, W. Qian, D.A.Putt, K. Jacobs, A. A. Elfarra, R. J. Krause and J. C. Parker, *Drug Metabolism and Disposition*, **26(1)**, 12, January (1998).
47. YC. Awasthi, HS.Grag, DD.Dao, CA.Partridge and SK.Srivastava, *Blood*, **58(4)**, 733, (1981).

References

48. M.D.Cordonnier, W.Laine, A.Joubert, C.Tardy, J.Goossens, M.Kouach, G.Briand, H.D.T.Mai, S.Michel, F.Tillequin, M.Koch, S.Leonce, A.Pierre and C.Bailly, *European Journal of Biochemistry*, **270(13)**, 2848, July (2003).
49. M. Bilzer, R.L.Siegel, R.H.Schirmer, T.P.M.Akerboom, H.Sies and G.E.Schulz, *Eur. J. Biochem.*, **138**, 373, (1984).
50. A. R. White, A. I. Bush, K.Beyreuther, C.L.Masters and R.Cappai, *Journal of Neurochemistry*, **72(5)**, 2092, May (1999).
51. DP. Jones, LA. Brown and P.Sternberg, *Toxicology*, **28**, (105, 2-3), 267, December (1995).
52. S. Aliya, P.Reddanna and K. Thyagaraju, *Molecular and Cellular Biochemistry*, **253**, 319, (2003).
53. J. H. Keen, W. H. Habig and W. B. Jakoby, *The Journal of Biological Chemistry*, **251(20)**, Issue of October 25, 6183, (1976).
54. M. Warholm, H. Jensson, M.K.Tahir and B.Mannervik, *Biochemistry*, **25**, 4119 (1986).
55. J. Csiszar, M. Szabo, E.Illes and K.Kurucz, *Acta. Biologica Szegediensis*, **46(3-4)**, 79, (2002).
56. S.P.Colowick and N.O.Kaplan, "Methods in Enzymology", **113**, (1985).
57. D. Sheehan, G. Meade, V.M.Foley and C.A.Dowd, *Biochem. J.*, **360**, 1, (2001).
58. J. A. Redick, W. B. Jakoby and J. Baron, *The journal of Biological Chemistry*, **257(24)**, Issue of December 25, 15200, (1982).
59. Y.Fen, W.Ping LU.Hong and Z.Dian, *Acta. Pharmacological Society*, **24 (10)**, 1033, October (2003).
60. DM. Townsend, kD.Tew, *Oncogene*, **20**, (22,47), 7369, October (2003).

References

61. S. H. Voss, R. Whalen and T. D. Boyer, *Biochem. J.*, **365**, 229, (2002).
62. G. W. Mainwaring, J. Nash, M. Davidson and T. Green, *Biochem. J.*, **314**, 445, (1996).
63. W. H. Habig, M. J. Pabst and W. B. Jakoby, *The journal of Biological Chemistry*, **249(22, 25)**, 7130, (1974).
64. I.Sinning, G. J. Kleywegt, S. W. Cowan, P.Reinemer, H.W.Din, R.Huber, G.L.Gilliland, R.V.Armstrong, Ji.Xinhua, P.G.Board, B.Olin, B.Mannervick and A.Jones, *Biochemistry*, **32**, 12949 (1993).
65. B. P. Block, *Inorganic synthesis*, IV (1953).
66. J. H. Price, A. N. Williamsson, R. F Schramamm and B. B. Wayland, *Inorganic Chemistry*, **11(6)**, (1972).
67. L. A. Bigelow, H. Etaough, *Organic Synthesis*, Collective **I** , (1948).
68. L.G.Marzilli, P.A. Marzilli and J.Halpern, *J.Am.Chem.Soc.*, **93**, 1374, (1971).
69. O.West, *J.Chem.Soc.*,**395**, (1954).
70. N.K.Jha and D.M.Joshi, *Synth.React.Inorg.Met-Org.Chem.*, **14**, 455, (1984).
71. E. W. Ainscough, A. M. Brodie, P.D.Buckley, A.K.Burrell, S.M.F.Kennedy and J.M.Waters, *J.Chem.Soc.Dalton Trans.*, 2663, (2000).
72. A.J.S.Al-Abdali, M. Sc. Thesis, Saddam University, Iraq (2002).
73. Y.R.Al-Hussuna, M.Sc. Thesis, Al-Nahrain University, Iraq (2005).
74. M. M. Bradford, *Anal. Biochem.*, **72**, 248, (1976).
75. J.R.Whitaker and R.A.Bernhard. "Experiments for: An Introduction to Enzymology". The Whiber Press, (1972).
76. M. J. Pabst, W. H. Habig and W. B. Jakoby, *The Journal of Biological chemistry*, **249(22)**, Issue of November 25, 7140, (1974).

References

77. K.H.Tan, D.J.Meyer, J.Belin and B.Ketterer, *Biochem.J.*, **220**, 243, (1984).
78. R.P.Saneto, Y.C.Awasthi and S.K.Srivastava, *Biochem.J.*, **205**, 213, (1982).
79. F.H.M.Al-Shikirhy, M.Sc. Thesis, Baghdad University, Iraq (2004).
80. P. C. Simons and D. L. Vander Jagt, *Analytical Biochemistry*, **82**, 334, (1977).
81. Dayagi and Y. Degini, "The Chemistry of Carbon-Nitrogen Double Bond", S. Patai, John Wiley and Sons interscience, New york, 64 (1970).
82. R. M. Silverstein, G. C. Bassler and T. C. Marril, "Spectrometric Identification of Organic Chemistry", John Wiely and sons, (1981).
83. R. P. Shukla and M. A. Jaiswal, *J. Indian Chem. Soc.*, **LX**, 1014, (1983).
84. O. P. Arora and N. S. Mishra, *J. Indian chem. Soc.*, **LIX**, 32, (1982).
85. N. M. Al-Abidy, M. Sc. Thesis, University of Baghdad, (1997).
86. N. S. Biradar and V. H. Kulkarni, *J. Inorg. Nucl. Chem.*, **23**, 3847, (1971).
87. P. S. Parbhu and S. S. Dodulah, *J. Indian Chem. Soc.*, **LX**, 546, (1983).
88. V. K. Agrawal and R. P. Mahesh, *J. Indian Chem. Soc.*, **LVIII**, 7367, (1981).
89. A. A. Ali and B. Shaubani, *Acta. Chim. Solv.*, **47**, 363, (2000).
90. A. K. Rana and J. R. Shah, *J. Indian Chem. Soc.*, **LVIII**, 1100, November (1981).
91. E. W. Ainsough and A. M. Brodie, *Chemistry-Institute of Fundamental Sciences*, 2663 (2000).
92. K. Arora, R. G. Goyal and S. S. Sharma, *Orient J. Chem.*, **15(2)**, 367 (1999).

References

93. S. M. Kagwanja, J. C. Jeffery, C. J. Jones, and J. A. McCleverty, *Polyhedron*, **15(17)**, 2959, (1996).
94. V. V. Ramanujam and B. Sivasankar, *J. Indian Chem. Soc.*, **LVIII**, 1152, December (1981).
95. M. K. Al-Maliki, M. Sc. Thesis, Al-Nahrain University, Iraq (2005).
96. N. S. Biradan and V. H. Kulkarni, *J. Indian Nucl. Chem.*, **33**, 3781, (1971).
97. J. N. R. Ruddick and J. R. Sams, *J. Organomet. Chem.*, **60**, 233, (1973).
98. S. Sarawat, S. G. Srivastava and C. R. Mehrotra, *J. Organomet. Chem.*, **129**, 155, (1977).
99. J. S. Graber, M. C. Harris and E. Sinn, *J. Inorg. Nucl. Chem.*, **30**, 1805, (1968).
100. P. Toyssie and J. Charette, *J. Spectrochim. Acta.*, **19**, 1407, (1963).
101. K. Ueno and E. A. Martell, *J. Phys. Chem.*, **60**, 1270, (1956).
102. L. T. Yildirim and O. Atakol, *Cryst. Res. Technol.*, **37**, (12), 1352, (2002).
103. N. Nakamoto, "Infrared and Raman Spectra of Inorganic and Coordination Compounds", John Wiley and Sons, Inc., (1978).
104. M. R. Gajenfragad and U. Agarwala, *Bulletin of the Chemical Society of Japan*, **48(3)**, 1024, (1975).
105. V. K. Agrawal, R. P. Mahesh and P. Singh, *J. Indian Chem. Soc.*, **LVIII**, 726, August (1981).
106. D. Nicholis, "Complexes and First-Row Transition Elements", Translated by Dr. W. I. Azeez, 141, (1984).
107. F. A. Cotton and G. Wilkinson, "Advanced Inorganic Chemistry", 538, (1972).
108. L. G. Miessler and A. D. Tarr, "Inorganic Chemistry", 2nd, Prentice-Hall, Inc., (1999).

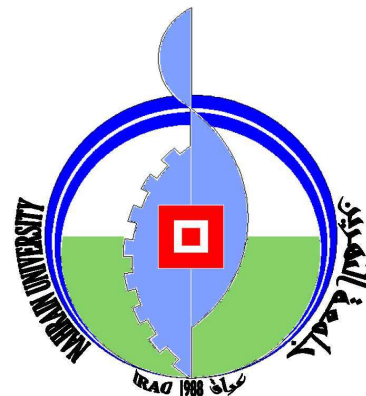
References

109. A. A. Alemi, B. Shaabani, K. A. Dilmaghani and S. T. Ganjall, *Molecules*, **6**, 417, (2001).
110. M. A. El-Rayoumi, M. El-Asser and F. Aladel-Halim, *J. Am. Chem. Soc.*, **39(3)**, 586, (1971).
111. P. W. Alexander and R. T. Steel, *Aust. J. Chem.*, **23**, 1183, (1970).
112. S. Saydam, E. Yilmaz and F. U. Fen, *Ve Muh Bilimleri Dergisi*, **12(2)**, 193, (2000).
113. B. N. Ghose and K. M. Lasisi, *Synth. React. Inorg. Met. Org. Chem.*, **16**, 1121, (1986).
114. A. B. P. Lever, "Inorganic Electronic Spectroscopy", Elsevier Publishing Company Amsterdam-London-New York (1968).
115. C. J. Ballhausen and H. B. Gray, "Coordination Chemistry", **I**, Edited by A. E. Martel, V. N. Reinhold Co., New York, 66 (1971).
116. K. K. Al-Janabi, M. Sc. Thesis, Baghdad University, Iraq (1998).
117. N. N. Green Wood and A. Earnshaw, "Chemistry of The Elements", University of Leeds, U.K. (1984).
118. J. E. Huheey, "Inorganic Chemistry, Principles of Structure and Reactivity", University of Maryland (1972).
119. N.H.Al-Mudallal, E.F.A.Al-Jumaily, S.J.Hamza, A.W.R.Hamad, *Al-Mustansiriya J.Sci.*, **15(1)**, (2004).
120. A.A.Al-Sheikhly.Ph.D.Thesis, Saddam University, (1999).
121. N.H.Al-Mudallal, E.F.A.Al-Jumaily, A.W.R.Hamad, S.J.Hamza, *Al-Mustansiriya J.Sci.*, **14(1)**, (2003).
122. P.J.Blackshear, "Systems for polyacrylamide gel electrophoresis. In: *Methods in Enzymology*'. (ed. Jakoby W.B.) **104**, 237, Academic Press, New York (1984).

Symbols and Abbreviations

FT.IR	Fourier Transform Infrared
UV-Vis	Ultraviolet Visible
DMSO	Dimethyl sulfoxide
B.M	Bohr Magnetron
EDTA	Ethylene diamine tetraacetic acid
DEAE	Diethyl amino ethyl-cellulose
SDS	Sodium dodecyl sulphate
TCA	Tri chloro acetic acid
TEMED	N,N,N,N-Tetra methyl ethylene diamine
Tris	Hydroxy methyl methane amine
BSA	Bovin serum albumin
CMC	Carboxy methyl cellulose
CDNB	1-chloro-2,4-dinitro benzene
GSH	Glutathione
GSTs	Glutathione S-transferase
Rm	Relative mobility
v	Stretching
γ	Out-of-plane bending

Republic of Iraq
Ministry of Higher Education
and Scientific Research
Al-Nahrain University
College of Science
Department of Chemistry



REACTIVITY OF SOME TRANSITION METAL COMPLEXES TOWARD GLUTATHIONE IN THE ABSENCE AND PRESENCE OF ISOLATED AND PURIFIED GLUTATHIONE S- TRANSFERASE

A Thesis

Submitted to the College of Science Al-Nahrain
University in partial fulfillment of the
requirements for the Degree of Master of
Science in Chemistry

By
ZAHRAA FARMAN AMEEN
(B.Sc. 1996)

May 2006

Rabii Al-Thani 1427



جمهورية العراق
وزارة التعليم العالي والبحث العلمي
جامعة النهرين
كلية العلوم
قسم الكيمياء

فعالية معقدات بعض العناصر
الانتقالية تجاه الغلوتاثيون
بوجود وغياب أنزيم غلوتاثيون-S-
ترانسفيريز المعزول والمنقى

رسالة

مقدمة إلى كلية العلوم- جامعة النهرين
وهي جزء من متطلبات نيل درجة الماجستير في الكيمياء

من قبل

زهراء فرمان أمين
بكالوريوس ١٩٩٦ (جامعة الكوفة)

آيار ٢٠٠٦

ربيع الثاني ١٤٢٧

Supervisors' certification

We certify that this thesis was prepared under our supervision at the Department of Chemistry, College of Science, Al-Nahrain University as a partial requirements for the **Degree of Master of Science in Chemistry.**

Signature:

**Name: Professor Dr.
Ayad H. Jassim**

Signature:

**Name: Professor Dr.
Essam F. Al-Jumaily**

Date:

Date:

In view of the available recommendations, I forward this thesis for debate by the Examining Committee.

Signature:

**Name: Assistant Professor Dr. Afaf Al-Derzi
Head of Chemistry Department
College of Science
Al-Nahrain University**

Examining Committee's Certification

We, the Examining Committee, certify that we read this thesis and have examined the student **Zahraa Farman Ameen**, in its contents and that, in our opinion; it is adequate as a thesis for the Degree of Master of Science, in Chemistry.

Chairman

Signature:

Name: Prof. Dr. Falih Hasan Musa Al-Musawi

Date:

Member

Signature:

Name: Assist. Prof. Salman Ali Ahmed

Abdali

Date:

Member

Signature

Name: Dr. Basim Ibrahim Al-

Date:

Member\advisor

Signature:

Name: Prof. Dr. Ayad H. Jassim

Jumaily

Date:

Member\advisor

Signature:

Name: Prof. Dr. Essam F. Al-

Date:

Approved for the College of Graduate Studies

Signature:

Name: Assist. Prof. Dr. LAITH ABDUL AZIZ AL-ANI

Address: Dean of the College of Science Al-Nahrain University

Date:

TO MY PARENTS...

TO MY BROTHERS...

TO MY SISTERS...

TO MY HASBUND...

ZAHRAA

بِسْمِ اللَّهِ الرَّحْمَنِ الرَّحِيمِ
وَعِنْدَهُ مَفَاتِحُ الْغَيْبِ لَا يَعْلَمُهَا إِلَّا هُوَ
وَيَعْلَمُ مَا فِي الْبُرِّ وَالْبَحْرِ وَمَا تَسْقُطُ
مِنْ وَرَقَةٍ إِلَّا يَعْلَمُهَا وَلَا حَبَّةٍ فِي
ظُلُمَاتِ الْأَرْضِ وَلَا رَطْبٍ وَلَا يَابِسٍ
إِلَّا فِي كِتَابٍ مُبِينٍ
صَدَقَ اللَّهُ الْعَظِيمُ

Abstract

A new set of Schiff bases have been prepared in this work, which include:

2-[(cyclohexylimino)methyl]phenol(L₁)

N[4(diethylamino)benzylidene]-N-(4-methoxyphenyl)amine(L₂)

1-[(4-methoxyphenyl)imino)methyl]-2-naphthol (L₃), along with their complexes, with Pt(IV), Au(III), Pd(II) and Cu(II) metal ions. All the Schiff bases and their metal complexes have been characterized using FT.IR, UV-Vis. Spectroscopy, CHN-elemental analysis, Magnetic Susceptibility, and Conductivity measurements.

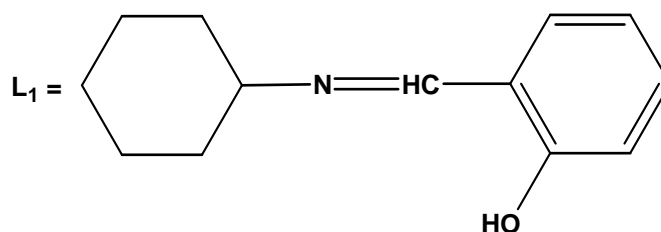
The following formula for the prepared complexes can be suggested:

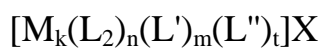
$[M_k(L_1)_n(L')_m]X$ for Pt(IV) $k=1, n=1, L'=Cl, m=4, X=0$

for Au(III) $k=1, n=1, L'=Cl, m=2, X=0$

for Pd(II) $k=1, n=2, L'=0, m=0, X=0$

for Cu(II) $k=2, n=8, L'=ONO_2, m=2, X=0$



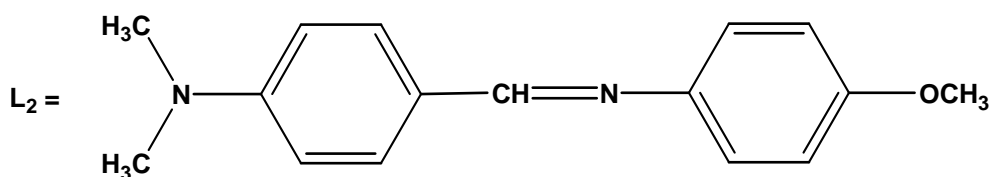


for Pt(IV) $k=2, n=4, L' = Cl, m=6, L''=0, t=0, X = Cl$

for Au(III) $k=1, n=6, L' = 0, m=0, L''=0, t=0, X = Cl$

for Pd(II) $k=2, n=4, L' = Cl, m=4, L''=H_2O, t=2, X = 0$

for Cu(II) $k=1, n=3, L' = ONO_2, m=1, L''=H_2O, t=2,$
 $X=NO_3$

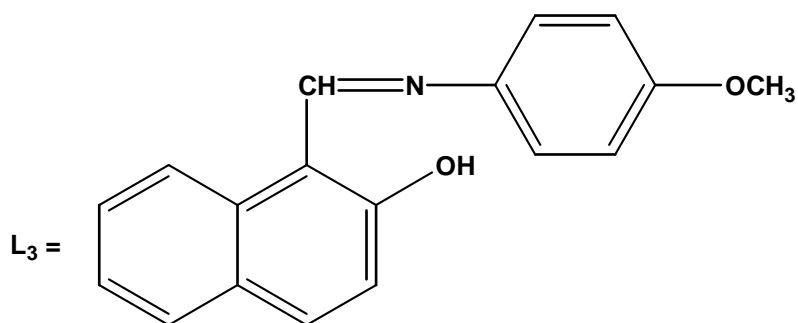


$[M_k(L_3)_n(L')_m]X$ for Pt(IV) $k=1, n=2, L' = Cl, m=2, X = Cl$

for Au(III) $k=1, n=2, L' = 0, m=0, X = Cl$

for Pd(II) $k=2, n=6, L' = 0, m=0, X = Cl$

for Cu(II) $k=1, n=2, L' = 0, m=0, X = 0$



The Glutathione S-transferase was isolated from rat liver and purified follow three steps, i.e. Ion Exchange Chromatography (using DEAE-Cellulose, then CM-Cellulose), finally using Gel Filtration Chromatography using Sephacryl S-200. Electrophoresis technique was used to estimate the purity of the purified enzyme and to measure its molecular weight.

The non-enzymatic and enzymatic reactivity's of eight of the prepared complexes toward glutathione were measured under physiological conditions (phosphate buffer 0.1M, pH=6.7, 30°C). 1-chloro 2,4-dinitrobenzene was used as standard substrate to assay the enzyme activity and for the comparative study of the conjugation reaction.

The rate and rate constant of the conjugation reaction were calculated, the reactivity (as reflected by the k_2 values) was found to follow the following sequence:



It was found that most cationic complexes (L_2Au , L_3Au , L_3Pd , L_3Pt , L_2Pt , and L_2Cu) were of greater reactivity than neutral complexes (L_2Pd , L_3Cu) and those gold (III) complexes where of highest k_2 values while copper (II) complexes having lowest values.

الخلاصة

تم تحضير ثلاث قواعد شف جديدة، والتي تتضمن:

2-[(cyclohexylimino)methyl]phenol(L₁)

N[4(diethylamino)benzylidene]-N-(4-methoxyphenyl)amine(L₂)

1-[(4-methoxyphenyl)imino)methyl]-2-naphthol (L₃)

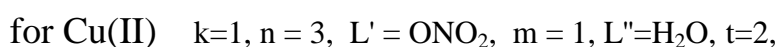
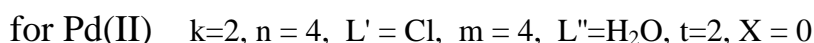
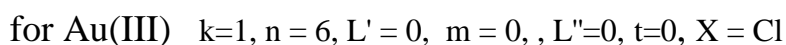
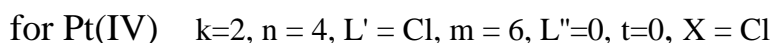
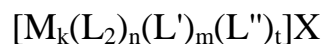
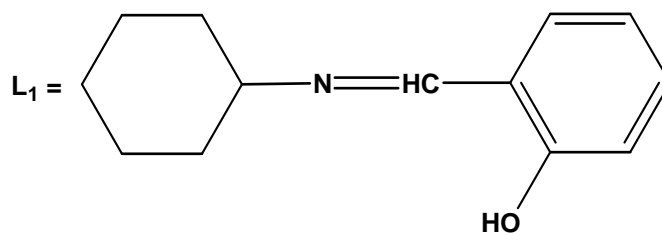
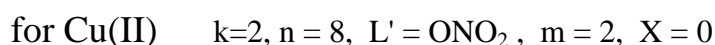
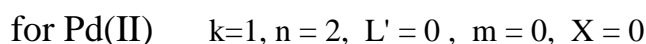
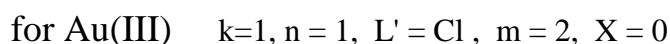
، Pt(IV), Au(III), Pd(II), Cu(II) كما حضرت معقداتها مع ايونات العناصر

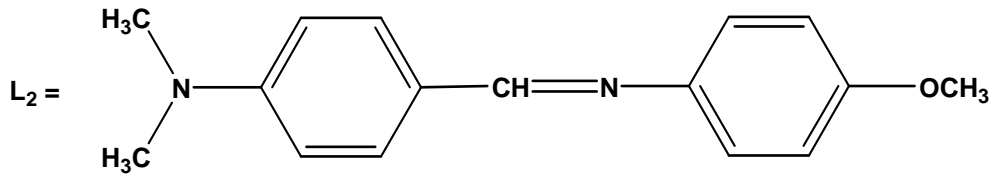
شخصت كل قواعد شف المحضرة ومعقداتها بواسطة الاشعة تحت الحمراء (FT.IR) والاشعة

فوق البنفسجية-المرئية (UV-Vis) والتحليل الدقيق للعناصر (C.H.N) وقياسات الحساسية

المغناطيسية والتوصيلية الكهربائية.

واقترحت الصيغ التالية للمعقدات:



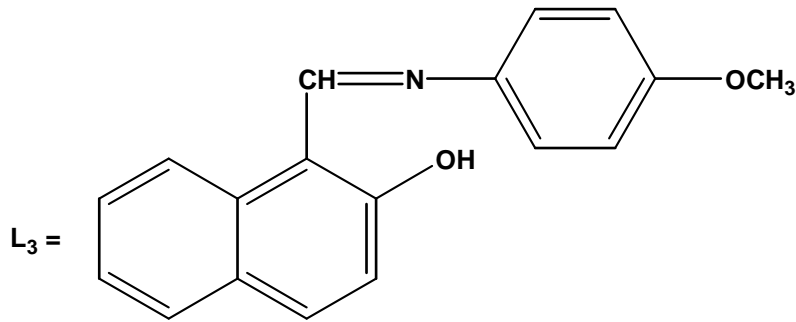


$[M_k(L_3)_n(L')_m]X$ for Pt(IV) $k=1, n=2, L'=Cl, m=2, X=Cl$

for Au(III) $k=1, n=2, L'=0, m=0, X=Cl$

for Pd(II) $k=2, n=6, L'=0, m=0, X=Cl$

for Cu(II) $k=1, n=2, L'=0, m=0, X=0$



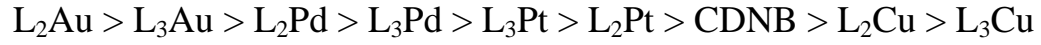
تم عزل إنزيم الكلوتاثيون S-ترانسفيريز من كبد الجرذان وتمت تنقيته بثلاث خطوات؛
كروماتوغرافيا التبادل الأيوني باستخدام DEAE-Cellulose وكروماتوغرافيا التبادل
الأيوني باستخدام CM-Cellulose وأخيرا باستخدام كروماتوغرافيا الترشيح الهلامي
باستخدام سيفاكريل S-200.

استخدمت تقنية الترحيل الكهربائي للكشف عن نقاوة الإنزيم المنقى وكذلك لتعيين وزنه
الجزئي.

درست فعالية ثمانية من المعقدات المحضرة تجاه الكلوتاثيون بوجود وغياب أنزيم
الكلوتاثيون S- ترانسفيريز تحت الظروف الفسلاجية (دارى الفوسفات $30^{\circ}C, pH7$,
 $0.1M$,

تم استخدام 1-Chloro2,4-dinitrobenzene كمادة أساس قياسي للكشف عن فعالية
إنزيم وكذلك للدراسة المقارنة لتفاعل التداخل.

حددت قيمة السرعة وثابت السرعة لتفاعل الاقتران، ووجد إن الفعالية تجاه الكلوتاثيون (والتي حددت من خلال قيمة k_2) قد اتبعت التسلسل الأتي:



حيث تبين إن المعقدات الأيونية الموجبة الشحنة

(L_2Au , L_3Au , L_3Pd , L_3Pt , L_2Pt , and L_2Cu) كانت أكثر فعالية من المعقدات

المتعادلة (L_2Pd , L_3Cu) كذلك وجد إن معقدات الذهب الثلاثي كانت تملك أعلى قيمة k_2 بينما

امتلكت معقدات النحاس (II) أقل قيمة للفعالية.

Acknowledgment

Above all else, I want to express my great thanks to my God Allah for his uncountable gifts and for helping me to present this thesis.

It is my pleasure to express deep appreciation to my supervisors Prof. Dr. Ayad H. Jassim Al-Khafaji, and Prof. Dr. Essam F. Al-Jumaili for their suggestions of the topic of this thesis and their guidance throughout the progresses of the research work.

I am grateful to the official authorities of Al-Nahrain University especially the chemistry department in college of science for helping me to accomplish my work; likewise to Genetic Engineering and Biotechnology Institute for the opportunity they offered me to continue my graduate study.

Special thanks go to my family for their patience and warm feelings and advice during my study.

Special thank to Mr. Mustafa Katan Al-Maliki for the printing and justifying of the thesis.

I wish also to thank all my friends and every one who helped me throughout this study.

Zahraa

2006

CHAPTER ONE

INTRODUCTION

CHAPTER TWO
MATERIALS AND
METHODS

CHAPTER THREE
RESULTS AND
DISCUSSION

References